UNIVERSITAT POLITÈCNICA
DE CATALUNYA
BARCELONATECH

Harmonic load flow formulation and numerical resolution

Asim Rashid

UNIVERSITAT POLITÈCNICA DE CATALUNYA

ESCOLA TÈCNICA SUPERIOR D'ENGINYERIA

INDUSTRIAL DE BARCELONA

DEPARTAMENT D'ENGINYERIA ELÈCTRICA

DOCTORAL THESIS

HARMONIC LOAD FLOW FORMULATION AND NUMERICAL RESOLUTION

PhD candidate: Asim Rashid

Supervisors: Juan José Mesas García

Luis Sainz Sapera

Barcelona, November 2018

Dedicated to my family

Acknowledgements

All praise and glory be to Allah, Who is greatest benefactor, and Whose help enabled me to complete this thesis.

I would like to thank my supervisors Prof. Juan José Mesas García and Prof. Luis Sainz Sapera for their guidance and motivation to complete this thesis, without their help and ideas I would not have been able to carry out this work.

Finally, special thanks to my father Abdul Rashid, my mother Rukhsana Rashid and the rest of the family. Their support has always been crucial in my life.

Abstract

As a continuation of the work done by the QSE (Electrical Supply Quality) research group at the UPC (Polytechnic University of Catalonia) on harmonic load flow in electric power networks, this thesis aims to study existing harmonic load flow formulations, as well as the numerical resolution of the nonlinear equation systems derived from these formulations, in order to propose improvements for the former and compare performances of numerical methods for the latter. The improvements in the harmonic load flow formulations are related to a reduction in the number of iterations, for which an improved formulation is proposed. The comparison of numerical resolution methods is focused on analysing harmonic load flow formulation convergences and accuracies.

The specific goals of the thesis are:

(1) To propose an improved formulation for the harmonic load flow problem. This formulation should be applicable to electrical networks with highly distorted voltages.

(2) To analyse the numerical resolution of all the considered harmonic load flow formulations (existing and improved) in terms of convergence and accuracy, by using a well-known numerical method (Newton-Raphson) and an alternative numerical method (Levenberg-Marquardt).

Table of Contents

List of Figures

List of Tables

List of Abbreviations

AC	Alternating Current
CHLF	Complete Harmonic Load Flow
$CHLF_F$	Complete Harmonic Load Flow (Fundamental)
$CHLF_H$	Complete Harmonic Load Flow (Harmonic)
$CHLF_m$	Complete Harmonic Load Flow (modified)
DC	Direct Current
EMTP	Electromagnetic Transients Program
FLF	Fundamental Load Flow
FLF_m	Fundamental Load Flow (modified)
HA	Harmonic Analysis
HD	Harmonic Distortion (individual)
HLF	Harmonic Load Flow
HP	Harmonic Penetration
HVDC	High-Voltage Direct Current
IUHLF	Improved Unified Harmonic Load Flow
NL	Nonlinear
NLL	Nonlinear Load
rms	root mean square
SHLF	Simplified Harmonic Load Flow
SMPS	Switch-Mode Power Supply
THD	Total Harmonic Distortion
UHLF	Unified Harmonic Load Flow
UPS	Uninterruptible Power Supply
VN	Voltage Node method

1. Introduction

1.1. State of the art

1.1.1. Fundamental load flow

The calculation of steady state voltages at fundamental frequency from the given power constraints in order to know about the static operation of an electric power system is known as fundamental load flow (FLF).

FLF formulation is important in planning, operation, control and calculating the performance of an electrical power system. The studies in relation to FLF are covered exclusively in bibliography [1 - 3]. The objective of FLF is the resolution of an electric network to find the steady state fundamental bus voltages. Table 1.1 summarises the unknowns for FLF if an AC network of n buses is considered $(i = 1, 2, \ldots, n)$: a Slack bus $(i = 1)$ and a number of PQ buses $(i = 2, \ldots, n)$. The absence of PV buses is assumed without loss of generality.

Stage	Bus	Data	Unknowns
FLF	Slack	$\underline{V}_1^1$	---
	PQ	P_i, Q_i (injected)	$\underline{V}_i^1$

Table 1.1: FLF formulation data and unknowns

The nonlinear equation system for FLF is as follows:

$$\underline{S}_i = \underline{V}_i^1 \left(\sum_{j=1}^{n} \underline{Y}_{ij}^1 \underline{V}_j^1 \right)^* \qquad (i = 2, \ldots, n) \tag{1.1}$$

where $\underline{Y}^1{}_{ij}$ are the ij^{th} elements of the network fundamental admittance matrix $\mathbf{Y}^1_{\mathbf{B}}$. The numerical resolution of the equation system (1.1) provides the fundamental voltages $\underline{V}_i^1$

$$\underline{V}_i^1 = V_i^1 \angle \underline{\delta_i^1} \qquad (i = 2, \ldots, n). \tag{1.2}$$

The fundamental currents injected at network buses can be given as

$$\mathbf{I}^1_{\mathbf{bus}} = \mathbf{Y}^1_{\mathbf{bus}} \cdot \mathbf{V}^1_{\mathbf{bus}} \quad \Rightarrow \quad \underline{I}_i^1 = \sum_{j=1}^{n} \underline{Y}_{ij}^1 \cdot \underline{V}_j^1 \qquad (i = 1, \ldots, n). \tag{1.3}$$

1.1.2. Harmonics in power systems

The average value of a periodic signal $x(t)$ is the average of all the values taken by that signal over one period.

$$X_{average} = \frac{1}{T}\int_0^T x(t)\,dt \tag{1.4}$$

If the periodic signal is sinusoidal, its average value is zero.

The root mean square (rms) value of a periodic signal $x(t)$ is the square root of the average value of the square of that signal over one period.

$$X = X_{rms} = \sqrt{\frac{1}{T}\int_0^T x^2(t)\,dt} \tag{1.5}$$

If the periodic signal is sinusoidal, its rms value is $X_{\max}/\sqrt{2}$.

The Fourier theorem states that under certain conditions (which are usually fulfilled in practice for a large number of functions) a periodic non-sinusoidal function can be decomposed into an infinite sum of functions (Fourier series) consisting of:

- a constant function (continuous component).
- a sinusoidal function of frequency *f* (fundamental component).
- infinite sinusoidal integer multi-frequency functions of *f* (harmonic components, or simply harmonics), the sinusoidal component whose frequency is *k* times the frequency of the fundamental component being called the harmonic *k* or *k*-th harmonic.

This decomposition is expressed mathematically by equation

$$x(t) = X_0 + \sum_{k=1}^{\infty} \sqrt{2}\cdot X_k \cdot \cos\left(k\omega t + \varphi_{X_k}\right) \tag{1.6}$$

where:

$x(t)$ is the periodic function object of the decomposition.

X_0 is the continuous component, which corresponds to the average value of $x(t)$.

$\sqrt{2}\cdot X_k \cdot \cos\left(k\omega t + \varphi_{X_k}\right)$ are the sinusoidal components (fundamental and harmonics), each characterized by:

X_k → rms value of the *k*-th sinusoidal component.

$k\omega$ → angular frequency (pulsation) of the *k*-th sinusoidal component, the order of said component being *k*.

φ_{X_k} → phase of the *k*-th sinusoidal component.

Thus, in the case of Fourier series decomposition of a non-sinusoidal periodic function, the rms value of said function can be calculated by using an alternative procedure derived from the mathematical expression (1.5) and which is discussed below (also in form of a mathematical expression):

$$X = X_{rms} = \sqrt{\sum_{k=0}^{\infty} X_k^2} \tag{1.7}$$

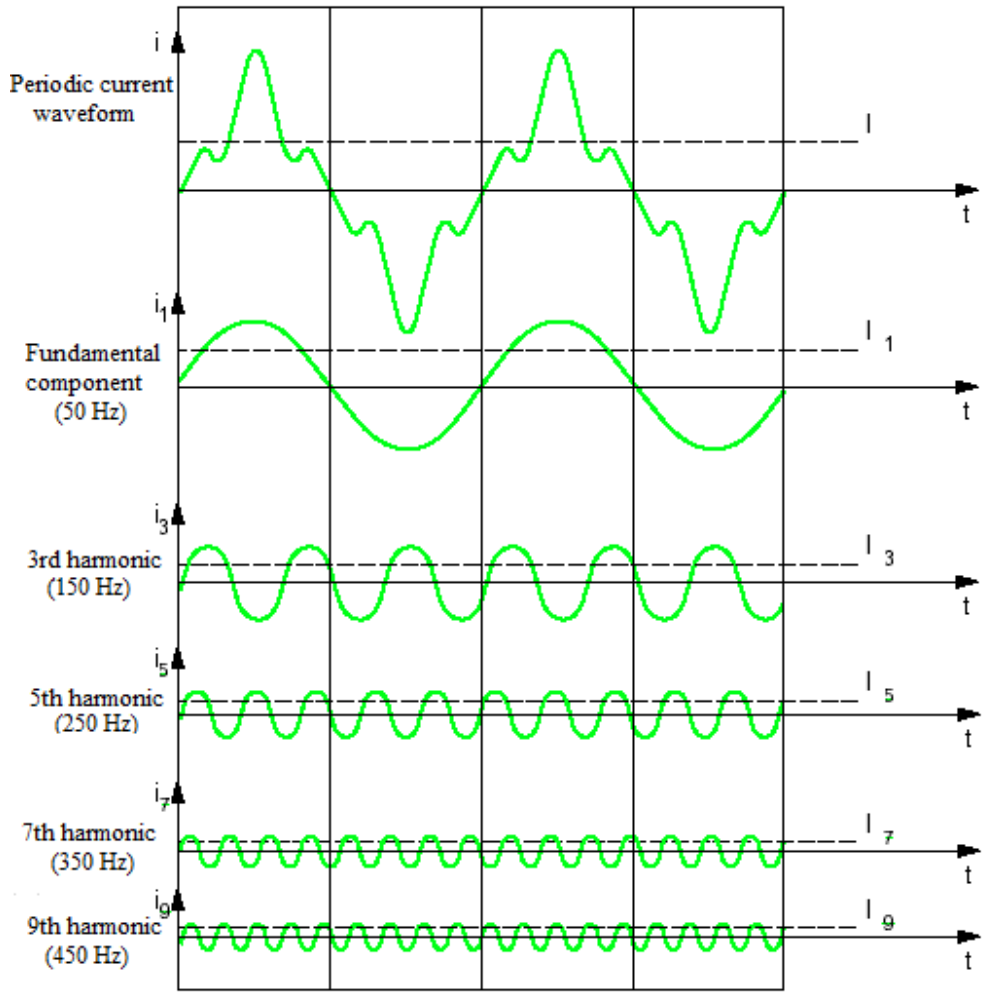

Figure 1.1: Example of a periodic signal of current of rms value *I* with harmonic content. Decomposition of said signal in its fundamental component and its harmonics of rms values I_k.

The continuous component and the harmonic sinusoidal components of a periodic signal constitute the distortion of its fundamental sinusoidal component. The part of that distortion due to harmonic sinusoidal components is called harmonic distortion. Figure 1.1 shows an example of a sinusoidal current wave affected only by harmonic distortion, resulting in a periodic signal of zero average current (without continuous component).

Of all the existing indicators for quantifying and evaluating the harmonic distortion of sinusoidal waves, the ones detailed below will be those used throughout this document.

The rms value, for the case of sinusoidal waves affected only by harmonic distortion, is defined from (1.7) adopting $k \geq 1$

$$X = X_{rms} = \sqrt{\sum_{k=1}^{\infty} X_k^2} \tag{1.8}$$

The individual harmonic distortion of order *k* is defined as the quotient between the rms value of the harmonic component *k* and the rms value of the fundamental component (in percent).

$$HD_{X_k} = \frac{X_k}{X_1} \cdot 100 \quad [\%] \tag{1.9}$$

The harmonic spectrum is defined as the graphic representation of the individual harmonic distortion values as a function of the harmonic order. This graphical representation usually incorporates the individual "harmonic" distortion (= 100%) of the fundamental component (as if it were one more harmonic) whenever it does not give rise to scaling problems.

The harmonic spectra associated with periodic non-sinusoidal functions are discrete or in discontinuous form. Thus, for the presence of such spectra to be more attractive, bar graphs are often used to represent them. An example is shown in Figure 1.2, which corresponds to that of a square wave signal.

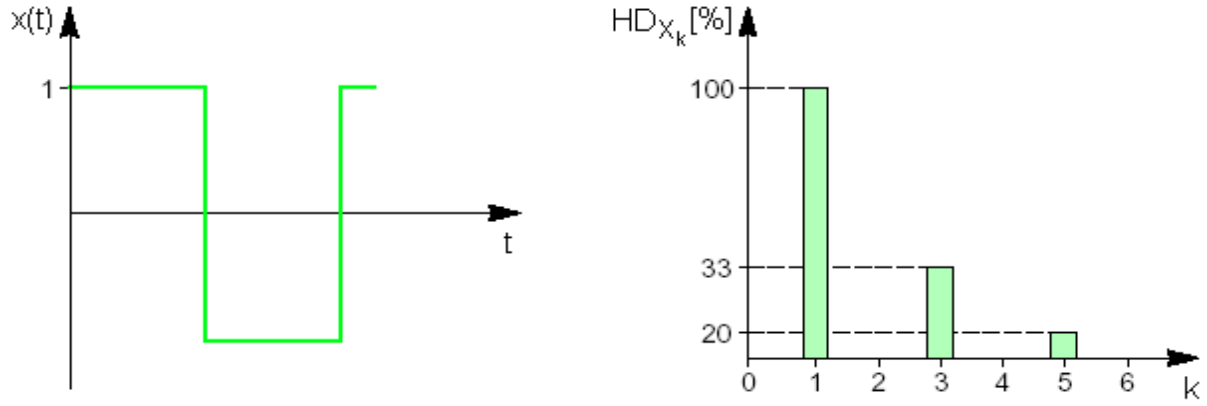

Figure 1.2: Signal of the square wave type and its harmonic spectrum (the highest individual harmonic distortions have been represented in it).

Total harmonic distortion is defined as the square root of the summation of the squares of individual harmonic distortions in percent.

$$THD_X = \sqrt{\sum_{k=2}^{\infty} HD_{X_k}^2} = \frac{\sqrt{\sum_{k=2}^{\infty} X_k^2}}{X_1} \cdot 100 \quad [\%] \tag{1.10}$$

The usual non-sinusoidal periodic regimes in Electrotechnics usually have negligible or no continuous component value. Thus, let it be a load (linear or nonlinear) excited with a voltage

$$u(t) = \sum_{k=1}^{\infty} \sqrt{2} \cdot U_k \cdot \cos\left(k\omega t + \varphi_{U_k}\right) \tag{1.11}$$

and crossed by a current

$$i(t) = \sum_{k=1}^{\infty} \sqrt{2} \cdot I_k \cdot \cos\left(k\omega t + \varphi_{I_k}\right). \tag{1.12}$$

Active power is defined as

$$P = \sum_{k=1}^{\infty} U_k \cdot I_k \cdot \cos\left(\varphi_{U_k} - \varphi_{I_k}\right) \tag{1.13}$$

and, adopting one of the multiple definitions found in the literature, reactive power as

$$Q = \sum_{k=1}^{\infty} U_k \cdot I_k \cdot \sin\left(\varphi_{U_k} - \varphi_{I_k}\right). \tag{1.14}$$

In addition, the product of the rms values of voltage and current is called apparent power

$$S = U \cdot I = \sqrt{\sum_{k=1}^{\infty} U_k^2} \cdot \sqrt{\sum_{k=1}^{\infty} I_k^2} = \sqrt{\sum_{k=1}^{\infty} U_k^2 \cdot \sum_{k=1}^{\infty} I_k^2} \tag{1.15}$$

In view of (1.13), (1.14) and (1.15) it is easy to verify that equality

$$P^2 + Q^2 = S^2, \tag{1.16}$$

typical of periodic sinusoidal regimes, is not met. In fact, for non-sinusoidal periodic regimes,

$$P^2 + Q^2 < S^2 \tag{1.17}$$

and the distortion power is defined as

$$D = \sqrt{S^2 - P^2 - Q^2}. \tag{1.18}$$

Since the existence of a continuous component is not being considered, it may be called harmonic distortion power itself.

Harmonics are generally caused by the distortion of the sinusoidal current waveform transmitted by nonlinear loads. Switch-mode power supplies (SMPSs), variable speed motors and drives, photocopiers, personal computers, laser printers, fax machines, battery chargers and uninterruptible power supplies (UPSs) are examples of nonlinear loads. In the last decade, there

were an increasing number of nonlinear loads connected to distribution systems. Unfortunately, these loads inject harmonic currents leading to problematic voltage distortion levels which may damage power quality. The effects of harmonics on power systems and their acceptable limits are well known [4 - 11]. For this reason, there are different studies in the literature that attempt to predict harmonic currents injected by nonlinear loads [9, 10] and determine harmonic voltages [10, 11, 12].

Controlling and reducing the harmonic distortion in power system is one of the main challenges of power engineer. The phenomena of harmonics are based on high frequencies usually the frequencies ranging from 50/60 Hz to 2.5 kHz. It is very important to keep in view the device characteristics at the harmonic frequency range. Some examples of harmonic producing loads are converters, transformers, discharge lamps, electrical machines and arc furnaces. In order to set a maximum limit to voltage distortion caused by harmonics and to have high quality power supplies, IEEE has set harmonic limits on power consumer so that the magnitude of harmonic distortions in power system remains reasonable. IEEE standard 519-2014 [6] puts limits on the allowable total harmonic distortion for “Low Voltage, General Distribution, General Sub-transmission, and High Voltage Systems and Dispersed Generation and Cogeneration".

1.1.3. Harmonic load flow analysis

In recent years, harmonic study and harmonic load analysis have become an integral component of electric power system design and analysis. It is estimated that in the next few years more than 50 percent electric loads in AC networks will be of nonlinear nature resulting in degradation and distortion of voltages and current waveforms in electric power systems. Harmonic studies are important because they are used to quantify the distorted voltages and current waveforms at various points in a power system and to determine whether dangerous resonant conditions exist and how they might be mitigated. The propagation of harmonics in the power system results in loss of life of equipment, power losses and also interfere with control and communication equipment in transmission system [11].

Procedures for analysing the steady state harmonic problem can be divided into time domain and frequency domain [14, 15, 16, 17]. The former, such as *Electromagnetic Transients Program (EMTP)*, are based on the numerical resolution of electric power system differential equations. They treat nonlinear load (NLL) equations directly, but require a high calculation effort to obtain steady state solutions and difficult management of power consumption loads. The latter, known as harmonic load flow (HLF) formulations, are reformulations of FLF which consider harmonic voltages and NLL state variables as additional unknowns to the fundamental voltages. Their main drawback is that NLL equations must be adapted to the frequency domain formulation. These frequency domain procedures pose nonlinear equation systems which must be numerically solved to directly obtain the fundamental and harmonic voltages of the network and the variables

characterising the NLL state. There are also hybrid procedures which work in both domains by using their respective advantages [18]. The procedures in the frequency domain are the most widely used in the literature, and Newton-Raphson is the most commonly employed numerical method to solve their nonlinear equation systems. Nevertheless, the numerical resolution of these equation systems has several difficulties such as long execution time, convergence problems and large computer memory requirements due to the significant number of involved unknowns. There are three important steps which must be considered when applying frequency domain methods to an AC network. These steps are:

- **Modelling of power system elements:** The elements connected in the network must be modelled in order to perform harmonic load flow studies. These elements can be decomposed in linear and nonlinear devices. Linear load modelling is a well-known topic but this is not true for nonlinear load topic which is still being studied [13, 19, 20]. The latter is very important in harmonic load flow because nonlinear loads are the network distorting devices and they exhibit a particular behaviour.

- **Formulation of the harmonic problem:** The problem formulation aims to pose the necessary equations to determine the fundamental and harmonic voltage and the variables which define nonlinear load behaviour. The great number of unknowns to solve in the harmonic load flow formulations leads authors to tackle the problem in several ways in order to reach a compromise between the simplicity and reliability of the formulation [21]. The simplest way is the harmonic penetration analysis which assumes no harmonic interaction between network and nonlinear loads [14, 21, 22]. The iterative harmonic analysis is the first modification of the harmonic penetration studies when considering harmonic voltage influence on the non–linear device behaviour. In particular, simplified harmonic load flow formulation is the most basic HLF formulation which takes into consideration the harmonic interaction in nonlinear load behaviour and improves the iterative harmonic analysis [23 - 27]. Complete harmonic load flow formulations are reformulations of the fundamental load flow in order to include nonlinear loads. This formulation is a natural modification of the fundamental load flow where the nonlinear device treatment and the harmonic voltage calculation have been included and are calculated simultaneously [28 - 31]. In this formulation, it can be assumed that power consumption is only due to fundamental voltages and currents or that power consumption is due to fundamental and harmonic voltages and currents [21]. The latter is the most complicated harmonic problem formulation but it provides the most accurate results. The other formulations can be used depending on the harmonic voltage level because all of them assume that harmonic voltage influence can be neglected in some part of the formulation equations. Another available HLF formulation is the unified harmonic load flow formulation [48, 49]. It is a modification of the complete harmonic load flow formulation which takes into account the approach used in the simplified harmonic load flow formulation.

1.1.4. Load flow numerical resolution

Newton-Raphson method is the numerical method most generally used in the literature for solving the nonlinear set of equations of the harmonic load flow formulation [14, 28, 35]. This method has the advantages of a relative simplicity and an excellent execution time, but for networks with high harmonic distortion and presence of nonlinear loads it can be divergent or convergent to a false solution [14, 40, 41]. Thus, there are different methods in the bibliography to improve the convergence of Newton-Raphson method, called, in general, modified Newton-Raphson methods [33, 36, 37, 38, 39]. These methods improve the convergence of Newton-Raphson method using a damping factor in the Newton-Raphson algorithm but do not ensure the global convergence because they can converge to a local minimum.

Newton-Raphson method suffers from convergence problems if starting points being proposed are not close to the solution. Therefore, need arises to explore other numerical methods for the numerical resolution of the HLF problem. The alternative method employed in this thesis for the numerical resolution of the HLF problem is the Levenberg-Marquardt method, which is based on the least-squares approach [44 - 47]. The optimization toolbox in MATLAB provides us with a built-in command *´fsolve´* [44] to apply this numerical method for our HLF problem without going into hustle of developing the code of the algorithm by oneself.

1.2. Objectives of the thesis

The thesis aims to study existing HLF formulations, as well as the numerical resolution of the nonlinear equation systems derived from these formulations, in order to propose improvements for the former and compare performances of numerical methods for the latter. The improvements in the HLF formulations are related to a reduction in the number of iterations, for which an improved formulation is proposed. The comparison of numerical resolution methods is focused on analysing HLF formulation convergences and accuracies. The specific goals of the thesis are presented below:

- To propose an improved formulation for the HLF problem. This formulation should be applicable to electrical networks with highly distorted voltages.
- To analyse the numerical resolution of all the considered HLF formulations (existing and improved) in terms of convergence and accuracy, by using a well-known numerical method (Newton-Raphson) and an alternative numerical method (Levenberg-Marquardt).

The above objectives have contributed along the following research lines:

- Study of existing HLF formulations and their numerical resolution.
- Practical implementation of programs which includes the main HLF formulations and their numerical resolution applied to AC networks.
- Comparison of the performances of both HLF formulations and numerical resolution methods. The comparison will be based on computational complexity, convergence properties and accuracy of results.
- Analysis of AC networks where the harmonic voltage distortion of nonlinear buses is increased.
- Study of an improved HLF formulation and its comparison with existing formulations.
- Study of numerical procedures for HLF resolution and their convergence properties.

1.3. Structure of the thesis

The structure of this thesis is described as follows:

Chapter 1 starts with state of the art explaining the basic concepts and theory behind HLF analysis. The concepts and theory underlying the FLF formulation and its associated set of equations are explained in detail. A description of harmonics in power systems and the main factors which introduce harmonics in AC networks are given. HLF and how it is different from FLF is introduced. Important methods found in literature to approach HLF analysis are also discussed. The chapter ends by discussing the load flow numerical resolution.

Chapter 2 discusses the main HLF formulations found in literature. The first is the harmonic penetration (HP), which is the simplest HLF formulation requiring a fewer number of equations but with some limitations in terms of accuracy if harmonics in AC networks exceed a certain level. Simplified harmonic load flow (SHLF) is described in detail, which is another important formulation where Thévenin equivalent circuits are employed to reduce the number of equations and hence the number of unknowns to be solved, but faces convergence problems since two numerical procedures linked by a Gauss-Seidel method to reach the solution. It is also presented the HLF formulation with the most number of equations and unknowns, which is the complete harmonic load flow (CHLF). This formulation faces convergence problems in its numerical resolution if the harmonic voltage distortion is increased in the system. It has two variants, one with power consideration at fundamental frequency ($CHLF_F$) and the other with power consideration at fundamental and harmonic frequencies ($CHLF_H$). $CHLF_F$ has the advantage of giving more accurate results than HP, same accurate results as SHLF, and less accurate results than $CHLF_H$. In fact, $CHLF_H$ is considered the most computational extensive HLF formulation as compared to the other HLF formulations. Regarding the unified harmonic load flow (UHLF), on which the improved formulation proposed in this thesis for the HLF problem will be based, is described in Chapter 4 for didactic reasons.

Chapter 3 discusses the numerical resolution of HLF formulations in detail. Different numerical methods being used in literature for obtaining the numerical solution of HLF problems are presented. The Newton-Raphson method is explored in HLF problems and some comments about its shortcomings are made. The fixed-point iteration method and its underlying basic concepts are described. In addition, some light is shed on using fixed-point iteration method with SHLF. Numerical methods which imply a nonlinear least-squares approach for function minimization are considered, such as the Gauss-Newton method and the Levenberg-Marquardt method.

Chapter 4 proposes an improved HLF formulation called improved unified harmonic load flow (IUHLF). This formulation is a derivation of the existing UHLF formulation and, as such, uses Thévenin equivalent circuits to reduce the number of equations and unknowns associated to an AC network. The main set of equations being used and associated unknowns for each bus (Slack, PQ and NL) are illustrated. The performance of IUHLF is compared with other known formulations. The comparison is done by evaluating properties such as convergence (number of iterations taken by each formulation) and accuracy in presence of harmonic voltage distortion.

Chapter 5 compares the Newton-Raphson method versus the nonlinear least-squares methods for the numerical resolution of HLF problems. A three-bus AC network is considered and the numerical solution of its associated HLF problem is obtained by applying the different HLF formulations separately and by using both the Newton-Raphson method and the nonlinear least-squares methods separately too. The comparison is done by evaluating properties such as convergence (number of iterations taken by each formulation) and accuracy in presence of harmonic voltage distortion.

Chapter 6 is based on the conclusions drawn on the study of the research topic and is followed by suggestions for future work in Chapter 7. Finally, Chapter 8 constitutes the bibliography listing all the literature being consulted and produced during the completion of this thesis.

2. Harmonic load flow formulation

HLF formulation is a modification of FLF formulation which includes the harmonic voltages and the NLL state variables [14, 15]. Many HLF formulations in the literature strive to find a compromise between simplicity (to reduce numerical convergence problems) and reliability (to provide accurate results) [21]. In order to analyse the harmonic problem, the following variables must be included in harmonic load flow:

- Fundamental bus voltages
- Harmonic bus voltages
- Variables which define the nonlinear load state.

This chapter presents the main formulations, from the simplest to the most complicated, when in electric power systems only the following types of buses are considered: Slack bus ($i = 1$), power consumption buses (PQ buses) ($i = 2,\ldots,c$) and buses feeding NLLs (NL buses) ($i = c + 1,\ldots,n$). The absence of PV buses in electric power systems is assumed without loss of generality. The usual assumption that power consumption is mainly due to the fundamental voltage and current components, i.e., $\underline{S}_i \approx \underline{V}^1_i \cdot (\underline{I}^1_i)^*$, is made. Even harmonics are not taken into account in the study as they are negligible due to the voltage and current half-wave symmetry.

It must be noted that one of the main formulations, which is known as unified harmonic load flow and only focuses on HVDC converters, will be presented in Chapter 4 for didactic reasons.

2.1. Harmonic penetration

Harmonic penetration (HP) is the simplest frequency domain procedure [21], [22], [23]. This formulation considers that NLL behaviour depends only on the fundamental voltages and their own state variables (i.e., no harmonic interaction is assumed in NLL behaviour). This allows NLL equations which define NLL behaviour to be incorporated into FLF. Thus, the nonlinear equation system of the modified FLF (FLF_m) is derived from the FLF equations, where NLLs are treated as PQ loads by adding the NLL equations.

Let it be a network with n buses $(i = 1,2,\ldots,n)$: a Slack bus $(i = 1)$, a number of PQ buses $(i = 2,\ldots,c)$ and a number of NL buses $(i = c+1,\ldots,n)$. HP is illustrated in Figure 2.1 and its data and unknowns are summarised in Table 2.1.

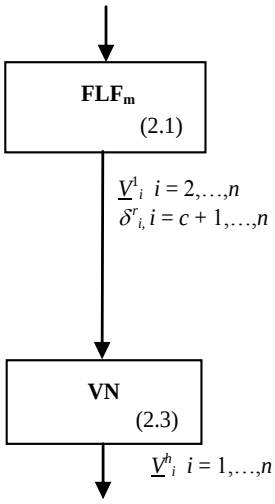

Figure 2.1: HP formulation flowchart

Stage	Bus	Data	Unknowns
FLF$_m$	Slack	$\underline{V}^1_1$	---
	PQ	P_i, Q_i (injected)	$\underline{V}^1_i$
	NL	D^m_i	$\underline{V}^1_i, \delta^r_i$
VN	Slack	X^1_1	$\underline{V}^h_1$
	PQ	$\underline{Y}^h_i = \underline{f}^h_{\underline{Y}_i}(V^1_i)$	$\underline{V}^h_i$
	NL	$\underline{I}^h_i$	$\underline{V}^h_i$

Table 2.1: HP formulation data and unknowns

The superscripts *r* and *m* are the indices of the NLL state variables and NLL data which define the NLL behaviour, respectively. Distorted voltages and currents will be expressed in terms of the summation of $k = 1,3,5,\ldots$ components: 1 is the fundamental component and $h = 3,5,7,\ldots$ are the harmonic components. The nonlinear equation system of the FLF$_m$ stage is

$$\begin{aligned}
&\underline{S}_i = \underline{V}^1_i \left(\sum_{j=1}^{n} \underline{Y}^1_{ij} \underline{V}^1_j \right)^* \qquad (i = 2,\ldots,c) \\
&\underline{V}^1_i (\underline{I}^1_i)^* = \underline{V}^1_i \left(\sum_{j=1}^{n} \underline{Y}^1_{ij} \underline{V}^1_j \right)^* \qquad (i = c+1,\ldots,n) \\
&nl^r_i (\underline{V}^1_i, \delta^r_i, D^m_i) = 0 \\
&(i = c+1,\ldots,n \;;\; r = 1,\ldots,r_{\max} \;;\; m = 1,\ldots,m_{\max}),
\end{aligned} \tag{2.1}$$

where $\underline{Y}^1_{ij}$ are the ij^{th} elements of the network fundamental admittance matrix $\mathbf{Y}^1_{\mathbf{B}}$, and $nl^r_i(\cdot) = 0$ represents the NLL equations. These equations depend on D^m_i (NLL data) and δ^r_i (NLL state variables). The NLL injected fundamental currents are expressed as

$$\underline{I}_i^1 = \underline{f}_i^1(\underline{V}_i^1, \delta_i^r, D_i^m)$$
$$(i = c+1,\ldots,n \ ; \ r = 1,\ldots,r_{\max} \ ; \ m = 1,\ldots,m_{\max}). \tag{2.2}$$

The numerical resolution of the equation system (2.1) provides the fundamental voltages $\underline{V}^1{}_i$ and the NLL state variables $\delta^r{}_i$ which are used to obtain the harmonic voltages $\underline{V}^h{}_i$ by the voltage node (VN) method. This method is based on the resolution of the linear system

$$\mathbf{Y}_\mathbf{B}^h \cdot \mathbf{V}_\mathbf{B}^h = \mathbf{I}_\mathbf{B}^h, \tag{2.3}$$

where the NLL injected harmonic currents $\underline{I}^h{}_i$ ($i = c + 1,\ldots,n$) and the Slack and PQ bus harmonic admittances $\underline{Y}^h{}_i$ ($i = 1,\ldots,c$) must be incorporated into the current vector $\mathbf{I}^h{}_\mathbf{B}$ and the network admittance matrix $\mathbf{Y}^h{}_\mathbf{B}$, respectively, and are determined as

$$\underline{I}_i^h = \underline{f}_i^h(\underline{V}_i^1, \delta_i^r, D_i^m)$$
$$(i = c+1,\ldots,n \ ; \ r = 1,\ldots,r_{\max} \ ; \ m = 1,\ldots,m_{\max})$$
$$\underline{Y}_1^h = \frac{1}{R_1 + j \cdot h \cdot X_1^1} \quad ; \quad R_1 \approx \frac{X_1^1}{20} \tag{2.4}$$
$$\underline{Y}_i^1 = \frac{-\underline{S}_i^*}{(V_i^1)^2} = \underline{f}_{Yi}^1(V_i^1) \quad ; \quad \underline{Y}_i^h = \underline{F}_{Yi}^h(\underline{Y}_i^1) \Rightarrow \underline{Y}_i^h = \underline{f}_{Yi}^h(V_i^1)$$
$$(i = 2,\ldots,c).$$

It must be noted that an X / R ratio equal to 20 is assumed in (2.4) for the Slack bus fundamental impedance.

This formulation allows the HLF problem to be tackled in a simple way, as with the FLF problem, but NLL sensitiveness to harmonic voltages could result in overestimation of the NLL polluting effect if harmonic voltage distortion is high.

2.2. Simplified harmonic load flow

Simplified harmonic load flow (SHLF) performs a fixed-point iteration method on a set of two nonlinear equation systems (labelled as N_1 and N_2) which are solved separately and in sequence by applying some iterative numerical method to each of them (see Figure 2.2) [21], [26], [27].

In a first stage, FLF_m is performed to obtain the fundamental voltages at all network buses and the NLL state variables. In order to integrate nonlinear loads into FLF_m, they are introduced as PQ loads. Subsequently, in a second stage, Harmonic Analysis (HA) is applied to obtain the fundamental and harmonic voltages at nonlinear buses and the NLL state variables. In HA stage, the network is reduced to nonlinear buses by using the Thévenin equivalent circuit at these buses. This enables to consider the harmonic interaction in nonlinear load behaviour.

After the performance of both stages, convergence is checked by comparing the fundamental voltages of FLF_m and HA at nonlinear buses. If the difference between voltages is smaller than a tolerance, the process is stopped and the fundamental voltages at all network buses, the harmonic voltages at nonlinear buses and the NLL state variables are those of the current iteration. Finally, the harmonic voltages at linear buses are obtained by the VN method (see Figure 2.2).

Let it be a network with n buses $(i = 1, 2, \ldots, n)$: a Slack bus $(i = 1)$, a number of PQ buses $(i = 2, \ldots, c)$ and a number of NL buses $(i = c+1, \ldots, n)$. SHLF is illustrated in Figure 2.2 and its data and unknowns are summarised in Table 2.2.

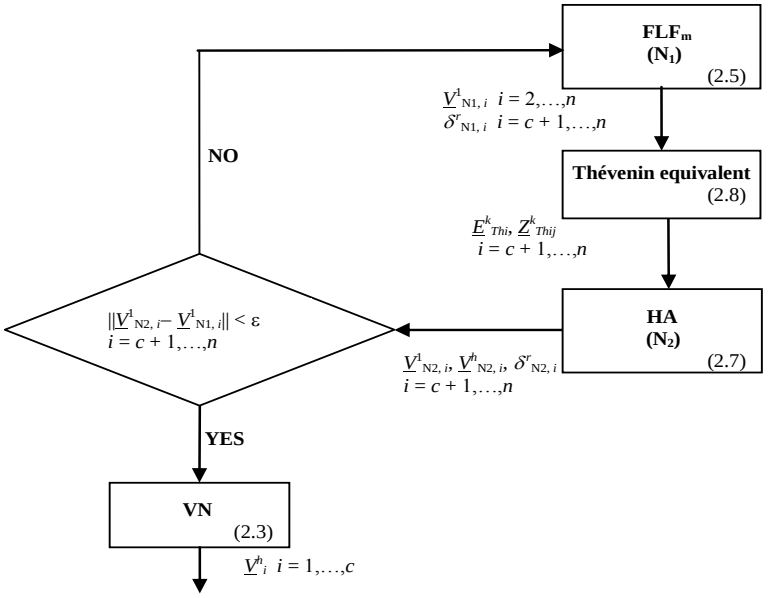

Figure 2.2: SHLF formulation flowchart

Stage	Bus	Data	Unknowns
FLF_m (N_1)	Slack	$\underline{V}^1_1$	---
	PQ	P_i, Q_i (injected)	$\underline{V}^1_{N_1,i}$
	NL	$\underline{V}^h_{N_2,i}, D^m_i$	$\underline{V}^1_{N_1,i}, \delta^r_{N_1,i}$
HA (N_2)	Slack	$\underline{V}^1_1, X^1_1$	---
	PQ	$\underline{Y}^k_i = \underline{f}^k_{Y_i}(V^1_{N_1,i})$	---
	NL	D^m_i	$\underline{V}^1_{N_2,i}, \underline{V}^h_{N_2,i}, \delta^r_{N_2,i}$
VN	Slack	X^1_1	$\underline{V}^h_1$
	PQ	$\underline{Y}^h_i = \underline{f}^h_{Y_i}(V^1_{N_1,i})$	$\underline{V}^h_i$
	NL	$\underline{I}^h_i$	---

Table 2.2: SHLF formulation data and unknowns

The superscripts *r* and *m* are the indices of the NLL state variables and NLL data which define the NLL behaviour, respectively. Distorted voltages and currents will be expressed in terms of the summation of $k = 1,3,5,\ldots$ components: 1 is the fundamental component and $h = 3,5,7,\ldots$ are the harmonic components.

The first nonlinear equation system N_1 is the FLF_m in HP considering NLL harmonic interaction, i.e.,

$$\begin{aligned}
&\underline{S}_i = \underline{V}^1_{\mathrm{N}_1,i}\left(\sum_{j=1}^{n}\underline{Y}^1_{ij}\underline{V}^1_{\mathrm{N}_1,j}\right)^* \qquad (i = 2,\ldots,c)\\
&\underline{V}^1_{\mathrm{N}_1,i}(\underline{I}^1_i)^* = \underline{V}^1_{\mathrm{N}_1,i}\left(\sum_{j=1}^{n}\underline{Y}^1_{ij}\underline{V}^1_{\mathrm{N}_1,j}\right)^* \qquad (i = c+1,\ldots,n)\\
&nl^r_i(\underline{V}^1_{\mathrm{N}_1,i}, \underline{V}^h_{\mathrm{N}_2,i}, \delta^r_{\mathrm{N}_1,i}, D^m_i) = 0\\
&(i = c+1,\ldots,n \;;\; r = 1,\ldots,r_{\max} \;;\; m = 1,\ldots,m_{\max}),
\end{aligned} \tag{2.5}$$

where the NLL injected fundamental currents are expressed as

$$\begin{aligned}
&\underline{I}^1_i = \underline{f}^1_i(\underline{V}^1_{\mathrm{N}_1,i}, \underline{V}^h_{\mathrm{N}_2,i}, \delta^r_{\mathrm{N}_1,i}, D^m_i)\\
&(i = c+1,\ldots,n \;;\; r = 1,\ldots,r_{\max} \;;\; m = 1,\ldots,m_{\max}).
\end{aligned} \tag{2.6}$$

Note that, although harmonic interaction is assumed in NLL behaviour, the harmonic voltages $\underline{V}^h{}_{\mathrm{N2},i}$ in the NLL functions $nl^r{}_i(\cdot) = 0$ and $\underline{I}^1{}_i = \underline{f}^1{}_i(\cdot)$ are data from the second nonlinear equation system N_2, where these variables are unknowns. Thus, the numerical resolution of (2.5) provides the fundamental voltages $\underline{V}^1{}_{\mathrm{N1},i}$ and the NLL state variables $\delta^r{}_{\mathrm{N1},i}$ which are used in the second nonlinear equation system.

Once (2.5) is solved, the linear network with the Slack and PQ buses (linear buses) is represented by its generalized Thévenin equivalent circuits "observed" from the NL buses [27]. The second nonlinear equation system N_2 is built by considering as unknowns only those of the NL buses. Its equations are based on Kirchhoff's second law applied to the fundamental and harmonic Thévenin equivalent circuits, and the NLL equations which define the NLL behaviour, i.e.,

$$\begin{aligned}
&\underline{V}^k_{\mathrm{N}_2,i} = \underline{E}^k_{Thi} + \sum_{j=c+1}^{n}\underline{Z}^k_{Thij}\underline{I}^k_i \qquad (i = c+1,\ldots,n)\\
&nl^r_i(\underline{V}^1_{\mathrm{N}_2,i}, \underline{V}^h_{\mathrm{N}_2,i}, \delta^r_{\mathrm{N}_2,i}, D^m_i) = 0\\
&(i = c+1,\ldots,n \;;\; r = 1,\ldots,r_{\max} \;;\; m = 1,\ldots,m_{\max}),
\end{aligned} \tag{2.7}$$

where the NLL fundamental and harmonic Thévenin equivalent circuit parameters and injected currents are expressed as

$$
\begin{aligned}
&\underline{E}^{k}_{Thi} = \underline{f}^{k}_{EThi}(\underline{V}^{1}_{\mathrm{N}_1,l}) \quad ; \quad \underline{Z}^{k}_{Thij} = \underline{f}^{k}_{ZThij}(\underline{V}^{1}_{\mathrm{N}_1,l}) \\
&(i = c+1,\ldots,n \ ; \ j = c+1,\ldots,n \ ; \ l = 2,\ldots,c) \\
&\underline{I}^{k}_{i} = \underline{f}^{k}_{i}(\underline{V}^{1}_{\mathrm{N}_2,i}, \underline{V}^{h}_{\mathrm{N}_2,i}, \delta^{r}_{\mathrm{N}_2,i}, D^{m}_{i}) \\
&(i = c+1,\ldots,n \ ; \ r = 1,\ldots,r_{\max} \ ; \ m = 1,\ldots,m_{\max}).
\end{aligned}
\tag{2.8}
$$

Note that the PQ bus fundamental voltages $\underline{V}^{1}_{\mathrm{N1},\,l}$ in the Thévenin equivalent circuit functions $\underline{E}^{k}_{Thi} = \underline{f}^{k}_{EThi}(\cdot)$ and $\underline{Z}^{k}_{Thij} = \underline{f}^{k}_{ZThij}(\cdot)$ are data from the first nonlinear equation system N_1, where these variables are unknowns. The numerical resolution of (2.7) provides the fundamental and harmonic voltages $\underline{V}^{k}_{\mathrm{N2},\,i}$ at NL buses and the NLL state variables $\delta^{r}_{\mathrm{N2},\,i}$. Convergence of the fixed-point iteration algorithm is checked by comparing the fundamental voltages at the NL buses obtained from the first and second nonlinear equation systems (i.e., $\underline{V}^{1}_{\mathrm{N1},\,i}$ and $\underline{V}^{1}_{\mathrm{N2},\,i}$). If convergence is reached, the VN method (2.3) is applied to determine the harmonic voltages $\underline{V}^{h}_{i}$ of the Slack and PQ buses. Otherwise, a new fixed-point iteration is made by using the results of (2.7) in the first nonlinear equation system.

This formulation takes into consideration the harmonic voltage influence on NLL behaviour without introducing the harmonic voltages at the Slack and PQ buses as unknowns of the nonlinear equations. However, it could pose convergence problems depending on the degree of decoupling between the two nonlinear equation systems (2.5) and (2.7).

2.3. Complete harmonic load flow

Complete harmonic load flow (CHLF) is a natural modification of FLF where NLL treatment and harmonic voltage calculation are included considering harmonic interaction in NLL behaviour. It is based on the simultaneous resolution of power equations at the PQ buses and harmonic current balance at the Slack and PQ buses, together with fundamental and harmonic current balance and NLL equations at the NL buses [21], [28 - 30].

How power is considered in power equations leads to two possible CHLF formulations.

2.3.1. Power consideration at fundamental frequency

The resulting CHLF formulation, called $\mathrm{CHLF_F}$, allows the resolution of the HLF problem to be reached by considering power only at fundamental frequency in power equations.

Let it be a network with n buses $(i = 1,2,\ldots,n)$: a Slack bus $(i = 1)$, a number of PQ buses $(i = 2,\ldots,c)$ and a number of NL buses $(i = c+1,\ldots,n)$. $\mathrm{CHLF_F}$ is illustrated in Figure 2.3 and its data and unknowns are summarised in Table 2.3.

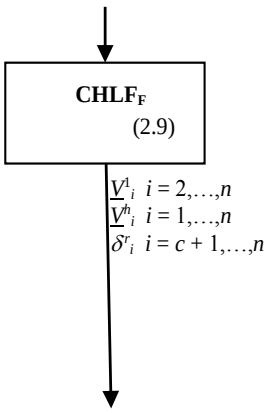

Figure 2.3: CHLF$_F$ formulation flowchart

Stage	Bus	Data	Unknowns
CHLF$_F$	Slack	$\underline{V}^1_1, X^1_1$	$\underline{V}^h_1$
	PQ	P_i, Q_i (injected)	$\underline{V}^1_i, \underline{V}^h_i$
	NL	D^m_i	$\underline{V}^1_i, \underline{V}^h_i, \delta^r_i$

Table 2.3: CHLF$_F$ formulation data and unknowns

The superscripts r and m are the indices of the NLL state variables and NLL data which define the NLL behaviour, respectively. Distorted voltages and currents will be expressed in terms of the summation of $k = 1,3,5,\ldots$ components: 1 is the fundamental component and $h = 3,5,7,\ldots$ are the harmonic components.

The nonlinear equation system of CHLF$_F$ is

$$\begin{aligned}
&\underline{S}_i = \underline{V}^1_i \left(\sum_{j=1}^{n} \underline{Y}^1_{ij} \underline{V}^1_j \right)^* \qquad (i = 2,\ldots,c) \\
&-\underline{Y}^h_i \underline{V}^h_i = \sum_{j=1}^{n} \underline{Y}^h_{ij} \underline{V}^h_j \qquad (i = 1,\ldots,c) \\
&\underline{I}^k_i = \sum_{j=1}^{n} \underline{Y}^k_{ij} \underline{V}^k_j \qquad (i = c+1,\ldots,n) \\
&nl^r_i (\underline{V}^1_i, \underline{V}^h_i, \delta^r_i, D^m_i) = 0 \\
&(i = c+1,\ldots,n \;;\; r = 1,\ldots,r_{\max} \;;\; m = 1,\ldots,m_{\max}),
\end{aligned} \tag{2.9}$$

where $\underline{Y}^k_{ij}$ are the ij^{th} elements of the network fundamental and harmonic admittance matrix $\mathbf{Y}^k_{\mathbf{B}}$, and $\underline{Y}^h_i$ are the Slack and PQ bus harmonic admittances (2.4). The NLL injected fundamental and harmonic currents are expressed as

$$\begin{aligned}
&\underline{I}^k_i = \underline{f}^k_i (\underline{V}^1_i, \underline{V}^h_i, \delta^r_i, D^m_i) \\
&(i = c+1,\ldots,n \;;\; r = 1,\ldots,r_{\max} \;;\; m = 1,\ldots,m_{\max}).
\end{aligned} \tag{2.10}$$

This formulation allows the HLF problem to be tackled as a single nonlinear equation system where the harmonic voltages at the Slack and PQ buses are also included as unknowns. This increases the number of unknowns to be determined significantly, which can result in a degradation of the convergence properties characterising numerical resolution methods.

2.3.2. Power consideration at fundamental and harmonic frequencies

The resulting CHLF formulation, called $CHLF_H$, allows the resolution of the HLF problem to be reached by considering power at fundamental and harmonic frequencies in power equations. The usual assumption that power consumption is mainly due to the fundamental voltage and current components is not made.

Let it be a network with n buses $(i = 1, 2, \ldots, n)$: a Slack bus $(i = 1)$, a number of PQ buses $(i = 2, \ldots, c)$ and a number of NL buses $(i = c+1, \ldots, n)$. $CHLF_H$ is illustrated in Figure 2.4 and its data and unknowns are summarised in Table 2.4.

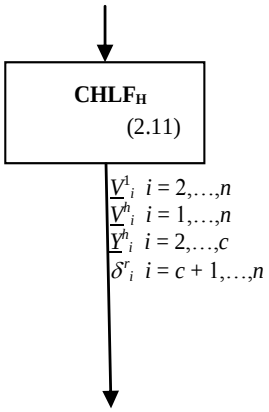

Figure 2.4: $CHLF_H$ formulation flowchart

Stage	Bus	Data	Unknowns
$CHLF_H$	Slack	$\underline{V}_1^1, X_1^1$	$\underline{V}_1^h$
	PQ	P_i, Q_i (injected)	$\underline{V}_i^1, \underline{V}_i^h, \underline{Y}_i^h$
	NL	D_i^m	$\underline{V}_i^1, \underline{V}_i^h, \delta_i^r$

Table 2.4: $CHLF_H$ formulation data and unknowns

The superscripts r and m are the indices of the NLL state variables and NLL data which define the NLL behaviour, respectively. Distorted voltages and currents will be expressed in terms of the summation of $k = 1, 3, 5, \ldots$ components: 1 is the fundamental component and $h = 3, 5, 7, \ldots$ are the harmonic components.

The nonlinear equation system of $CHLF_H$ is

$$
\begin{aligned}
&\underline{S}_i = \sum_{k=1}^{3,5,\ldots} \underline{V}_i^k \left(\sum_{j=1}^{n} \underline{Y}_{ij}^k \underline{V}_j^k \right)^* \qquad (i = 2,\ldots,c) \\
&-\underline{S}_i = \sum_{k=1}^{3,5,\ldots} \left(\underline{Y}_i^k \right)^* \cdot \left(V_i^k \right)^2 \qquad (i = 2,\ldots,c) \\
&-\underline{Y}_i^h \underline{V}_i^h = \sum_{j=1}^{n} \underline{Y}_{ij}^h \underline{V}_j^h \qquad (i = 1,\ldots,c) \\
&\underline{I}_i^k = \sum_{j=1}^{n} \underline{Y}_{ij}^k \underline{V}_j^k \qquad (i = c+1,\ldots,n) \\
&nl_i^r (\underline{V}_i^1, \underline{V}_i^h, \delta_i^r, D_i^m) = 0 \\
&(i = c+1,\ldots,n \;;\; r = 1,\ldots,r_{\max} \;;\; m = 1,\ldots,m_{\max}),
\end{aligned}
\tag{2.11}
$$

where $\underline{Y}^k_{ij}$ are the ij^{th} elements of the network fundamental and harmonic admittance matrix $\mathbf{Y}^k_{\mathbf{B}}$, and $\underline{Y}^h_i$ are the Slack and PQ bus harmonic admittances (2.4). The NLL injected fundamental and harmonic currents are expressed as

$$
\begin{aligned}
&\underline{I}_i^k = \underline{f}_i^k (\underline{V}_i^1, \underline{V}_i^h, \delta_i^r, D_i^m) \\
&(i = c+1,\ldots,n \;;\; r = 1,\ldots,r_{\max} \;;\; m = 1,\ldots,m_{\max}).
\end{aligned}
\tag{2.12}
$$

Similarly to CHLF_F, this formulation allows the HLF problem to be tackled as a single nonlinear equation system where the harmonic voltages at the Slack and PQ buses are also included as unknowns. However, additional unknowns must be determined: the PQ bus harmonic admittances.

3. Numerical methods for harmonic load flow resolution

HLF calculation can be regarded as the resolution of a nonlinear equation system formulated as a set of q equations in q unknowns $F(x) = 0$:

$$\left\{ f_i\left(x_1, x_2, \ldots, x_q\right) = 0 \quad (i = 1, \ldots, q). \right. \tag{3.1}$$

The numerical resolution of this system provides the fundamental and harmonic bus voltages and the NLL state variables. Multiple solutions are mathematically possible for the above nonlinear equation system, but usually only one is physically admissible. Several numerical methods can solve this system, among which Newton-Raphson is the most widely used in the bibliography. Fixed-point iteration methods, such as the Gauss-Seidel method, can also be used but have poorer convergence properties. The SHLF formulation is an example of these iterative approaches.

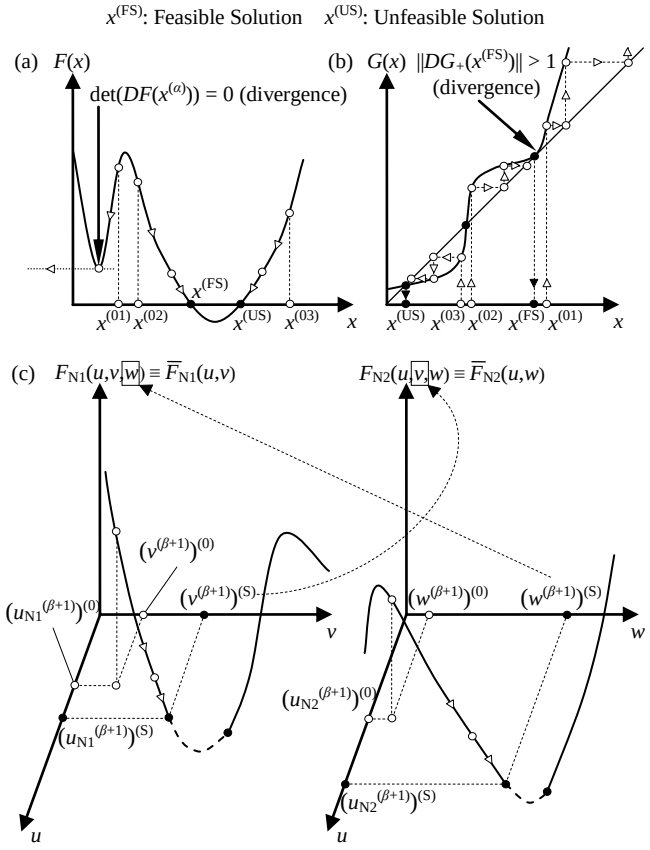

Figure 3.1: Numerical methods: (a) Newton-Raphson method. (b) Fixed-point iteration method. (c) Iteration β+1 of SHLF fixed-point iteration method.

3.1. Newton-Raphson method

The Newton-Raphson method can be algorithmically expressed as

$$x^{(\alpha+1)} = x^{(\alpha)} - DF^{-1}(x^{(\alpha)}) \cdot F(x^{(\alpha)}), \tag{3.2}$$

which is applied from the initial value $x^{(0)}$ to the problem solution $x^{(S)}$, with $DF(x)$ being the Jacobian matrix of the nonlinear equation system and α+1 the Newton-Raphson iteration. The Jacobian matrix is called true Jacobian matrix if it is calculated for all iterations, whereas it is called constant Jacobian matrix if it is only calculated for the first iteration, remaining unchanged for the rest of iterations. Algorithm convergence can be checked from the conditions $||F(x^{(\alpha+1)})|| < \varepsilon$ or $||x^{(\alpha+1)} - x^{(\alpha)}|| < \varepsilon$, where ε is a fixed error. The main drawback of this method is that convergence to the problem solution is only assured if the initial value is close to the solution and $\det(DF(x^{(\alpha)})) \neq 0$ for all $x^{(\alpha)}$. Otherwise (more likely in HLF than in FLF due to initial values of harmonic voltages far from the solution), it can lead to divergence or an unfeasible solution. This is illustrated in Figure 3.1(a). If the initial value is $x^{(01)}$, there exists a value $x^{(\alpha)}$ where $\det(DF(x^{(\alpha+1)})) = 0$, and this may cause divergence. When the initial value is $x^{(02)}$, convergence to the feasible solution $x^{(FS)}$ may occur because $x^{(02)}$ is close to $x^{(FS)}$ and $\det(DF(x^{(\alpha)})) \neq 0$ for all $x^{(\alpha)}$. However, if the initial value is $x^{(03)}$, convergence to an unfeasible solution $x^{(US)}$ may occur because $x^{(03)}$ is closer to $x^{(US)}$ than to $x^{(FS)}$.

There are also modified Newton-Raphson methods [33, 39] which consist of the iteration process of the algorithm

$$x^{(\alpha+1)} = x^{(\alpha)} - \lambda^{(\alpha)} DF^{-1}(x^{(\alpha)}) \cdot F(x^{(\alpha)}). \tag{3.3}$$

The Newton-Raphson method is included in (3.3) when a factor $\lambda^{(\alpha)} = 1$ is chosen for all iterations. The Newton-Raphson method converges to the correct solution quickly if the initial value is close to the solution, but a bad choice of the initial value may lead the algorithm to diverge or face convergence problems. The modified Newton-Raphson method uses the damping factor $\lambda^{(\alpha)}$ to reduce the significance of the term

$$DF^{-1}(x^{(\alpha)}) \cdot F(x^{(\alpha)}). \tag{3.4}$$

This in turn avoids the large jumps being caused by Newton-Raphson method in the iterative process thereby improving the overall convergence of the algorithm.

There are many ways in the literature to define a value for the damping factor [39], but the most commonly used term is

$$\lambda^{(\alpha)} = \frac{1}{2^{n^{(\alpha)}}}. \tag{3.5}$$

The parameter $n^{(\alpha)}$ is calculated starting from $n^{(0)} = 0$ and in such a way that the term $\left\|F(x^{(\alpha)})\right\|$ will be strictly decreasing, i.e., $\left\|F(x^{(\alpha)})\right\| > \left\|F(x^{(\alpha+1)})\right\|$.

3.2. Fixed-point iteration method

The nonlinear equation system $F(x) = 0$ can occasionally be reformulated as a set of q equations in q unknowns $x = G(x)$:

$$\left\{x_i = g_i\left(x_1, x_2, \ldots, x_q\right) \qquad (i = 1, \ldots, q). \right. \tag{3.6}$$

Most fixed-point iteration methods can be algorithmically expressed as

$$x^{(\beta+1)} = G(x^{(\beta)}), \tag{3.7}$$

which is applied from the initial value $x^{(0)}$ to the problem solution $x^{(S)}$, with $G(x)$ being a nonlinear equation system derived from $F(x)$ and β+1 the fixed-point iteration. Algorithm convergence is checked from the condition $||x^{(\beta+1)} - x^{(\beta)}|| < \varepsilon$, where ε is a fixed error. The main drawback of this method is that convergence to the problem solution is only assured if the initial value is close to the solution and $||DG(x^{(S)})|| < 1$. Otherwise, it can lead to divergence or an unfeasible solution. This is illustrated in Figure 3.1(b). If the initial value is $x^{(01)}$, then $||DG_{+}(x^{(FS)})|| > 1$, and this causes divergence. When the initial value is $x^{(02)}$, convergence to the feasible solution $x^{(FS)}$ occurs because $x^{(02)}$ is close to $x^{(FS)}$ and $||DG_{-}(x^{(FS)})|| < 1$. However, if the initial value is $x^{(03)}$, convergence to an unfeasible solution $x^{(US)}$ occurs because $x^{(03)}$ is closer to $x^{(US)}$ than to $x^{(FS)}$.

One of the main fixed-point iteration methods is the Gauss-Seidel method, whose associated algorithm is

$$\left\{x_i^{(\beta+1)} = g_i\left(x_1^{(\beta+1)}, \ldots, x_{i-1}^{(\beta+1)}, x_i^{(\beta+1)} \ldots, x_q^{(\beta)}\right) \qquad (i = 1, \ldots, q). \right. \tag{3.8}$$

At each fixed-point iteration β+1, the equations of (3.8) are used separately and in sequence. Thus, $g_1(\cdot)$ allows $x_1^{(\beta+1)}$ to be obtained, $g_2(\cdot)$ allows $x_2^{(\beta+1)}$ to be obtained, and so on.

If it is not possible to reformulate the nonlinear equation system $F(x) = 0$ as $x = G(x)$, the previous algorithm must be rewritten as follows:

$$\left\{f_i\left(x_1^{(\beta+1)}, \ldots, x_i^{(\beta+1)}, x_{i+1}^{(\beta)}, \ldots, x_q^{(\beta)}\right) = 0 \qquad (i = 1, \ldots, q). \right. \tag{3.9}$$

At each fixed-point iteration β+1, the equations of (3.9) are solved separately and in sequence by applying some iterative numerical method to each of them. Thus, the numerical resolution of

$f_1(\cdot) = 0$ allows $x_1^{(\beta+1)}$ to be obtained, the numerical resolution of $f_2(\cdot) = 0$ allows $x_2^{(\beta+1)}$ to be obtained, and so on.

3.3. Simplified harmonic load flow fixed-point iteration method

The fixed-point iteration method of SHLF formulation can be regarded as the application of the Gauss-Seidel method to a set of two nonlinear equation systems:

$$\begin{cases} F_{\mathrm{N}_1}(u, v, w) = 0 \\ F_{\mathrm{N}_2}(u, v, w) = 0 \end{cases}. \tag{3.10}$$

The Gauss-Seidel method is applied to (3.10) by using the following algorithm:

$$\begin{cases} F_{\mathrm{N}_1}\left(u_{\mathrm{N}_1}^{(\beta+1)}, v^{(\beta+1)}, w^{(\beta)}\right) = 0 \\ F_{\mathrm{N}_2}\left(u_{\mathrm{N}_2}^{(\beta+1)}, v^{(\beta+1)}, w^{(\beta+1)}\right) = 0 \end{cases}. \tag{3.11}$$

At each fixed-point iteration β+1, the nonlinear equation systems of (3.11) are solved separately and in sequence by applying the Newton-Raphson method to each of them (see Figure 3.1(c)). Thus, the numerical resolution of $F_{\mathrm{N1}}(\cdot) = 0$ allows $v^{(\beta+1)}$ (and $u_{\mathrm{N1}}^{(\beta+1)}$) to be obtained by applying the iterative scheme

$$\begin{cases} x_{\mathrm{N}_1} = \begin{bmatrix} u & v \end{bmatrix}^T \;;\; \left(x_{\mathrm{N}_1}^{(\beta+1)}\right)^{(0)} = \left[\left(u_{\mathrm{N}_2}^{(\beta)}\right)^{(\mathrm{S})} \left(v^{(\beta)}\right)^{(\mathrm{S})}\right]^T \\ \left(x_{\mathrm{N}_1}^{(\beta+1)}\right)^{(\alpha+1)} = \left(x_{\mathrm{N}_1}^{(\beta+1)}\right)^{(\alpha)} - D\bar{F}_{\mathrm{N}_1}^{-1}\left(\left(x_{\mathrm{N}_1}^{(\beta+1)}\right)^{(\alpha)}\right)\bar{F}_{\mathrm{N}_1}\left(\left(x_{\mathrm{N}_1}^{(\beta+1)}\right)^{(\alpha)}\right) \end{cases}, \tag{3.12}$$

the numerical resolution of $F_{\mathrm{N2}}(\cdot) = 0$ allows $w^{(\beta+1)}$ (and $u_{\mathrm{N2}}^{(\beta+1)}$) to be obtained by applying the iterative scheme

$$\begin{cases} x_{\mathrm{N}_2} = \begin{bmatrix} u & w \end{bmatrix}^T \;;\; \left(x_{\mathrm{N}_2}^{(\beta+1)}\right)^{(0)} = \left[\left(u_{\mathrm{N}_1}^{(\beta+1)}\right)^{(\mathrm{S})} \left(w^{(\beta)}\right)^{(\mathrm{S})}\right]^T \\ \left(x_{\mathrm{N}_2}^{(\beta+1)}\right)^{(\alpha+1)} = \left(x_{\mathrm{N}_2}^{(\beta+1)}\right)^{(\alpha)} - D\bar{F}_{\mathrm{N}_2}^{-1}\left(\left(x_{\mathrm{N}_2}^{(\beta+1)}\right)^{(\alpha)}\right)\bar{F}_{\mathrm{N}_2}\left(\left(x_{\mathrm{N}_2}^{(\beta+1)}\right)^{(\alpha)}\right) \end{cases}, \tag{3.13}$$

and so on.

Section 2.2 identifies the unknowns u_{N1}, u_{N2}, v and w with those of SHLF formulation:

$$
\begin{aligned}
&u_{\mathrm{N}_1} = \left(u_{\mathrm{N}_1,\mathrm{I}}, u_{\mathrm{N}_1,\mathrm{II}}\right) = \left(\underline{V}^1_{\mathrm{N}_1,i}, \delta^r_{\mathrm{N}_1,i}\right) \\
&(i = c+1,\ldots,n \ ; \ r = 1,\ldots,r_{\max}) \\
&u_{\mathrm{N}_2} = \left(u_{\mathrm{N}_2,\mathrm{I}}, u_{\mathrm{N}_2,\mathrm{II}}\right) = \left(\underline{V}^1_{\mathrm{N}_2,i}, \delta^r_{\mathrm{N}_2,i}\right) \\
&(i = c+1,\ldots,n \ ; \ r = 1,\ldots,r_{\max}) \\
&v = \underline{V}^1_{\mathrm{N}_1,i} \qquad (i = 2,\ldots,c) \\
&w = \underline{V}^h_{\mathrm{N}_2,i} \qquad (i = c+1,\ldots,n).
\end{aligned}
\tag{3.14}
$$

Instead of the usual condition to check fixed-point iteration algorithm convergence

$$
\left\| \left(v^{(\beta+1)}, w^{(\beta+1)}\right) - \left(v^{(\beta)}, w^{(\beta)}\right) \right\| < \varepsilon, \tag{3.15}
$$

where ε is a fixed error, an alternative condition is used to check SHLF fixed-point iteration algorithm convergence:

$$
\left\| u^{(\beta+1)}_{\mathrm{N}_2,\mathrm{I}} - u^{(\beta+1)}_{\mathrm{N}_1,\mathrm{I}} \right\| < \varepsilon. \tag{3.16}
$$

Convergence problems associated with the SHLF fixed-point iteration method are similar to those of the fixed-point iteration method described in Section 3.2.

3.4. A minimization approach: nonlinear least-squares methods

The nonlinear equation system is of the form

$$
\begin{cases}
f_1\left(x_1, x_2, \ldots, x_n\right) = 0 \\
f_2\left(x_1, x_2, \ldots, x_n\right) = 0 \\
\qquad \vdots \\
f_n\left(x_1, x_2, \ldots, x_n\right) = 0
\end{cases}, \tag{3.17}
$$

in which the function F has the range

$$
\begin{aligned}
&\mathbf{F} : R^n \to R^n \\
&\mathbf{X} \mapsto \mathbf{F}\left(\mathbf{X}\right)
\end{aligned}
\tag{3.18}
$$

where

$$
\mathbf{X} = \begin{pmatrix} x_1 \\ x_2 \\ \vdots \\ x_n \end{pmatrix} \quad \text{and} \quad \mathbf{F}\left(\mathbf{X}\right) = \begin{pmatrix} f_1\left(x_1, x_2, \ldots, x_n\right) \\ f_2\left(x_1, x_2, \ldots, x_n\right) \\ \vdots \\ f_n\left(x_1, x_2, \ldots, x_n\right) \end{pmatrix}.
$$

The values of **X** for which the nonlinear equation system (3.17) is satisfied are called solutions of **F(X)**

$$\mathbf{F}(\mathbf{X}) = \mathbf{0}. \tag{3.19}$$

There are numerous mathematically correct solutions which satisfy (3.17), but we are looking for a physically possible solution through numerical resolution of the nonlinear equation system.

Harmonic load flow formulations usually comprise of nonlinear equation systems in which the number of unknowns is equal to the number of equations, so they can be categorized as determined systems. If we opt for a starting point which is sufficiently close to the solution, then Newton-Raphson method can be a good selection for the numerical resolution of the harmonic load flow problem. The main advantages for using this method are rapid convergence and simplicity of the numerical method. The algorithm for the *m*-th iteration (*m*) is

$$\mathbf{X}^{(m+1)} = \mathbf{X}^{(m)} - \left(\mathbf{JF}\left(\mathbf{X}^{(m)}\right)\right)^{-1} \cdot \mathbf{F}\left(\mathbf{X}^{(m)}\right), \tag{3.20}$$

where

$$\mathbf{JF}(\mathbf{X}) = \begin{pmatrix} \frac{\partial f_1}{\partial x_1}(\mathbf{X}) & \frac{\partial f_1}{\partial x_2}(\mathbf{X}) & \cdots & \frac{\partial f_1}{\partial x_n}(\mathbf{X}) \\ \frac{\partial f_2}{\partial x_1}(\mathbf{X}) & \frac{\partial f_2}{\partial x_2}(\mathbf{X}) & \cdots & \frac{\partial f_2}{\partial x_n}(\mathbf{X}) \\ \vdots & \vdots & \ddots & \vdots \\ \frac{\partial f_n}{\partial x_1}(\mathbf{X}) & \frac{\partial f_n}{\partial x_2}(\mathbf{X}) & \cdots & \frac{\partial f_n}{\partial x_n}(\mathbf{X}) \end{pmatrix}$$ is the Jacobian matrix of function **F(X).**

MATLAB has been used as a software tool for the creation of a custom developed program to analyse the harmonic formulations and the electrical network example proposed in Chapter 4. This software tool provides a built-in calculation routine '*fsolve*' [44] for the numerical resolution of the nonlinear equation system by optimization techniques (applying the Gauss-Newton method by default). However, the software does not have a built-in calculation routine for applying the Newton-Raphson method, which seems surprising, as Newton-Raphson is the most commonly used method for the numerical resolution of these types of problems due to its simplicity of implementation.

There is always a possibility of implementing the method by oneself as done in this thesis memory to get results of different HLF formulations for comparison purposes. One logical explanation of not having a built-in calculation routine is that the Gauss-Newton method becomes the Newton-Raphson method when it is close to the solution sought. Taking into account, as already mentioned, that for each one of nonlinear equation systems that are intended

to be solved we will try to have a starting point sufficiently close to its solution, using '*fsolve*' applying the Gauss-Newton method is equivalent in these conditions to apply the Newton-Raphson method.

In order to justify the explanation given in the above paragraphs, we are going to discuss briefly the theoretical foundations of optimization techniques applied to the numerical resolution of nonlinear equation systems keeping in view specially the Gauss-Newton method.

In general, it is usually less computationally expensive to find the minimum of a scalar function of several variables (linear or nonlinear) than to find solutions of a nonlinear equation system defined by a vector function of several variables. This advantage, together with the fact that through minimization of a certain scalar function of several variables one can find solutions for both determined and overdetermined nonlinear equation systems, prompts the use of optimization for all these type of problems.

Specifically, the optimization problem that arises to deal with nonlinear equation systems of type (3.17) is

$$[\text{MIN}]\ S\left(x_1, x_2, \ldots, x_n\right) = \sum_{i=1}^{n} \left(f_i\left(x_1, x_2, \ldots, x_n\right)\right)^2 \tag{3.21}$$

(known as the nonlinear least-squares problem), the solution sought from any of these systems being the point $\mathbf{X}^*$ at which the function S associated with the system presents its global or absolute minimum. At this point, this function S must vanish, since it is a determined nonlinear equation system.

To solve numerically the proposed optimization problem, the Gauss-Newton method (belonging to the family of quasi-Newton methods) can be applied. This method is based on the fact that the point at which S presents its global minimum can be seen as the point at which the gradient of S equals zero, i.e., $\mathbf{X}^*$ is such that

$$\vec{\nabla} S\left(\mathbf{X}^*\right) = \begin{pmatrix} \dfrac{\partial S}{\partial x_1}\left(\mathbf{X}^*\right) \\ \dfrac{\partial S}{\partial x_2}\left(\mathbf{X}^*\right) \\ \vdots \\ \dfrac{\partial S}{\partial x_n}\left(\mathbf{X}^*\right) \end{pmatrix} = 0. \tag{3.22}$$

Newton-Raphson method can be applied to solve $\vec{\nabla} S\left(\mathbf{X}\right) = 0$. The expression of the algorithm for the optimization problem will be

$$\mathbf{X}^{(m+1)} = \mathbf{X}^{(m)} - \left(\mathbf{H}S\left(\mathbf{X}^{(m)}\right)\right)^{-1} \cdot \vec{\nabla} S\left(\mathbf{X}^{(m)}\right), \tag{3.23}$$

where $\mathbf{H}S(\mathbf{X})$ is the Hessian matrix of S and is given as

$$\mathbf{H}S(\mathbf{X}) = \mathbf{J}\left(\vec{\nabla} S(\mathbf{X})\right) = \begin{pmatrix} \frac{\partial^2 S}{\partial x_1^2}(\mathbf{X}) & \frac{\partial^2 S}{\partial x_1 \partial x_2}(\mathbf{X}) & \cdots & \frac{\partial^2 S}{\partial x_1 \partial x_n}(\mathbf{X}) \\ \frac{\partial^2 S}{\partial x_2 \partial x_1}(\mathbf{X}) & \frac{\partial^2 S}{\partial x_2^2}(\mathbf{X}) & \cdots & \frac{\partial^2 S}{\partial x_2 \partial x_n}(\mathbf{X}) \\ \vdots & \vdots & \ddots & \vdots \\ \frac{\partial^2 S}{\partial x_n \partial x_1}(\mathbf{X}) & \frac{\partial^2 S}{\partial x_n \partial x_2}(\mathbf{X}) & \cdots & \frac{\partial^2 S}{\partial x_n^2}(\mathbf{X}) \end{pmatrix}.$$

3.4.1. Gauss-Newton method

From (3.21), the gradient $\vec{\nabla} S\left(\mathbf{X}^{(m)}\right)$ and the Hessian matrix $\mathbf{H}S(\mathbf{X})$ can be written as:

$$\begin{cases} \vec{\nabla} S(\mathbf{X}) = 2 \cdot \left(\mathbf{JF}(\mathbf{X})\right)^{\mathrm{T}} \cdot \mathbf{F}(\mathbf{X}) \\ \mathbf{H}S(\mathbf{X}) = 2 \cdot \left(\mathbf{JF}(\mathbf{X})\right)^{\mathrm{T}} \cdot \mathbf{JF}(\mathbf{X}) + 2 \cdot \sum_{i=1}^{n} \mathbf{H}f_i(\mathbf{X}) \cdot f_i(\mathbf{X}) \end{cases} \tag{3.24}$$

Equations (3.24) gives us an opportunity to modify the Newton-Raphson expression being applied for minimization of S.We are going to replace the gradient function $\vec{\nabla} S(\mathbf{X})$ and the Hessian function $\mathbf{H}S(\mathbf{X})$ in the algorithm (3.23) with a small modification:

$$\begin{cases} \vec{\nabla} S(\mathbf{X}) = 2 \cdot \left(\mathbf{JF}(\mathbf{X})\right)^{\mathrm{T}} \cdot \mathbf{F}(\mathbf{X}) \\ \mathbf{H}S(\mathbf{X}) \approx 2 \cdot \left(\mathbf{JF}(\mathbf{X})\right)^{\mathrm{T}} \cdot \mathbf{JF}(\mathbf{X}) \end{cases} \tag{3.25}$$

Placing (3.25) into (3.23) gives us Gauss-Newton method. The reason why the method works with an approximation rather than a true Hessian of S is as follows:

- The Gauss-Newton method calculates a point from the previous one following directions of decrease of S. For any direction to be a direction of decrease of S, $\mathbf{H}S(\mathbf{X}^{(m)})$ must be positive definite. The approximation of $\mathbf{H}S(\mathbf{X}^{(m)})$ taken for the Gauss-Newton method, given that it is positive semidefinite for every point in which it is evaluated, when it is far from the minimum, it is practically guaranteed that it is following directions of decrease of S (except for those points where this approach is not positive definite, a problem that can be overcome by means of an evolution of the Gauss-Newton method known as the

Levenberg-Marquardt method, also available in the computer package that has been used as a programming tool).

- When the starting point is close to the minimum then, in addition to the condition of the Hessian matrix being positive semidefinite, from (3.24) it is true that:

$$\begin{cases} \vec{\nabla} S\left(\mathbf{X}\right) = 2 \cdot \left(\mathbf{JF}\left(\mathbf{X}\right)\right)^{\mathrm{T}} \cdot \mathbf{F}\left(\mathbf{X}\right) \\ \mathbf{H}S\left(\mathbf{X}\right) = 2 \cdot \left(\mathbf{JF}\left(\mathbf{X}\right)\right)^{\mathrm{T}} \cdot \mathbf{JF}\left(\mathbf{X}\right) \end{cases} \tag{3.26}$$

and, after replacing (3.26) in (3.23), operating a bit we will get to

$$\begin{aligned} \mathbf{X}^{(m+1)} &= \mathbf{X}^{(m)} - \left(\mathbf{H}S\left(\mathbf{X}^{(m)}\right)\right)^{-1} \cdot \vec{\nabla} S\left(\mathbf{X}^{(m)}\right) \\ &= \mathbf{X}^{(m)} - \left(2 \cdot \left(\mathbf{JF}\left(\mathbf{X}^{(m)}\right)\right)^{\mathrm{T}} \cdot \mathbf{JF}\left(\mathbf{X}^{(m)}\right)\right)^{-1} \cdot 2 \cdot \left(\mathbf{JF}\left(\mathbf{X}^{(m)}\right)\right)^{\mathrm{T}} \cdot \mathbf{F}\left(\mathbf{X}^{(m)}\right) \\ &= \mathbf{X}^{(m)} - \left(\mathbf{JF}\left(\mathbf{X}^{(m)}\right)\right)^{-1} \cdot \left(\left(\mathbf{JF}\left(\mathbf{X}^{(m)}\right)\right)^{\mathrm{T}}\right)^{-1} \cdot 2^{-1} \cdot 2 \cdot \left(\mathbf{JF}\left(\mathbf{X}^{(m)}\right)\right)^{\mathrm{T}} \cdot \mathbf{F}\left(\mathbf{X}^{(m)}\right) \\ &= \mathbf{X}^{(m)} - \left(\mathbf{JF}\left(\mathbf{X}^{(m)}\right)\right)^{-1} \cdot \mathbf{F}\left(\mathbf{X}^{(m)}\right) \end{aligned} \tag{3.27}$$

which is the algorithmic expression corresponding to the Newton-Raphson method (3.20). This demonstrates the equivalence between the Gauss-Newton method and the Newton-Raphson method when the starting point is close to the solution we are looking for.

If a starting point is close enough to the solution of (3.19) and the Newton-Raphson method is guaranteed to converge towards it, then previously demonstrated equivalence suggests that, in the context of numerical minimization of the function S in which the Gauss-Newton method is applied, that same starting point must also be sufficiently close to the point for which S presents its global minimum. This assumption turns out to be true in reality and, consequently, in spite of the property of local convergence Gauss-Newton method exhibits, none of the nonlinear equation systems that are intended to be solved are at risk of converging towards a non-global local minimum.

3.4.2. Levenberg-Marquardt method

The Hessian matrix $\mathbf{H}S\left(\mathbf{X}^{(m)}\right)$ may, under some circumstances, become singular or nearly singular. In this case, the step size $\Delta\mathbf{X}^{(m)} = \mathbf{X}^{(m+1)} - \mathbf{X}^{(m)}$ might not be a descent direction and may become very large. To avoid this situation, Levenberg in 1944 [45] and Marquardt in 1963 [46] proposed a damped Gauss-Newton method. The expression for the algorithm is as follows:

$$\mathbf{X}^{(m+1)} = \mathbf{X}^{(m)} - \left(\left(\mathbf{JF}\left(\mathbf{X}^{(m)} \right) \right)^{\mathrm{T}} \cdot \mathbf{JF}\left(\mathbf{X}^{(m)} \right) + \mu \cdot \mathbf{I} \right)^{-1} \cdot \left(\mathbf{JF}\left(\mathbf{X}^{(m)} \right) \right)^{\mathrm{T}} \cdot \mathbf{F}\left(\mathbf{X}^{(m)} \right) \tag{3.28}$$

The damping factor μ has the following effects on the expression of the algorithm:

- For all $\mu > 0$; the coefficient matrix becomes positive definite and the resulting step size $\Delta\mathbf{X}^{(m)}$ is in descent direction.
- One drawback of μ is that if we set $\mu > 0$; the term $\left(\left(\mathbf{JF}\left(\mathbf{X}^{(m)} \right) \right)^{\mathrm{T}} \cdot \mathbf{JF}\left(\mathbf{X}^{(m)} \right) + \mu \cdot \mathbf{I} \right)^{-1}$ will lose its form as true Hessian, even if all f_i are equal to zero, and the convergence property of Newton-Raphson may be lost. To overcome such a condition, one strategy is to update μ iteration by iteration. If the algorithm is making good progress we decrease μ towards zero but if algorithm is not making progress we increase the value of μ.
- We can observe how well the algorithm is progressing by computing the ratio:

$$\rho = \frac{S\left(\mathbf{X}^{(m+1)} \right) - S\left(\mathbf{X}^{(m)} \right)}{\left(\vec{\nabla} S\left(\mathbf{X}^{(m)} \right) \right)^{\mathrm{T}} \cdot \Delta\mathbf{X}^{(m)} + \frac{1}{2} \cdot \left(\Delta\mathbf{X}^{(m)} \right)^{\mathrm{T}} \cdot \mathbf{H}S\left(\mathbf{X}^{(m)} \right) \cdot \Delta\mathbf{X}^{(m)}} \tag{3.29}$$

  The numerator is the decrease in function value for a single iteration, whereas the denominator is the decrease predicted by the local quadratic model, i.e.

$$S\left(\mathbf{X}^{(m+1)} \right) \approx S\left(\mathbf{X}^{(m)} \right) + \left(\vec{\nabla} S\left(\mathbf{X}^{(m)} \right) \right)^{\mathrm{T}} \cdot \Delta\mathbf{X}^{(m)} + \frac{1}{2} \cdot \left(\Delta\mathbf{X}^{(m)} \right)^{\mathrm{T}} \cdot \mathbf{H}S\left(\mathbf{X}^{(m)} \right) \cdot \Delta\mathbf{X}^{(m)} \tag{3.30}$$

  If this ratio is close to one, we assume that the local quadratic model is good and therefore a decrease in μ is required. However, if $\rho << 1$, we increase the damping factor μ.

- There are also techniques available in literature [47] for controlling the step size $\Delta\mathbf{X}^{(m)}$ also called the "trust region" approaches. The basic idea is minimizing the function $\left\| \mathbf{JF}\left(\mathbf{X}^{(m)} \right) \cdot \Delta\mathbf{X}^{(m)} + \mathbf{F}\left(\mathbf{X}^{(m)} \right) \right\|^2$ with the additional constraint (step size limitation)

$$\left\| \Delta\mathbf{X}^{(m)} \right\| \le \delta . \tag{3.31}$$

  This inequality defines what is called the "trust region" about the current point $\mathbf{X}^{(m)}$, where we think our quadratic approximation is valid.

  If it is assumed that $\left\| \Delta\mathbf{X}^{(m)} \right\| < \delta$, the gradient of $\left\| \mathbf{JF}\left(\mathbf{X}^{(m)} \right) \cdot \Delta\mathbf{X}^{(m)} + \mathbf{F}\left(\mathbf{X}^{(m)} \right) \right\|^2$ with respect to the components of $\Delta\mathbf{X}^{(m)}$ must be zero. That is:

$$
\begin{gathered}
2\cdot\left(\left(\mathbf{JF}\left(\mathbf{X}^{(m)}\right)\right)^{\mathrm{T}}\cdot\mathbf{JF}\left(\mathbf{X}^{(m)}\right)\cdot\Delta\mathbf{X}^{(m)}+\left(\mathbf{JF}\left(\mathbf{X}^{(m)}\right)\right)^{\mathrm{T}}\cdot\mathbf{F}\left(\mathbf{X}^{(m)}\right)\right)=0 \\
\Downarrow \\
\left(\mathbf{JF}\left(\mathbf{X}^{(m)}\right)\right)^{\mathrm{T}}\cdot\mathbf{JF}\left(\mathbf{X}^{(m)}\right)\cdot\Delta\mathbf{X}^{(m)}+\left(\mathbf{JF}\left(\mathbf{X}^{(m)}\right)\right)^{\mathrm{T}}\cdot\mathbf{F}\left(\mathbf{X}^{(m)}\right)=0 \\
\Downarrow \\
\left(\mathbf{JF}\left(\mathbf{X}^{(m)}\right)\right)^{\mathrm{T}}\cdot\mathbf{JF}\left(\mathbf{X}^{(m)}\right)\cdot\Delta\mathbf{X}^{(m)}=-\left(\mathbf{JF}\left(\mathbf{X}^{(m)}\right)\right)^{\mathrm{T}}\cdot\mathbf{F}\left(\mathbf{X}^{(m)}\right) \\
\Downarrow \\
\Delta\mathbf{X}^{(m)}=-\left(\left(\mathbf{JF}\left(\mathbf{X}^{(m)}\right)\right)^{\mathrm{T}}\cdot\mathbf{JF}\left(\mathbf{X}^{(m)}\right)\right)^{-1}\cdot\left(\mathbf{JF}\left(\mathbf{X}^{(m)}\right)\right)^{\mathrm{T}}\cdot\mathbf{F}\left(\mathbf{X}^{(m)}\right) \\
\Downarrow \\
\mathbf{X}^{(m+1)}-\mathbf{X}^{(m)}=-\left(\left(\mathbf{JF}\left(\mathbf{X}^{(m)}\right)\right)^{\mathrm{T}}\cdot\mathbf{JF}\left(\mathbf{X}^{(m)}\right)\right)^{-1}\cdot\left(\mathbf{JF}\left(\mathbf{X}^{(m)}\right)\right)^{\mathrm{T}}\cdot\mathbf{F}\left(\mathbf{X}^{(m)}\right) \\
\Downarrow \\
\mathbf{X}^{(m+1)}=\mathbf{X}^{(m)}-\left(\left(\mathbf{JF}\left(\mathbf{X}^{(m)}\right)\right)^{\mathrm{T}}\cdot\mathbf{JF}\left(\mathbf{X}^{(m)}\right)\right)^{-1}\cdot\left(\mathbf{JF}\left(\mathbf{X}^{(m)}\right)\right)^{\mathrm{T}}\cdot\mathbf{F}\left(\mathbf{X}^{(m)}\right) \\
\Downarrow \\
\mathbf{X}^{(m+1)}=\mathbf{X}^{(m)}-\left(\left(\mathbf{JF}\left(\mathbf{X}^{(m)}\right)\right)^{\mathrm{T}}\cdot\mathbf{JF}\left(\mathbf{X}^{(m)}\right)+0\cdot\mathbf{I}\right)^{-1}\cdot\left(\mathbf{JF}\left(\mathbf{X}^{(m)}\right)\right)^{\mathrm{T}}\cdot\mathbf{F}\left(\mathbf{X}^{(m)}\right)
\end{gathered}
\tag{3.32}
$$

Setting $0=\mu$, (3.28) is obtained (it being $\mu=0$).

If it is assumed that $\left\|\Delta\mathbf{X}^{(m)}\right\|=\delta$, we can write this constraint as $\left\|\Delta\mathbf{X}^{(m)}\right\|^2-\delta^2=0$. Then, there exists such a value $\lambda\neq 0$ for which the gradient of $\left\|\mathbf{JF}\left(\mathbf{X}^{(m)}\right)\cdot\Delta\mathbf{X}^{(m)}+\mathbf{F}\left(\mathbf{X}^{(m)}\right)\right\|^2$ is proportional to the gradient of $\left\|\Delta\mathbf{X}^{(m)}\right\|^2-\delta^2$, both gradients taken with respect to the components of $\Delta\mathbf{X}^{(m)}$. The gradient of $\left\|\Delta\mathbf{X}^{(m)}\right\|^2-\delta^2$ is $2\cdot\Delta\mathbf{X}^{(m)}$. Therefore:

$$
\begin{gathered}
2\cdot\left(\left(\mathbf{JF}\left(\mathbf{X}^{(m)}\right)\right)^{\mathrm{T}}\cdot\mathbf{JF}\left(\mathbf{X}^{(m)}\right)\cdot\Delta\mathbf{X}^{(m)}+\left(\mathbf{JF}\left(\mathbf{X}^{(m)}\right)\right)^{\mathrm{T}}\cdot\mathbf{F}\left(\mathbf{X}^{(m)}\right)\right)=\lambda\cdot 2\cdot\Delta\mathbf{X}^{(m)} \\
\Downarrow \\
\left(\mathbf{JF}\left(\mathbf{X}^{(m)}\right)\right)^{\mathrm{T}}\cdot\mathbf{JF}\left(\mathbf{X}^{(m)}\right)\cdot\Delta\mathbf{X}^{(m)}+\left(\mathbf{JF}\left(\mathbf{X}^{(m)}\right)\right)^{\mathrm{T}}\cdot\mathbf{F}\left(\mathbf{X}^{(m)}\right)=\lambda\cdot\Delta\mathbf{X}^{(m)} \\
\Downarrow \\
\left(\mathbf{JF}\left(\mathbf{X}^{(m)}\right)\right)^{\mathrm{T}}\cdot\mathbf{JF}\left(\mathbf{X}^{(m)}\right)\cdot\Delta\mathbf{X}^{(m)}-\lambda\cdot\mathbf{I}\cdot\Delta\mathbf{X}^{(m)}=-\left(\mathbf{JF}\left(\mathbf{X}^{(m)}\right)\right)^{\mathrm{T}}\cdot\mathbf{F}\left(\mathbf{X}^{(m)}\right) \\
\Downarrow \\
\left(\left(\mathbf{JF}\left(\mathbf{X}^{(m)}\right)\right)^{\mathrm{T}}\cdot\mathbf{JF}\left(\mathbf{X}^{(m)}\right)-\lambda\cdot\mathbf{I}\right)\cdot\Delta\mathbf{X}^{(m)}=-\left(\mathbf{JF}\left(\mathbf{X}^{(m)}\right)\right)^{\mathrm{T}}\cdot\mathbf{F}\left(\mathbf{X}^{(m)}\right) \\
\Downarrow \\
\Delta\mathbf{X}^{(m)}=-\left(\left(\mathbf{JF}\left(\mathbf{X}^{(m)}\right)\right)^{\mathrm{T}}\cdot\mathbf{JF}\left(\mathbf{X}^{(m)}\right)-\lambda\cdot\mathbf{I}\right)^{-1}\cdot\left(\mathbf{JF}\left(\mathbf{X}^{(m)}\right)\right)^{\mathrm{T}}\cdot\mathbf{F}\left(\mathbf{X}^{(m)}\right) \\
\Downarrow \\
\mathbf{X}^{(m+1)}-\mathbf{X}^{(m)}=-\left(\left(\mathbf{JF}\left(\mathbf{X}^{(m)}\right)\right)^{\mathrm{T}}\cdot\mathbf{JF}\left(\mathbf{X}^{(m)}\right)-\lambda\cdot\mathbf{I}\right)^{-1}\cdot\left(\mathbf{JF}\left(\mathbf{X}^{(m)}\right)\right)^{\mathrm{T}}\cdot\mathbf{F}\left(\mathbf{X}^{(m)}\right) \\
\Downarrow \\
\mathbf{X}^{(m+1)}=\mathbf{X}^{(m)}-\left(\left(\mathbf{JF}\left(\mathbf{X}^{(m)}\right)\right)^{\mathrm{T}}\cdot\mathbf{JF}\left(\mathbf{X}^{(m)}\right)-\lambda\cdot\mathbf{I}\right)^{-1}\cdot\left(\mathbf{JF}\left(\mathbf{X}^{(m)}\right)\right)^{\mathrm{T}}\cdot\mathbf{F}\left(\mathbf{X}^{(m)}\right)
\end{gathered}
\tag{3.33}
$$

Setting $-\lambda=\mu$, (3.28) is obtained (it being $\mu\neq 0$).

4. An improved harmonic load flow formulation

4.1. Formulation of the harmonic problem

The proposed HLF formulation, known as improved unified harmonic load flow (IUHLF) [51], derives from the unified harmonic load flow (UHLF) [48, 49]. Both formulations are a modification of the CHLF ($CHLF_m$) which takes into account the Thévenin equivalent circuit approach used in SHLF to avoid considering the harmonic voltages at the Slack and PQ buses as unknowns.

Let it be a network with n buses $(i = 1, 2, \ldots, n)$: a Slack bus $(i = 1)$, a number of PQ buses $(i = 2, \ldots, c)$ and a number of NL buses $(i = c+1, \ldots, n)$. UHLF and IUHLF formulations are illustrated in Figure 4.1 and their data and unknowns are summarised in Table 4.1.

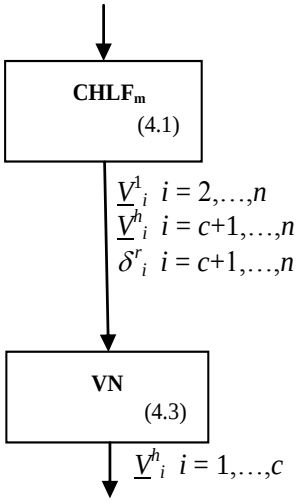

Figure 4.1: UHLF / IUHLF formulation flowchart

Stage	Bus	Data	Unknowns
CHLF$_m$	Slack	$\underline{V}^1_1$	---
	PQ	P_i, Q_i (injected)	$\underline{V}^1_i$
	NL	D^m_i	$\underline{V}^1_i, \underline{V}^h_i, \delta^r_i$
VN	Slack	X^1_1	$\underline{V}^h_1$
	PQ	$\underline{Y}^h_i = \underline{f}^h_{Yi}\left(V^1_i\right)$	$\underline{V}^h_i$
	NL	$\underline{I}^h_i$	---

Table 4.1: UHLF / IUHLF formulation data and unknowns

The superscripts r and m are the indices of the NLL state variables and NLL data which define the NLL behaviour, respectively. Distorted voltages and currents will be expressed in terms of

the summation of $k = 1,3,5,\ldots$ components: 1 is the fundamental component and $h = 3,5,7,\ldots$ are the harmonic components.

UHLF formulation [48, 49] is based on the simultaneous resolution of the power equations at the PQ buses, Kirchhoff's second law applied to the fundamental and harmonic Thévenin equivalent circuits, and the NLL equations defining HVDC converter behaviour, i.e.,

$$\begin{aligned}
&\underline{S}_i = \underline{V}_i^1 \left(\sum_{j=1}^{n} \underline{Y}_{ij}^1 \underline{V}_j^1 \right)^* \qquad (i = 2,\ldots,c) \\
&\underline{V}_i^k = \underline{E}_{Thi}^k + \sum_{j=c+1}^{n} \underline{Z}_{Thij}^k \underline{I}_i^k \qquad (i = c+1,\ldots,n) \\
&hvdc_i^r(\underline{V}_i^1, \underline{V}_i^h, \delta_i^r, D_i^m) = 0 \\
&(i = c+1,\ldots,n \;;\; r = 1,\ldots,r_{\max} \;;\; m = 1,\ldots,m_{\max}),
\end{aligned} \tag{4.1}$$

where $\underline{Y}^1_{ij}$ are the ij^{th} elements of the network fundamental admittance matrix $\mathbf{Y}^1_{\mathbf{B}}$, $\underline{I}^k_i$ is defined as

$$\begin{aligned}
&\underline{I}_i^k = \underline{f}_i^k(\underline{V}_i^1, \underline{V}_i^h, \delta_i^r, D_i^m) \\
&(i = c+1,\ldots,n \;;\; r = 1,\ldots,r_{\max} \;;\; m = 1,\ldots,m_{\max}),
\end{aligned} \tag{4.2}$$

and $hvdc^r_i(\cdot) = 0$ represents the HVDC converter equations. HVDC converters are the only sort of nonlinear load analysed and considered in [48, 49] for the UHLF formulation, probably because the authors only knew the model of this nonlinear load and they did not know how to include others.

The fundamental and harmonic Thévenin equivalent circuits of the linear network "observed" from the NL buses (i.e., $\underline{E}^k_{Thi}$ and $\underline{Z}^k_{Thij}$) are determined in each of the iterations to be used in the corresponding equations since $\underline{E}^k_{Thi} = \underline{f}^k_{EThi}(\underline{V}^1_l)$ and $\underline{Z}^k_{Thij} = \underline{f}^k_{ZThij}(\underline{V}^1_l)$ ($l = 2,\ldots,c$). The use of a constant Jacobian matrix is proposed in [48] to carry out the numerical resolution of (4.1) by the Newton-Raphson method. Holding the Jacobian matrix constant leads to a larger number of faster iterations to obtain the overall solution, [49]. However, if voltages are highly distorted, this number of iterations may still be larger or convergence to the solution might even not be achieved. The numerical resolution of (4.1) provides the fundamental voltages at the PQ and NL buses, the harmonic voltages at the NL buses and the NLL state variables. Subsequently, the VN method (4.3) is applied to determine the harmonic voltages at the Slack and PQ buses. This method is based on the resolution of the linear system

$$\mathbf{Y}^h_{\mathbf{B}} \cdot \mathbf{V}^h_{\mathbf{B}} = \mathbf{I}^h_{\mathbf{B}} \tag{4.3}$$

This formulation allows the HLF problem to be tackled as a single nonlinear equation system, considering NLL harmonic interaction but not including the harmonic voltages at the Slack and PQ buses as unknowns.

Another UHLF formulation could be considered, namely removing the following equations of Kirchhoff's second law applied to the fundamental Thévenin equivalent circuits from (4.1):

$$\underline{V}_i^1 = \underline{E}_{Thi}^1 + \sum_{j=c+1}^{n} \underline{Z}_{Thij}^1 \underline{I}_i^1 \qquad (i = c+1,\ldots,n), \tag{4.4}$$

and incorporating the following power equations derived from HVDC converters when treated as PQ loads into (4.1) instead:

$$\underline{V}_i^1 (\underline{I}_i^1)^* = \underline{V}_i^1 \left(\sum_{j=1}^{n} \underline{Y}_{ij}^1 \underline{V}_j^1 \right)^* \qquad (i = c+1,\ldots,n). \tag{4.5}$$

However, this alternative UHLF formulation is discarded due to the high degree of nonlinearity of equations in (4.5) compared to those in (4.4).

Two features of the considered UHLF formulation are as follows [48, 49]:

- The formulation is oriented to the presence of a specific sort of nonlinear load in the electrical network: HVDC converters.

- The Newton-Raphson method with constant Jacobian matrix is applied for the numerical resolution of (4.1).

While these two features could be good enough for electrical networks with the presence of HVDC converters and in a context of scarcely distorted voltages, [48, 49], they could not be convenient for electrical networks with the presence of any sort of nonlinear load or in scenarios of highly distorted voltages.

To overcome these limitations, an enhanced UHLF formulation called IUHLF formulation is presented. The two improvements over the UHLF formulation are as follows:

- The proposed formulation is oriented to the presence of any sort of nonlinear load in the electrical network. Therefore, $hvdc^r_i(\cdot) = 0$ in (4.1) must be replaced by $nl^r_i(\cdot) = 0$.

- The Newton-Raphson method with true Jacobian matrix is applied for the numerical resolution of (4.1). It allows the increase in the number of iterations which is inherent to the presence of highly distorted voltages in electrical networks to be smaller.

4.2. Discussion on the improved HLF formulation strengths

The main IUHLF formulation strengths over other HLF formulations for electrical networks with highly distorted voltages are:

- In contrast to HP formulation, NLL harmonic interaction is considered in IUHLF formulation.

- The numerical resolution of IUHLF formulation is carried out by applying the Newton-Raphson method to a single nonlinear equation system, whereas the numerical resolution of SHLF formulation requires the application of the Gauss-Seidel method to a set of two nonlinear equation systems. The application of a fixed-point iteration method to the set of two systems in SHLF formulation hinders the global numerical resolution of the HLF problem, to such a point that high harmonic distortions might lead to very different values of u_{N1} and u_{N2}. Therefore, convergence of SHLF formulation is improved by IUHLF formulation.

- The number of unknowns at $CHLF_m$ stage in IUHLF formulation is smaller than in CHLF formulation (the harmonic voltages at the Slack and PQ buses are not unknowns at that stage). Thus, convergence of IUHLF formulation is likely better than that of CHLF formulation.

- The use of Newton-Raphson method with true Jacobian matrix allows convergence of UHLF formulation to be enhanced by IUHLF formulation.

- Unlike UHLF formulation, IUHLF formulation is applicable to electrical networks with the presence of any kind of nonlinear load.

- IUHLF formulation exhibits the same accuracy as SHLF, CHLF and UHLF formulations (and better accuracy than HP formulation) because of the NLL harmonic interaction consideration in all four.

4.3. Number of real equations required by the different HLF formulations

Let it be a network with n buses $(i = 1, 2, \ldots, n)$: a Slack bus $(i = 1)$, a number of PQ buses $(i = 2, \ldots, c)$ and *a single NL bus* $(i = c + 1 = n)$. The superscripts r and m are the indices of the NLL state variables and NLL data which define the NLL behaviour, respectively. Distorted voltages and currents will be expressed in terms of the summation of $k = 1, 3, 5, \ldots$ components: 1 is the fundamental component and $h = 3, 5, 7, \ldots$ are the harmonic components. Let k_m be the total number of frequencies which includes fundamental and the first odd harmonic frequencies of an AC network whose harmonic load flow we intend to perform. Let r_{max} be the number of NLL state variables being found for *the N identical NLL* in *the single NL bus*. Tables 4.2 and 4.3 allow the number of real equations required by the different HLF formulations (UHLF only if NLL ≡ HVDC converter) for the numerical resolution of the considered AC network to be calculated.

Bus	HP	SHLF	CHLF	UHLF / IUHLF
Slack	---	---	$-\underline{Y}_1^h \underline{V}_1^h = \sum_{j=1}^{n} \underline{Y}_{1j}^h \underline{V}_j^h$	---
PQ	$\underline{S}_i = \underline{V}_i^1 \left(\sum_{j=1}^{n} \underline{Y}_{ij}^1 \underline{V}_j^1 \right)^*$	FLF$_m$ $\underline{S}_i = \underline{V}_{\mathrm{N}_1,i}^1 \left(\sum_{j=1}^{n} \underline{Y}_{ij}^1 \underline{V}_{\mathrm{N}_1,j}^1 \right)^*$ HA ---	$\underline{S}_i = \underline{V}_i^1 \left(\sum_{j=1}^{n} \underline{Y}_{ij}^1 \underline{V}_j^1 \right)^*$ $-\underline{Y}_i^h \underline{V}_i^h = \sum_{j=1}^{n} \underline{Y}_{ij}^h \underline{V}_j^h$	$\underline{S}_i = \underline{V}_i^1 \left(\sum_{j=1}^{n} \underline{Y}_{ij}^1 \underline{V}_j^1 \right)^*$
NL	$\underline{V}_i^1 (\underline{I}_i^1)^* = \underline{V}_i^1 \left(\sum_{j=1}^{n} \underline{Y}_{ij}^1 \underline{V}_j^1 \right)^*$ $nl_i^r (\underline{V}_i^1, \delta_i^r, D_i^m) = 0$	FLF$_m$ $\underline{V}_{\mathrm{N}_1,i}^1 (\underline{I}_i^1)^* = \underline{V}_{\mathrm{N}_1,i}^1 \left(\sum_{j=1}^{n} \underline{Y}_{ij}^1 \underline{V}_{\mathrm{N}_1,j}^1 \right)^*$ $nl_i^r (\underline{V}_{\mathrm{N}_1,i}^1, \underline{V}_{\mathrm{N}_2,i}^h, \delta_{\mathrm{N}_1,i}^r, D_i^m) = 0$ HA $\underline{V}_{\mathrm{N}_2,i}^k = \underline{E}_{Thi}^k + \sum_{j=c+1}^{n} \underline{Z}_{Thij}^k \underline{I}_i^k$ $nl_i^r (\underline{V}_{\mathrm{N}_2,i}^1, \underline{V}_{\mathrm{N}_2,i}^h, \delta_{\mathrm{N}_2,i}^r, D_i^m) = 0$	$\underline{I}_i^k = \sum_{j=1}^{n} \underline{Y}_{ij}^k \underline{V}_j^k$ $nl_i^r (\underline{V}_i^1, \underline{V}_i^h, \delta_i^r, D_i^m) = 0$	$\underline{V}_i^k = \underline{E}_{Thi}^k + \sum_{j=c+1}^{n} \underline{Z}_{Thij}^k \underline{I}_i^k$ $nl_i^r (\underline{V}_i^1, \underline{V}_i^h, \delta_i^r, D_i^m) = 0$

Table 4.2: Equations required by the different HLF formulations

Bus	HP	SHLF	CHLF	UHLF / IUHLF
Slack	0	0	$2 \cdot (k_m\text{-}1)$	0
PQ	$2 \cdot (c\text{-}1)$	FLF$_m$ $2 \cdot (c\text{-}1)$ HA 0	$2 \cdot (c\text{-}1) \cdot k_m$	$2 \cdot (c\text{-}1)$
NL	$2 \cdot (n\text{-}c) + r_{max}$	FLF$_m$ $2 \cdot (n\text{-}c) + r_{max}$ HA $2 \cdot (n\text{-}c) \cdot k_m + r_{max}$	$2 \cdot (n\text{-}c) \cdot k_m + r_{max}$	$2 \cdot (n\text{-}c) \cdot k_m + r_{max}$

Table 4.3: Number of real equations required by the different HLF formulations

4.4. Electrical network example

Without loss of generality in the conclusions, an academic electrical LV network example is considered for which the equations and unknowns are shown for each HLF formulation. It is a 3-bus system in which first bus is the Slack bus $(i = 1)$, second bus is the PQ bus $(i = 2)$, and third bus is the nonlinear bus $(i = 3)$ to which *N identical single-phase uncontrolled rectifiers* [50] are connected (i.e., UHLF formulation is not applicable). Let's consider the first odd ten frequencies,

i.e., $k = 1,3,5,7,9,.....,19$ (i.e., those of the most significant harmonics for the study), so we have k_m = 10, and the NLL state variables of single-phase uncontrolled rectifiers, i.e., r_{max} = 2. The electrical network is given in Figure 4.2.

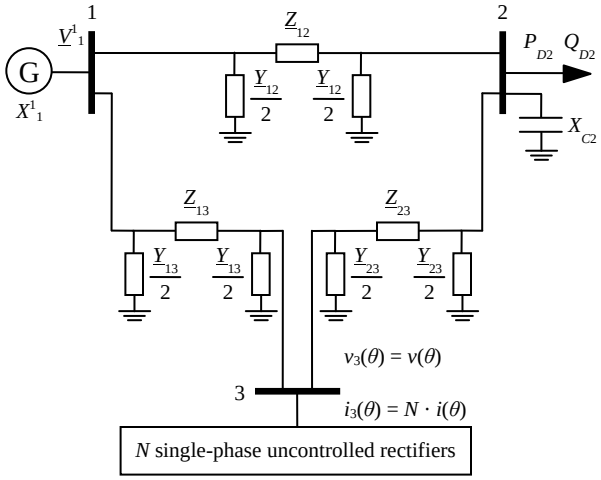

Figure 4.2(a): Three-bus network.

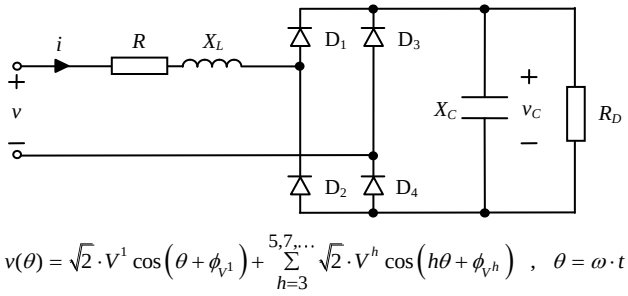

Figure 4.2(b): Single-phase uncontrolled rectifier circuit.

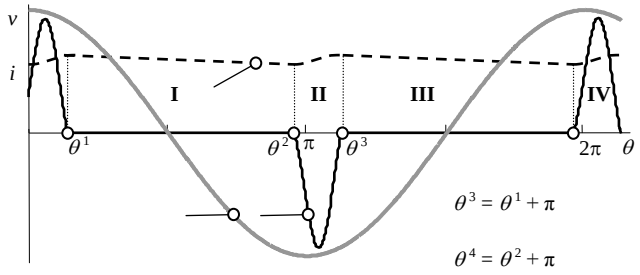

Figure 4.2(c): Supply voltage v, ac current i and dc voltage v_C waveforms.

The data for the electrical network considered in Figure 4.2 are shown in Table 4.4. For the purpose of simplicity and ease of comparison of results between different harmonic formulations, all the values of the AC network are converted into per unit values. The base values for power and voltage used to transform the data into per unit values are as follows:

$$S_B = 2500\,\text{VA};\;\; V_B = 220\,\text{V} \tag{4.6}$$

Element	#	Type	Data	Values (pu)
Bus	1	Slack	$\underline{V}^1_1$ X^1_1	$1\angle 0^o$ 4.6168e-3
	2	PQ	$P_2 = -P_{D2}$ $Q_2 = -Q_{D2}$	-0.8 -0.6
	3	NL	R , X_L X_C , R_D	0.0207,0.0130 1.1579,11.0021
Shunt	2-0	Capacitor	X_{C2}	1.6667
Branch	1-2	Line	$\underline{Z}_{12}$ $\underline{Y}_{12}$	5.1653e-4+j5.1653e-3 j6.4533e-3
	2-3	Line	$\underline{Z}_{23}$ $\underline{Y}_{23}$	5.1653e-4+j5.1653e-3 j6.4533e-3
	1-3	Line	$\underline{Z}_{13}$ $\underline{Y}_{13}$	5.1653e-4+j5.1653e-3 j6.4533e-3

Table 4.4: Network data for Figure 4.2

The basic idea is to study the harmonic voltages at buses and the currents injected into the network by the *N* single-phase uncontrolled rectifiers. The main parameters defining the behaviour of the nonlinear device are the commutation times t_3^1 and t_3^2 as shown in Figure 4.2. The fundamental and harmonic currents injected by the *N* single-phase uncontrolled rectifiers will be:

$$\underline{I}_3^k = N \cdot \underline{f}_3^k(\underline{V}_3^1, \underline{V}_3^h, t_3^1, t_3^2, R_3, X_{L3}, X_{C3}, R_{D3}) \tag{4.7}$$

$\underline{f}^k_3$ is described in [13, 50]. Resonance is introduced in the AC network to observe the characteristics of harmonic voltages under the presence of resonance at a certain harmonic frequency. The resonant frequency in the electrical network depends on the following expression:

$$X_1^1 = \frac{X_{C2}}{h_{res}^2} \tag{4.8}$$

For the electrical network example resonant frequency is set at $h_{res} = 15$, which means that we will observe an increase in harmonic voltage at 15-th harmonic. The admittance matrix for the above-proposed example considering the fundamental component is as follows:

$$\mathbf{Y}_{\mathbf{B}}^{1}=\begin{bmatrix}\underline{Y}_{11}^{1} & \underline{Y}_{12}^{1} & \underline{Y}_{13}^{1}\\ \underline{Y}_{21}^{1} & \underline{Y}_{22}^{1} & \underline{Y}_{23}^{1}\\ \underline{Y}_{31}^{1} & \underline{Y}_{32}^{1} & \underline{Y}_{33}^{1}\end{bmatrix} \tag{4.9}$$

The elements that constitute the admittance matrix are as follows

$$\begin{aligned}
&\underline{Y}_{11}^{1}=\frac{1}{\underline{Z}_{12}^{1}}+\frac{\underline{Y}_{12}^{1}}{2}+\frac{\underline{Y}_{13}^{1}}{2}+\frac{1}{\underline{Z}_{13}^{1}}\\
&\underline{Y}_{22}^{1}=\frac{1}{\underline{Z}_{12}^{1}}+\frac{\underline{Y}_{12}^{1}}{2}+\frac{\underline{Y}_{23}^{1}}{2}+\frac{1}{\underline{Z}_{23}^{1}}+\underline{Y}_{C2}^{1}\\
&\underline{Y}_{33}^{1}=\frac{1}{\underline{Z}_{13}^{1}}+\frac{\underline{Y}_{13}^{1}}{2}+\frac{\underline{Y}_{23}^{1}}{2}+\frac{1}{\underline{Z}_{23}^{1}}\\
&\underline{Y}_{12}^{1}=-\frac{1}{\underline{Z}_{12}^{1}},\ \ \underline{Y}_{13}^{1}=-\frac{1}{\underline{Z}_{13}^{1}},\ \ \underline{Y}_{23}^{1}=-\frac{1}{\underline{Z}_{23}^{1}}\\
&\underline{Y}_{21}^{1}=\underline{Y}_{12}^{1},\ \ \underline{Y}_{31}^{1}=\underline{Y}_{13}^{1},\ \ \underline{Y}_{32}^{1}=\underline{Y}_{23}^{1}
\end{aligned} \tag{4.10}$$

4.4.1. Harmonic penetration

HP formulation data and unknowns for the electrical network given in Figure 4.2 are summarised in Table 4.5.

Stage	Bus	Data	Unknowns	Number of real unknowns
FLF$_m$	Slack	$\underline{V}_1^1$	---	0
	PQ	P_2, Q_2	$\underline{V}_2^1$	2
	NL	$R_3, X_{L3}, X_{C3}, R_{D3}$	$\underline{V}_3^1, t_3^1, t_3^2$	4
VN	Slack	X_1^1	$\underline{V}_1^h$	18
	PQ	$\underline{Y}_2^h = \underline{f}_{Y_2}^h(V_2^1)$	$\underline{V}_2^h$	18
	NL	$\underline{I}_3^h$	$\underline{V}_3^h$	18

Table 4.5: HP formulation data and unknowns for the electrical network example

FLF$_m$ stage is solved by using the following nonlinear equation system:

$$
\begin{aligned}
&\mathrm{Re}\left\{\underline{V}_2^1\left(\underline{Y}_{21}^1\underline{V}_1^1+\underline{Y}_{22}^1\underline{V}_2^1+\underline{Y}_{23}^1\underline{V}_3^1\right)^*\right\}-P_2=0\\
&\mathrm{Im}\left\{\underline{V}_2^1\left(\underline{Y}_{21}^1\underline{V}_1^1+\underline{Y}_{22}^1\underline{V}_2^1+\underline{Y}_{23}^1\underline{V}_3^1\right)^*\right\}-Q_2=0\\
&\mathrm{Re}\left\{\underline{V}_3^1\left(\underline{Y}_{31}^1\underline{V}_1^1+\underline{Y}_{32}^1\underline{V}_2^1+\underline{Y}_{33}^1\underline{V}_3^1\right)^*\right\}-\mathrm{Re}\left\{\underline{V}_3^1\left(\underline{I}_3^1\right)^*\right\}=0\\
&\mathrm{Im}\left\{\underline{V}_3^1\left(\underline{Y}_{31}^1\underline{V}_1^1+\underline{Y}_{32}^1\underline{V}_2^1+\underline{Y}_{33}^1\underline{V}_3^1\right)^*\right\}-\mathrm{Im}\left\{\underline{V}_3^1\left(\underline{I}_3^1\right)^*\right\}=0\\
&nl_3^1(\underline{V}_3^1,t_3^1,t_3^2,R_3,X_{L3},X_{C3},R_{D3})=0\\
&nl_3^2(\underline{V}_3^1,t_3^1,t_3^2,R_3,X_{L3},X_{C3},R_{D3})=0
\end{aligned}
\tag{4.11}
$$

$nl^1{}_3$ and $nl^2{}_3$ are described in [13, 50]. The fundamental current injected by the N single-phase uncontrolled rectifiers will be:

$$
\underline{I}_3^1=N\cdot\underline{f}_3^1(\underline{V}_3^1,t_3^1,t_3^2,R_3,X_{L3},X_{C3},R_{D3}) \tag{4.12}
$$

The number of real equations required in the numerical resolution of HP for the electrical network example are summarised in Table 4.6 for each bus.

Stage	Bus	Number of real equations
FLF$_\mathbf{m}$	Slack	0
	PQ	2·(2-1)=2
	NL	2·(3-2)+2=4

Table 4.6: Number of real equations required by HP formulation

The harmonic voltages of the AC network are then obtained by applying the voltage node (VN) method:

$$
\mathbf{V}_\mathbf{B}^h=(\mathbf{Y}_\mathbf{Bm}^h)^{-1}\cdot\mathbf{I}_\mathbf{Bm}^h, \tag{4.13}
$$

where $\mathbf{V}_\mathbf{B}^h$ is the h-order bus voltage vector. This vector can be given as

$$
\mathbf{V}_\mathbf{B}^h=\begin{bmatrix}\underline{V}_1^h\\ \underline{V}_2^h\\ \underline{V}_3^h\end{bmatrix} \tag{4.14}
$$

$\mathbf{Y}_\mathbf{Bm}^h$ is the h-order modified bus admittance matrix. This matrix is obtained by integrating the harmonic admittances at Slack bus and the harmonic admittances at PQ buses into the h-order bus admittance matrix $\mathbf{Y}_\mathbf{B}^h$

$$\mathbf{Y}_{\mathbf{Bm}}^{h}=\begin{bmatrix}\underline{Y}_{11\mathrm{m}}^{h} & \underline{Y}_{12}^{h} & \underline{Y}_{13}^{h}\\ \underline{Y}_{21}^{h} & \underline{Y}_{22\mathrm{m}}^{h} & \underline{Y}_{23}^{h}\\ \underline{Y}_{31}^{h} & \underline{Y}_{32}^{h} & \underline{Y}_{33}^{h}\end{bmatrix} \tag{4.15}$$

The elements that constitute the admittance matrix are as follows

$$\begin{aligned}
&\underline{Y}_{11\mathrm{m}}^{h}=\frac{1}{\underline{Z}_{12}^{h}}+\frac{\underline{Y}_{12}^{h}}{2}+\frac{\underline{Y}_{13}^{h}}{2}+\frac{1}{\underline{Z}_{13}^{h}}+\underline{Y}_{1}^{h}\\
&\underline{Y}_{22\mathrm{m}}^{h}=\frac{1}{\underline{Z}_{12}^{h}}+\frac{\underline{Y}_{12}^{h}}{2}+\frac{\underline{Y}_{23}^{h}}{2}+\frac{1}{\underline{Z}_{23}^{h}}+\underline{Y}_{C2}^{h}+\underline{Y}_{2}^{h}\\
&\underline{Y}_{33}^{1}=\frac{1}{\underline{Z}_{13}^{h}}+\frac{\underline{Y}_{13}^{h}}{2}+\frac{\underline{Y}_{23}^{h}}{2}+\frac{1}{\underline{Z}_{23}^{h}}\\
&\underline{Y}_{12}^{h}=-\frac{1}{\underline{Z}_{12}^{h}},\quad \underline{Y}_{13}^{h}=-\frac{1}{\underline{Z}_{13}^{h}},\quad \underline{Y}_{23}^{h}=-\frac{1}{\underline{Z}_{23}^{h}}\\
&\underline{Y}_{21}^{h}=\underline{Y}_{12}^{h},\quad \underline{Y}_{31}^{h}=\underline{Y}_{13}^{h},\quad \underline{Y}_{32}^{h}=\underline{Y}_{23}^{h}
\end{aligned} \tag{4.16}$$

The harmonic admittances at Slack bus are

$$\underline{Y}_{1}^{h}=\frac{1}{R_1+j\cdot h\cdot X_1^1},\quad R_1\approx\frac{X_1^1}{20}. \tag{4.17}$$

The harmonic admittances at PQ bus are

$$\underline{Y}_{2}^{h}=\frac{1}{R_2+j\cdot h\cdot X_2^1},\quad R_2+jX_2^1=\frac{1}{\underline{Y}_{2}^{1}},\quad \underline{Y}_{2}^{1}=\frac{-(P_2+jQ_2)^{*}}{\left(V_2^1\right)^2},\quad \underline{Y}_{C2}^{k}=\frac{1}{-j\cdot k\cdot X_{C2}} \tag{4.18}$$

$\mathbf{I}_{\mathbf{Bm}}^{h}$ is the *h*-order modified bus current vector. This vector can be given as

$$\mathbf{I}_{\mathbf{Bm}}^{h}=\begin{bmatrix}\underline{0}_1\\ \underline{0}_2\\ \underline{I}_3^h\end{bmatrix}=\begin{bmatrix}\underline{0}_1\\ \underline{0}_2\\ N\cdot\underline{f}_3^{\,h}(\underline{V}_3^1,t_3^1,t_3^2,R_3,X_{L3},X_{C3},R_{D3})\end{bmatrix} \tag{4.19}$$

4.4.2. Simplified harmonic load flow

SHLF formulation data and unknowns for the electrical network given in Figure 4.2 are summarised in Table 4.7.

Stage	Bus	Data	Unknowns	Number of real unknowns
FLF_m (N_1)	Slack	$\underline{V}_1^1$	---	0
	PQ	P_2, Q_2	$\underline{V}_{N_1,2}^1$	2
	NL	$\underline{V}_{N_2,3}^h, R_3, X_{L3}, X_{C3}, R_{D3}$	$\underline{V}_{N_1,3}^1, t_{N_1,3}^1, t_{N_1,3}^2$	4
HA (N_2)	Slack	$\underline{V}_1^1, X_1^1$	---	0
	PQ	$\underline{Y}_2^k = \underline{f}_{Y_2}^k(V_{N_1,2}^1)$	---	0
	NL	$R_3, X_{L3}, X_{C3}, R_{D3}$	$\underline{V}_{N_2,3}^1, \underline{V}_{N_2,3}^h, t_{N_2,3}^1, t_{N_2,3}^2$	22
VN	Slack	X_1^1	$\underline{V}_1^h$	18
	PQ	$\underline{Y}_2^h = \underline{f}_{Y_2}^h(V_{N_1,2}^1)$	$\underline{V}_2^h$	18
	NL	$\underline{I}_3^h$	---	0

Table 4.7: SHLF formulation data and unknowns for the electrical network example

First of all, numerical resolution of FLF_m and HA stages must be performed in order to address the voltage node (VN) method. FLF_m stage will imply to solve the following equation system:

$$\begin{aligned}
&\mathrm{Re}\left\{\underline{V}_{N_1,2}^1\left(\underline{Y}_{21}^1\underline{V}_1^1+\underline{Y}_{22}^1\underline{V}_{N_1,2}^1+\underline{Y}_{23}^1\underline{V}_{N_1,3}^1\right)^*\right\}-P_2=0\\
&\mathrm{Im}\left\{\underline{V}_{N_1,2}^1\left(\underline{Y}_{21}^1\underline{V}_1^1+\underline{Y}_{22}^1\underline{V}_{N_1,2}^1+\underline{Y}_{23}^1\underline{V}_{N_1,3}^1\right)^*\right\}-Q_2=0\\
&\mathrm{Re}\left\{\underline{V}_{N_1,3}^1\left(\underline{Y}_{31}^1\underline{V}_1^1+\underline{Y}_{32}^1\underline{V}_{N_1,2}^1+\underline{Y}_{33}^1\underline{V}_{N_1,3}^1\right)^*\right\}-\mathrm{Re}\left\{\underline{V}_{N_1,3}^1\left(\underline{I}_3^1\right)^*\right\}=0\\
&\mathrm{Im}\left\{\underline{V}_{N_1,3}^1\left(\underline{Y}_{31}^1\underline{V}_1^1+\underline{Y}_{32}^1\underline{V}_{N_1,2}^1+\underline{Y}_{33}^1\underline{V}_{N_1,3}^1\right)^*\right\}-\mathrm{Im}\left\{\underline{V}_{N_1,3}^1\left(\underline{I}_3^1\right)^*\right\}=0\\
&nl_3^1(\underline{V}_{N_1,3}^1,\underline{V}_{N_2,3}^h,t_{N_1,3}^1,t_{N_1,3}^2,R_3,X_{L3},X_{C3},R_{D3})=0\\
&nl_3^2(\underline{V}_{N_1,3}^1,\underline{V}_{N_2,3}^h,t_{N_1,3}^1,t_{N_1,3}^2,R_3,X_{L3},X_{C3},R_{D3})=0
\end{aligned} \tag{4.20}$$

The fundamental current injected by the *N* single-phase uncontrolled rectifiers will be:

$$\underline{I}_3^1 = N\cdot\underline{f}_3^1(\underline{V}_{N_1,3}^1,\underline{V}_{N_2,3}^h,t_{N_1,3}^1,t_{N_1,3}^2,R_3,X_{L3},X_{C3},R_{D3}) \tag{4.21}$$

The harmonic voltages of the nonlinear load $\underline{V}^{h}_{\mathrm{N2,3}}$ are found by the numerical resolution of the HA stage.

In HA stage, the harmonic voltages $\underline{V}^{h}_{\mathrm{N2,3}}$ are found by converting the AC network to its Thévenin equivalent thereby eliminating all other buses and considering the unknowns at nonlinear bus only. Thévenin equivalent is calculated for fundamental and harmonic frequencies. The system for the fundamental frequency is shown in Figure 4.3 where the impedance at the bus 2 has been calculated under the hypothesis that power is produced by fundamental frequency only. This hypothesis allows not only the admittance of PQ bus at fundamental frequency to be modelled, but also at harmonic frequencies.

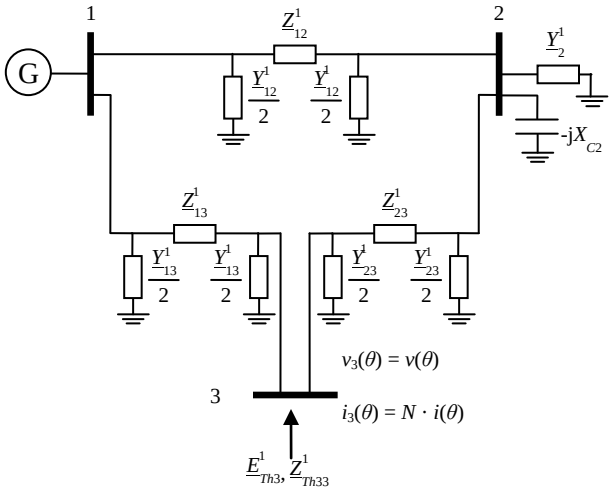

Figure 4.3: System under study for fundamental frequency

Figure 4.4 shows the AC network for the harmonic frequencies. The harmonic admittances at Slack bus are provided by equation (4.17) whereas harmonic admittances at PQ bus are provided by equation (4.18).

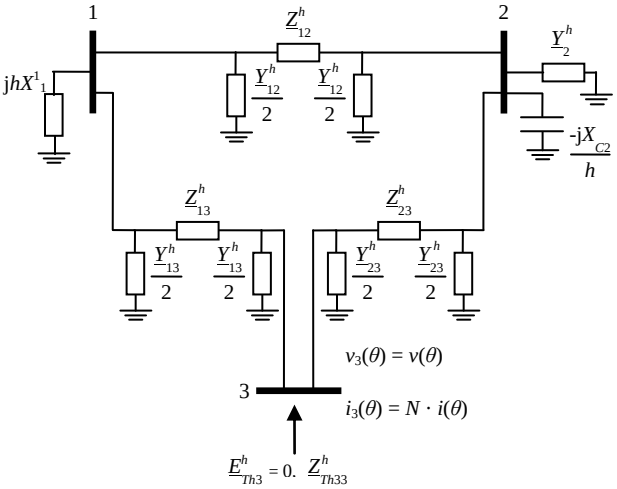

Figure 4.4: System under study for harmonic frequencies

Once the Thévenin equivalent of the AC network is seen from the nonlinear bus, the study of the problem is reduced to the equations corresponding to the circuits shown in Figure 4.5 and Figure 4.6 together with the equations that define the behaviour of the nonlinear load:

$$\begin{aligned} &\underline{V}^{k}_{\mathrm{N}_2,3} = \underline{E}^{k}_{Th3} + \underline{Z}^{k}_{Th33}\underline{I}^{k}_{3} \\ &nl^{1}_{3}(\underline{V}^{1}_{\mathrm{N}_2,3}, \underline{V}^{h}_{\mathrm{N}_2,3}, t^{1}_{\mathrm{N}_2,3}, t^{2}_{\mathrm{N}_2,3}, R_3, X_{L3}, X_{C3}, R_{D3}) = 0 \\ &nl^{2}_{3}(\underline{V}^{1}_{\mathrm{N}_2,3}, \underline{V}^{h}_{\mathrm{N}_2,3}, t^{1}_{\mathrm{N}_2,3}, t^{2}_{\mathrm{N}_2,3}, R_3, X_{L3}, X_{C3}, R_{D3}) = 0 \end{aligned} \tag{4.22}$$

where

$$\begin{aligned} &\underline{E}^{k}_{Th3} = \underline{f}^{k}_{ETh3}(\underline{V}^{1}_{\mathrm{N}_1,2}) \quad ; \quad \underline{Z}^{k}_{Th33} = \underline{f}^{k}_{ZTh33}(\underline{V}^{1}_{\mathrm{N}_1,2}) \\ &\underline{I}^{k}_{3} = N \cdot \underline{f}^{k}_{3}(\underline{V}^{1}_{\mathrm{N}_2,3}, \underline{V}^{h}_{\mathrm{N}_2,3}, t^{1}_{\mathrm{N}_2,3}, t^{2}_{\mathrm{N}_2,3}, R_3, X_{L3}, X_{C3}, R_{D3}) \end{aligned} \tag{4.23}$$

$\underline{V}^{1}_{\mathrm{N1,2}}$ are found by the numerical resolution of the $\mathrm{FLF_m}$ stage.

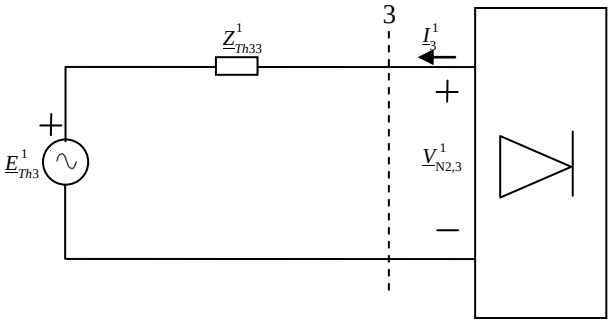

Figure 4.5: Thévenin equivalent circuit for fundamental frequency

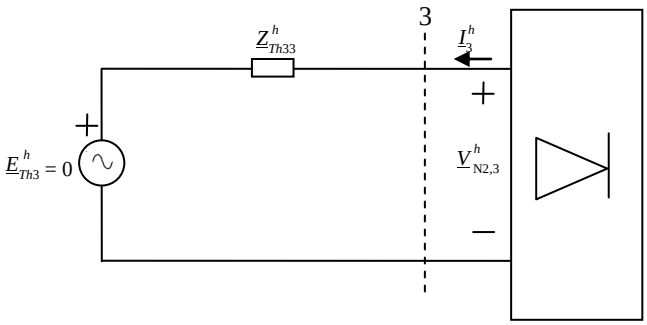

Figure 4.6: Thévenin equivalent circuit for harmonic frequencies

The HA stage will provide the fundamental voltages (in addition to harmonic voltages and nonlinear load unknowns) at bus 3, which are then compared to fundamental voltages of $\mathrm{FLF_m}$ stage at bus 3. This will indicate whether the iterative process between both nonlinear equation systems $\mathrm{N_1}$ and $\mathrm{N_2}$ has finished or not.

The number of real equations required in the numerical resolution of SHLF for the electrical network example are summarised in Table 4.8 for each bus.

Stage	Bus	Number of real equations
FLF_m (N_1)	Slack	0
	PQ	2·(2-1)=2
	NL	2·(3-2)+2=4
HA (N_2)	Slack	0
	PQ	0
	NL	2·(3-2)·10+2=22

Table 4.8: Number of real equations required by SHLF formulation

Once the iterative process between both nonlinear equation systems N_1 and N_2 has finished, the harmonic voltages for the rest of the electrical network can be calculated through the voltage node (VN) method by using equations (4.13) - (4.19).

4.4.3. Complete harmonic load flow

If power only at fundamental frequency is considered in power equations, CHLF formulation data and unknowns for the electrical network given in Figure 4.2 are summarised in Table 4.9.

Stage	Bus	Data	Unknowns	Number of real unknowns
CHLF	Slack	$\underline{V}_1^1, X_1^1$	$\underline{V}_1^h$	18
	PQ	P_2, Q_2	$\underline{V}_2^1, \underline{V}_2^h$	20
	NL	$R_3, X_{L3}, X_{C3}, R_{D3}$	$\underline{V}_3^1, \underline{V}_3^h, t_3^1, t_3^2$	22

Table 4.9: CHLF formulation data and unknowns for the electrical network example

CHLF implies to solve the following equation system:

$$
\begin{aligned}
&\mathrm{Re}\left\{\underline{V}_2^1\left(\underline{Y}_{21}^1\underline{V}_1^1+\underline{Y}_{22}^1\underline{V}_2^1+\underline{Y}_{23}^1\underline{V}_3^1\right)^*\right\}-P_2=0\\
&\mathrm{Im}\left\{\underline{V}_2^1\left(\underline{Y}_{21}^1\underline{V}_1^1+\underline{Y}_{22}^1\underline{V}_2^1+\underline{Y}_{23}^1\underline{V}_3^1\right)^*\right\}-Q_2=0\\
&\mathrm{Re}\left\{\underline{Y}_{11}^h\underline{V}_1^h+\underline{Y}_{12}^h\underline{V}_2^h+\underline{Y}_{13}^h\underline{V}_3^h\right\}-\mathrm{Re}\left\{-\underline{Y}_1^h\cdot\underline{V}_1^h\right\}=0\\
&\mathrm{Im}\left\{\underline{Y}_{11}^h\underline{V}_1^h+\underline{Y}_{12}^h\underline{V}_2^h+\underline{Y}_{13}^h\underline{V}_3^h\right\}-\mathrm{Im}\left\{-\underline{Y}_1^h\cdot\underline{V}_1^h\right\}=0\\
&\mathrm{Re}\left\{\underline{Y}_{21}^h\underline{V}_1^h+\underline{Y}_{22}^h\underline{V}_2^h+\underline{Y}_{23}^h\underline{V}_3^h\right\}-\mathrm{Re}\left\{-\underline{Y}_2^h\cdot\underline{V}_2^h\right\}=0\\
&\mathrm{Im}\left\{\underline{Y}_{21}^h\underline{V}_1^h+\underline{Y}_{22}^h\underline{V}_2^h+\underline{Y}_{23}^h\underline{V}_3^h\right\}-\mathrm{Im}\left\{-\underline{Y}_2^h\cdot\underline{V}_2^h\right\}=0\\
&\mathrm{Re}\left\{\underline{Y}_{31}^k\underline{V}_1^k+\underline{Y}_{32}^k\underline{V}_2^k+\underline{Y}_{33}^k\underline{V}_3^k\right\}-\mathrm{Re}\left\{\underline{I}_3^k\right\}=0\\
&\mathrm{Im}\left\{\underline{Y}_{31}^k\underline{V}_1^k+\underline{Y}_{32}^k\underline{V}_2^k+\underline{Y}_{33}^k\underline{V}_3^k\right\}-\mathrm{Im}\left\{\underline{I}_3^k\right\}=0\\
&nl_3^1(\underline{V}_3^1,\underline{V}_3^h,t_3^1,t_3^2,R_3,X_{L3},X_{C3},R_{D3})=0\\
&nl_3^2(\underline{V}_3^1,\underline{V}_3^h,t_3^1,t_3^2,R_3,X_{L3},X_{C3},R_{D3})=0
\end{aligned}
\tag{4.24}
$$

where

$$
\underline{I}_3^k=N\cdot\underline{f}_3^k(\underline{V}_3^1,\underline{V}_3^h,t_3^1,t_3^2,R_3,X_{L3},X_{C3},R_{D3}) \tag{4.25}
$$

The number of real equations required in the numerical resolution of CHLF for the electrical network example are summarised in Table 4.10 for each bus.

Stage	Bus	Number of real equations
CHLF	Slack	2·(10-1)=18
	PQ	2·(2-1)·10=20
	NL	2·(3-2)·10+2=22

Table 4.10: Number of real equations required by CHLF formulation

4.4.4. Improved unified harmonic load flow

IUHLF formulation data and unknowns for the electrical network given in Figure 4.2 are summarised in Table 4.11.

Stage	Bus	Data	Unknowns	Number of real unknowns
CHLF$_m$	Slack	$\underline{V}_1^1$	---	0
	PQ	P_2, Q_2	$\underline{V}_2^1$	2
	NL	$R_3, X_{L3}, X_{C3}, R_{D3}$	$\underline{V}_3^1, \underline{V}_3^h, t_3^1, t_3^2$	22

VN	Slack	X_1^1	$\underline{V}_1^h$	18
	PQ	$\underline{Y}_2^h = \underline{f}_{Y_2}^h\left(V_2^1\right)$	$\underline{V}_2^h$	18
	NL	$\underline{I}_3^h$	---	---

Table 4.11: IUHLF formulation data and unknowns for the electrical network example

IUHLF implies to solve the following equation system:

$$\begin{aligned}
&\mathrm{Re}\left\{\underline{V}_2^1\left(\underline{Y}_{21}^1\underline{V}_1^1+\underline{Y}_{22}^1\underline{V}_2^1+\underline{Y}_{23}^1\underline{V}_3^1\right)^*\right\}-P_2=0\\
&\mathrm{Im}\left\{\underline{V}_2^1\left(\underline{Y}_{21}^1\underline{V}_1^1+\underline{Y}_{22}^1\underline{V}_2^1+\underline{Y}_{23}^1\underline{V}_3^1\right)^*\right\}-Q_2=0\\
&\underline{V}_3^k=\underline{E}_{Th3}^k+\underline{Z}_{Th33}^k\underline{I}_3^k\\
&nl_3^1(\underline{V}_3^1,\underline{V}_3^h,t_3^1,t_3^2,R_3,X_{L3},X_{C3},R_{D3})=0\\
&nl_3^2(\underline{V}_3^1,\underline{V}_3^h,t_3^1,t_3^2,R_3,X_{L3},X_{C3},R_{D3})=0
\end{aligned} \tag{4.26}$$

where

$$\begin{aligned}
&\underline{E}_{Th3}^k=\underline{f}_{ETh3}^k(\underline{V}_2^1)\quad;\quad \underline{Z}_{Th33}^k=\underline{f}_{ZTh33}^k(\underline{V}_2^1)\\
&\underline{I}_3^k=N\cdot\underline{f}_3^k(\underline{V}_3^1,\underline{V}_3^h,t_3^1,t_3^2,R_3,X_{L3},X_{C3},R_{D3})
\end{aligned} \tag{4.27}$$

The number of real equations required in the numerical resolution of IUHLF for the electrical network example are summarised in Table 4.12 for each bus.

Stage	Bus	Number of real equations
$CHLF_m$	Slack	0
	PQ	2·(2-1)=2
	NL	2·(3-2)·10+2=22

Table 4.12: Number of real equations required by IUHLF formulation

Once $CHLF_m$ stage has finished, the harmonic voltages for the rest of the electrical network can be calculated through the voltage node (VN) method by using equations (4.13) - (4.19).

4.4.5. Obtained results

The obtained results for the studied electrical network and for HP, SHLF, CHLF and IUHLF formulations are shown through Tables 4.13 to 4.20. The main goal of this subsection is to compare these results. In order to analyse the effect of the harmonic voltage distortion level on the obtained results for the four HLF formulations, this level is varied by connecting a number *N*

of nonlinear loads to the network. Five harmonic voltage distortion levels are considered and applied to the electrical network, from N=1 (the lowest level) to N=5 (the highest level).

It was observed that SHLF, CHLF and IUHLF formulations, for the first odd ten frequencies and the five harmonic voltage distortion levels considered, lead to almost same results with very little difference. Therefore, in order to avoid repetition of the same set of values for SHLF, CHLF and IUHLF formulations, average results are shown in Tables 4.14, 4.16, 4.18 and 4.20.

	N=1	N=2	N=3	N=4	N=5
$\underline{V}_1^1$	1∠0°	1∠0°	1∠0°	1∠0°	1∠0°
$\underline{V}_1^3$	0.0022∠-170.5737°	0.0044∠-170.6555°	0.0067∠-170.7373°	0.0089∠-170.8190°	0.0111∠-170.9007°
$\underline{V}_1^5$	0.0037∠137.0732°	0.0074∠136.9369°	0.0110∠136.8006°	0.0147∠136.6645°	0.0184∠136.5284°
$\underline{V}_1^7$	0.0052∠84.6883°	0.0103∠84.4974°	0.0155∠84.3067°	0.0207∠84.1161°	0.0258∠83.9256°
$\underline{V}_1^9$	0.0069∠32.5513°	0.0138∠32.3060°	0.0207∠32.0607°	0.0276∠31.8156°	0.0345∠31.5707°
$\underline{V}_1^{11}$	0.0097∠-19.1712°	0.00194∠-19.4711°	0.0291∠-19.7708°	0.0388∠-20.0703°	0.0484∠-20.3697°
$\underline{V}_1^{13}$	0.00194∠-70.7979°	0.0388∠-71.1524°	0.0582∠-71.5066°	0.0776∠-71.8606°	0.0969∠-72.2144°
$\underline{V}_1^{15}$	0.0276∠65.9631°	0.0551∠65.5546°	0.0826∠65.1463°	0.1102∠64.7383°	0.1377∠64.3305°
$\underline{V}_1^{17}$	0.0045∠17.3675°	0.0090∠16.9042°	0.0135∠16.4411°	0.0180∠15.9783°	0.0225∠15.5158°
$\underline{V}_1^{19}$	0.0015∠-22.5044°	0.0030∠-23.0222°	0.0044∠-23.5398°	0.0059∠-24.0571°	0.0074∠-24.5741°

Table 4.13: Fundamental and harmonic voltages (pu) at Slack bus by using HP formulation

	N=1	N=2	N=3	N=4	N=5
$\underline{V}_1^1$	1∠0°	1∠0°	1∠0°	1∠0°	1∠0°
$\underline{V}_1^3$	0.002∠155.8072°	0.0034∠130.5895°	0.0044∠106.2158°	0.0052∠94.08°	0.0059∠83.8087°
$\underline{V}_1^5$	0.0032∠80.9822°	0.0057∠38.9187°	0.0073∠-1.4791°	0.0086∠-21.8606°	0.0097∠-39.0493°
$\underline{V}_1^7$	0.0045∠6.0294°	0.0079∠-52.9363°	0.0103∠-109.0621°	0.0121∠-137.8979°	0.0135∠-162.1044°
$\underline{V}_1^9$	0.006∠-68.8258°	0.0104∠-144.7858°	0.0137∠143.7026°	0.016∠106.1569°	0.0177∠74.7992°
$\underline{V}_1^{11}$	0.0083∠-143.4911°	0.0143∠123.4071°	0.019∠36.8384°	0.022∠-9.7036°	0.0243∠-48.3791°
$\underline{V}_1^{13}$	0.0163∠141.6107°	0.0277∠31.1249°	0.0366∠-70.2612°	0.0421∠-126.1237°	0.0463∠-172.3285°
$\underline{V}_1^{15}$	0.0222∠-105.3589°	0.037∠126.3498°	0.0474∠10.1693°	0.0545∠-55.4411°	0.0599∠-109.4859°
$\underline{V}_1^{17}$	0.0034∠-178.1487°	0.0053∠34.9699°	0.0062∠-96.5023°	0.0072∠-172.7242°	0.0079∠124.7265°
$\underline{V}_1^{19}$	0.0009∠119.0576°	0.0013∠-47.3375°	0.0009∠165.2717°	0.0011∠73.4039°	0.0013∠-1.3899°

Table 4.14: Fundamental and harmonic voltages (pu) at Slack bus by using SHLF, CHLF and IUHLF formulations

At Slack bus, the comparison of harmonic voltage values between HP and the rest of the formulation leads to observation that for low distortion the results are almost similar for harmonic voltage amplitudes, but not for angles as there is too much difference of harmonic voltage angles between HP and the rest of the formulations. Similarly, when distortion is increased by increasing the number *N* of nonlinear loads, HP leads to high harmonic voltage values as compared to rest of the harmonic formulations.

	N=1	*N*=2	*N*=3	*N*=4	*N*=5
$\underline{V}_2^1$	0.9996∠-0.1717°	0.9995∠-0.1854°	0.9993∠-0.1990°	0.9992∠-0.2126°	0.9990∠-0.2262°
$\underline{V}_2^3$	0.0031∠-170.9078°	0.0062∠-170.989°	0.0092∠-171.072°	0.0123∠-171.153°	0.0154∠-171.235°
$\underline{V}_2^5$	0.0052∠136.8484°	0.0104∠136.7120°	0.0155∠136.5758°	0.0207∠136.4396°	0.0259∠136.3035°
$\underline{V}_2^7$	0.0075∠84.5040°	0.0149∠84.3131°	0.0224∠84.1224°	0.0298∠83.9318°	0.0373∠83.7412°
$\underline{V}_2^9$	0.0103∠32.3825°	0.0206∠32.1372°	0.0309∠31.8919°	0.0412∠31.6469°	0.0515∠31.4019°
$\underline{V}_2^{11}$	0.0152∠-19.3373°	0.0303∠-19.6372°	0.0455∠-19.9369°	0.0606∠-20.2365°	0.0758∠-20.5358°
$\underline{V}_2^{13}$	0.0322∠-70.9701°	0.0644∠-71.3254°	0.0965∠-71.6788°	0.1287∠-72.0328°	0.1608∠-72.3866°
$\underline{V}_2^{15}$	0.0492∠65.7775°	0.0984∠65.3690°	0.1475∠64.9607°	0.1966∠64.5527°	0.2457∠64.1449°
$\underline{V}_2^{17}$	0.0088∠17.1604°	0.0176∠16.6971°	0.0264∠16.2340°	0.0352∠15.7712°	0.0440∠15.3087°
$\underline{V}_2^{19}$	0.0032∠-22.7432°	0.0097∠-23.2610°	0.0097∠-23.7786°	0.0129∠-24.2959°	0.0161∠-24.8129°

Table 4.15: Fundamental and harmonic voltages (pu) at PQ bus by using HP formulation

	N=1	*N*=2	*N*=3	*N*=4	*N*=5
$\underline{V}_2^1$	0.9996∠-0.1684°	0.9994∠-0.1735°	0.9993∠-0.174°	0.9992∠-0.1748°	0.9991∠-0.1746°
$\underline{V}_2^3$	0.0027∠155.4731°	0.0047∠130.2553°	0.006∠105.8817°	0.0072∠93.7458°	0.0081∠83.4745°
$\underline{V}_2^5$	0.0045∠80.7573°	0.0079∠38.6939°	0.0102∠-1.704°	0.0121∠-22.0854°	0.0136∠-39.2742°
$\underline{V}_2^7$	0.0065∠5.8451°	0.0114∠-53.1206°	0.0148∠-109.246°	0.0174∠-138.0822°	0.0194∠-162.2887°
$\underline{V}_2^9$	0.009∠-68.9945°	0.0155∠-144.9546°	0.0205∠143.5338°	0.0239∠105.9881°	0.0265∠74.6304°
$\underline{V}_2^{11}$	0.013∠-143.6572°	0.0224∠123.2409°	0.0297∠36.6723°	0.0344∠-9.8698°	0.038∠-48.5452°
$\underline{V}_2^{13}$	0.027∠141.4385°	0.046∠30.9527°	0.0607∠-70.4334°	0.0698∠-126.2959°	0.0769∠-172.5007°
$\underline{V}_2^{15}$	0.0397∠-105.5445°	0.0661∠126.1642°	0.0846∠9.9837°	0.0973∠-55.6268°	0.1069∠-109.6715°
$\underline{V}_2^{17}$	0.0066∠-178.3558°	0.0104∠34.7628°	0.0121∠-96.7094°	0.014∠-172.9313°	0.0154∠124.5194°
$\underline{V}_2^{19}$	0.002∠118.8188°	0.0027∠-47.5763°	0.0021∠165.0329°	0.0025∠73.1651°	0.0028∠-1.6287°

Table 4.16: Fundamental and harmonic voltages (pu) at PQ bus by using SHLF, CHLF and IUHLF formulations

At PQ bus, HP is able to correctly estimate the fundamental voltages for all number *N* of nonlinear loads when we compare their values with those of the other formulations, but results in

overestimation of the harmonic voltages when distortion is increased. This is due to the fact that HP is a modified form of fundamental load flow without considering the harmonic interaction of nonlinear bus with AC network.

	N=1	*N*=2	*N*=3	*N*=4	*N*=5
$\underline{V}_3^1$	0.9996∠-0.1604°	0.9993∠-0.1337°	0.9990∠-0.1609°	0.9987∠-0.1881°	0.9984∠-0.2153°
$\underline{V}_3^3$	0.0039∠-170.9224°	0.0077∠-170.0042°	0.0116∠-171.0860°	0.0154∠-171.1678°	0.0193∠-171.2494°
$\underline{V}_3^5$	0.0063∠136.8841°	0.0126∠136.7477°	0.0189∠136.6115°	0.0252∠136.4753°	0.0315∠136.3392°
$\underline{V}_3^7$	0.0087∠84.5744°	0.0173∠84.3836°	0.0260∠84.1928°	0.0346∠84.0022°	0.0433∠83.8117°
$\underline{V}_3^9$	0.0112∠32.4883°	0.0224∠32.2429°	0.0336∠31.9977°	0.0448∠31.7526°	0.0559∠31.5077°
$\underline{V}_3^{11}$	0.0150∠-19.1901°	0.0300∠-19.4900°	0.0451∠-19.7897°	0.0601∠-20.0892°	0.0751∠-20.3886°
$\underline{V}_3^{13}$	0.0282∠-70.7694°	0.0564∠-71.1238°	0.0846∠-71.4780°	0.1128∠-71.8320°	0.1409∠-72.1858°
$\underline{V}_3^{15}$	0.0366∠66.0539°	0.0731∠65.6454°	0.1096∠65.2371°	0.1462∠64.8291°	0.1826∠64.4213°
$\underline{V}_3^{17}$	0.0052∠17.5573°	0.0104∠17.0940°	0.0156∠16.6309°	0.0208∠15.1681°	0.0260∠15.7056°
$\underline{V}_3^{19}$	0.0014∠-22.1160°	0.0027∠-23.6339°	0.0041∠-23.1515°	0.0054∠-23.6687°	0.0068∠-24.1857°

Table 4.17: Fundamental and harmonic voltages (pu) at NL bus by using HP formulation

	N=1	*N*=2	*N*=3	*N*=4	*N*=5
$\underline{V}_3^1$	0.9996∠-0.0998°	0.9992∠-0.11°	0.9989∠-0.1108°	0.9987∠-0.1123°	0.9985∠-0.1119°
$\underline{V}_3^3$	0.0034∠155.4584°	0.006∠130.2407°	0.0076∠105.8671°	0.009∠93.7313°	0.0102∠83.46°
$\underline{V}_3^5$	0.0055∠80.793°	0.0097∠38.7296°	0.0124∠-1.6683°	0.0148∠-22.0497°	0.0165∠-39.2385°
$\underline{V}_3^7$	0.0076∠5.9155°	0.0132∠-53.0501°	0.0172∠-109.176°	0.0202∠-138.0118°	0.0225∠-162.2183°
$\underline{V}_3^9$	0.0097∠-68.8888°	0.0169∠-144.8488°	0.0222∠143.6396°	0.0259∠106.0939°	0.0288∠74.7362°
$\underline{V}_3^{11}$	0.0129∠-143.51°	0.0222∠123.3882°	0.0294∠36.8195°	0.034∠-9.7225°	0.0376∠-48.398°
$\underline{V}_3^{13}$	0.0237∠141.6392°	0.0403∠31.1534°	0.0532∠-70.2326°	0.0612∠-126.0951°	0.0674∠-172.2999°
$\underline{V}_3^{15}$	0.0295∠-105.2681°	0.0491∠126.4406°	0.0629∠10.2601°	0.0723∠-55.3503°	0.0795∠-109.3951°
$\underline{V}_3^{17}$	0.0039∠-177.9589°	0.0062∠35.1597°	0.0072∠-96.3125°	0.0083∠-172.5344°	0.0091∠124.9163°
$\underline{V}_3^{19}$	0.0008∠119.4459°	0.0012∠-46.9492°	0.0009∠165.66°	0.001∠73.7922°	0.0012∠-1.0016°

Table 4.18: Fundamental and harmonic voltages (pu) at NL bus by using SHLF, CHLF and IUHLF formulations

At NL bus, non-interaction hypothesis of the nonlinear load with the AC network results in high harmonic voltages for the bus as evident from the comparison of the harmonic voltage values between the two tables. The difference of values is more significant when distortion is increased by increasing the number *N* of nonlinear loads.

	N=1	N=2	N=3	N=4	N=5
$\underline{I}_3^1$	0.1623∠153.5356°	0.3244∠153.5083°	0.4865∠153.4811°	0.6484∠153.4538°	0.8103∠153.4266°
$\underline{I}_3^3$	0.1564∠100.6490°	0.3127∠100.5672°	0.4689∠100.4855°	0.6250∠100.4038°	0.7810∠100.3222°
$\underline{I}_3^5$	0.1451∠47.8948°	0.2902∠47.7586°	0.4352∠47.6223°	0.5801∠47.4862°	0.7249∠47.3502°
$\underline{I}_3^7$	0.1295∠-4.6183°	0.2589∠-4.8091°	0.3882∠-4.9998°	0.5175∠-5.1904°	0.6467∠-5.3808°
$\underline{I}_3^9$	0.1107∠-56.7439°	0.2213∠-56.9893°	0.3319∠-57.2344°	0.4424∠-57.4795°	0.5528∠-57.7244°
$\underline{I}_3^{11}$	0.0902∠-108.2631°	0.1804∠-108.5629°	0.2705∠-108.8626°	0.3606∠-109.1621°	0.4506∠-109.4614°
$\underline{I}_3^{13}$	0.0696∠-158.8128°	0.1392∠-159.1671°	0.2088∠-159.5213°	0.2783∠-159.8752°	0.3478∠-160.2289°
$\underline{I}_3^{15}$	0.0503∠152.2782°	0.1007∠151.8694°	0.1509∠151.4607°	0.2012∠151.0523°	0.2514∠150.6442°
$\underline{I}_3^{17}$	0.0336∠106.4127°	0.0672∠105.9494°	0.1007∠105.4862°	0.1342∠105.0234°	0.1677∠104.5608°
$\underline{I}_3^{19}$	0.0204∠66.8878°	0.06131∠66.3699°	0.06131∠65.8523°	0.0817∠63.335°	0.1020∠64.8180°

Table 4.19: Fundamental and harmonic currents (pu) at NL bus by using HP formulation

	N=1	N=2	N=3	N=4	N=5
$\underline{I}_3^1$	0.1432∠142.3349°	0.2506∠133.9323°	0.317∠125.784°	0.3795∠121.7551°	0.4272∠118.3384°
$\underline{I}_3^3$	0.1378∠67.0299°	0.241∠41.8122°	0.3067∠17.4386°	0.3659∠5.3029°	0.4112∠-4.9684°
$\underline{I}_3^5$	0.1276∠-8.1962°	0.2228∠-50.2596°	0.2865∠-90.6574°	0.3395∠-111.0388°	0.3803∠-128.2276°
$\underline{I}_3^7$	0.1133∠-83.2772°	0.1972∠-142.2428°	0.2569∠161.6314°	0.302∠132.7957°	0.3369∠108.5892°
$\underline{I}_3^9$	0.0961∠-158.121°	0.1666∠125.919°	0.2196∠54.4074°	0.2559∠16.8618°	0.2842∠-14.4959°
$\underline{I}_3^{11}$	0.0773∠127.417°	0.1331∠34.3152°	0.1767∠-52.2534°	0.2044∠-98.7954°	0.2259∠-137.4708°
$\underline{I}_3^{13}$	0.0584∠53.5959°	0.0994∠-56.8899°	0.1313∠-158.2759°	0.151∠145.8617°	0.1663∠99.6569°
$\underline{I}_3^{15}$	0.0406∠-19.0438°	0.0676∠-147.3355°	0.0866∠96.4837°	0.0996∠30.8729°	0.1094∠-23.1721°
$\underline{I}_3^{17}$	0.025∠-89.1035°	0.0397∠124.015°	0.0462∠-7.4572°	0.0535∠-83.6791°	0.0588∠-146.2284°
$\underline{I}_3^{19}$	0.0127∠-151.5502°	0.0173∠42.0546°	0.0131∠-105.3362°	0.0157∠162.796°	0.0174∠88.0022°

Table 4.20: Fundamental and harmonic currents (pu) at NL bus by using SHLF, CHLF and IUHLF formulations

At NL bus, it can be noticed that the higher the *N* value is, the greater the obtained fundamental and harmonic currents are for all formulations. In addition, regarding HP formulation, this increase in the obtained currents is clearly proportional to the *N* value.

It is seen that HP offers simplicity and a fewer number of equations to be used for the numerical resolution of the harmonic problem, but the technique often leads to incorrect results due to the hypothesis of non-interaction between the nonlinear load and AC network.

Other HLF formulations consider the interaction between the nonlinear load and AC network, usually leading to correct results. However, the procedure followed differs from one formulation to another:

- The HLF formulations which offer harmonic interaction with a fewer number of equations to be used for the numerical resolution of the harmonic problem are UHLF and IUHLF. This is achieved by transforming the AC network to its Thévenin equivalent and not considering the harmonic voltages of Slack and PQ buses in the numerical resolution of the harmonic problem. The harmonic voltages of Slack and PQ buses are found later after the numerical resolution by applying the voltage node method.

- CHLF is the most computationally extensive formulation and requires the largest number of equations to be solved during the numerical resolution of the harmonic problem. This is because this particular formulation considers the harmonic interaction at each bus, i.e., the Slack bus, the PQ bus and the NL bus thereby increasing the number of unknowns to be determined for reaching the numerical solution of the harmonic problem.

- SHLF also offers harmonic interaction with few equations to be used for the numerical resolution of the harmonic problem, but it carries the disadvantage of the implementation of two numerical procedures in order to reach the numerical solution of the harmonic problem.

5. Newton-Raphson method vs. nonlinear least-squares methods in harmonic load flow resolution

In this chapter we are going to present the results of different harmonic formulations and try to make discussions and observations based on the results thereby validating and concluding the theory proposed in previous chapters. The HLF problem associated with the three-bus network in Figure 5.1(a) is solved by using the HLF formulations in Chapter 2 (HP, SHLF and CHLF) and the improved HLF formulation in Chapter 4 (IUHLF) so as to compare their performances. Typical NLLs, specifically single-phase uncontrolled rectifiers, connected to bus 3, and an increasing number N of these NLLs at the bus, are considered to analyse the behaviour of the different formulations in a context of high voltage distortion.

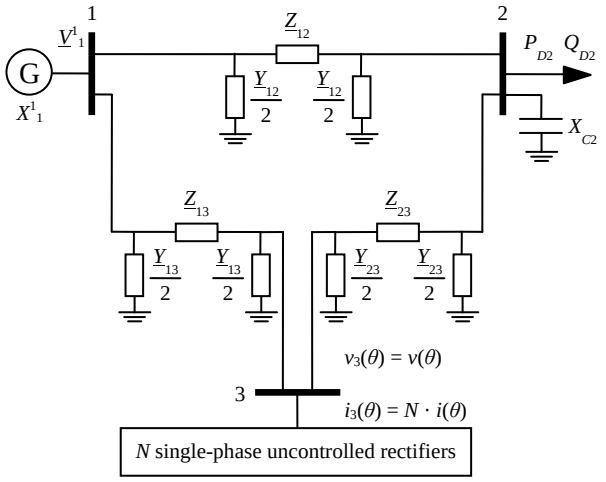

Figure 5.1(a): Three-bus network.

The circuit of a single-phase uncontrolled rectifier [50] is shown in Figure 5.1(b) and its supply voltage v, ac consumed current i and dc voltage waveforms are depicted in Figure 5.1(c), where $\omega = 2\pi \cdot f$ and f is the fundamental frequency of the supply system. A distorted supply voltage v is considered in the rectifier model to allow harmonic interaction to be assumed in NLL behaviour. The commutation angles θ^i are the NLL state variables, whose values must be determined irrespective of HLF formulation, i.e., they are always unknowns in the HLF resolution. The half-wave symmetry hypothesis is considered; therefore, only θ^1 and θ^2 must be determined since the commutation angles verify the relation $\theta^{j+2} = \theta^j + \pi$ (j = 1, 2).

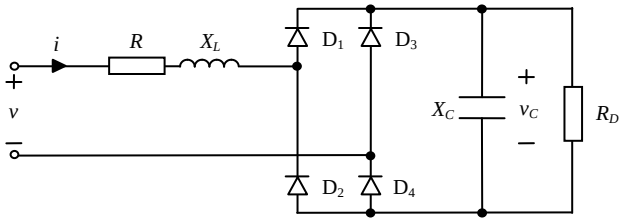

$$v(\theta) = \sqrt{2} \cdot V^1 \cos\left(\theta + \phi_{V^1}\right) + \sum_{h=3}^{5,7,\ldots} \sqrt{2} \cdot V^h \cos\left(h\theta + \phi_{V^h}\right) \quad , \quad \theta = \omega \cdot t$$

Figure 5.1(b): Single-phase uncontrolled rectifier circuit.

Resonance is also introduced in the AC network to observe the characteristics of harmonic voltages under the influence of resonances.

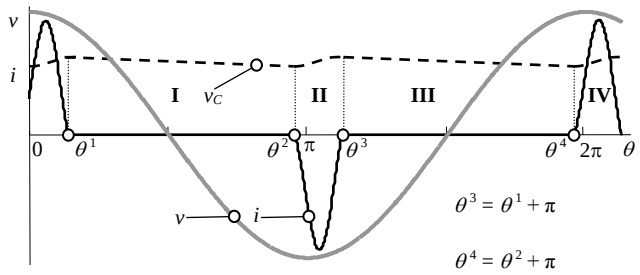

Figure 5.1(c): Supply voltage v, ac current i and dc voltage v_C waveforms.

The data of the whole network were summarised in Table 4.4.

5.1. Study of HLF formulation convergences

To reach the numerical solution of the proposed electrical network, two numerical methods are used. The first is the Newton-Raphson method, which is one of the most famous methods conventionally used for the numerical resolution of AC networks. The second is the Levenberg-Marquardt method (which includes Gauss-Newton method as a particular case), based on nonlinear least-squares approach. The basic idea is to observe the convergence of HLF formulations under both numerical methods and also to compare the effectiveness of both numerical methods when deployed for the numerical resolution of the harmonic problem.

5.1.1. Newton-Raphson method

The evolutions of $||x^{(\alpha+1)} - x^{(\alpha)}||$ and $||F(x)||$ for the AC network, when HP, SHLF, CHLF and IUHLF formulations are used and the Newton-Raphson method is applied, are given in Figure 5.2. As we know that Newton-Raphson method exhibits better convergence if the starting point is close to the solution, a starting point was chosen for all used HLF formulations, which was close to the solution of the harmonic problem.

From a common initial value $x^{(0)}$ for all used formulations, Newton-Raphson convergence was checked from the condition $||x^{(\alpha+1)} - x^{(\alpha)}|| < 10^{-3}$, and the terms of the Jacobian matrix were calculated by the finite difference approach (the only feasible choice for complicated networks). SHLF fixed-point iteration convergence was checked by considering $\varepsilon = 10^{-5}$ in equation (3.16).

Figure 5.2(a) shows the evolution of $||x^{(\alpha+1)} - x^{(\alpha)}||$ versus the Newton-Raphson iteration (α+1) for all used formulations and five different numbers N of single-phase uncontrolled rectifiers. The purpose of increasing N is to increase the voltage distortion in the AC network and observe the convergence of different HLF formulations under unstable conditions. In SHLF formulation, evolutions associated with the FLF_m and HA stages are plotted in sequence.

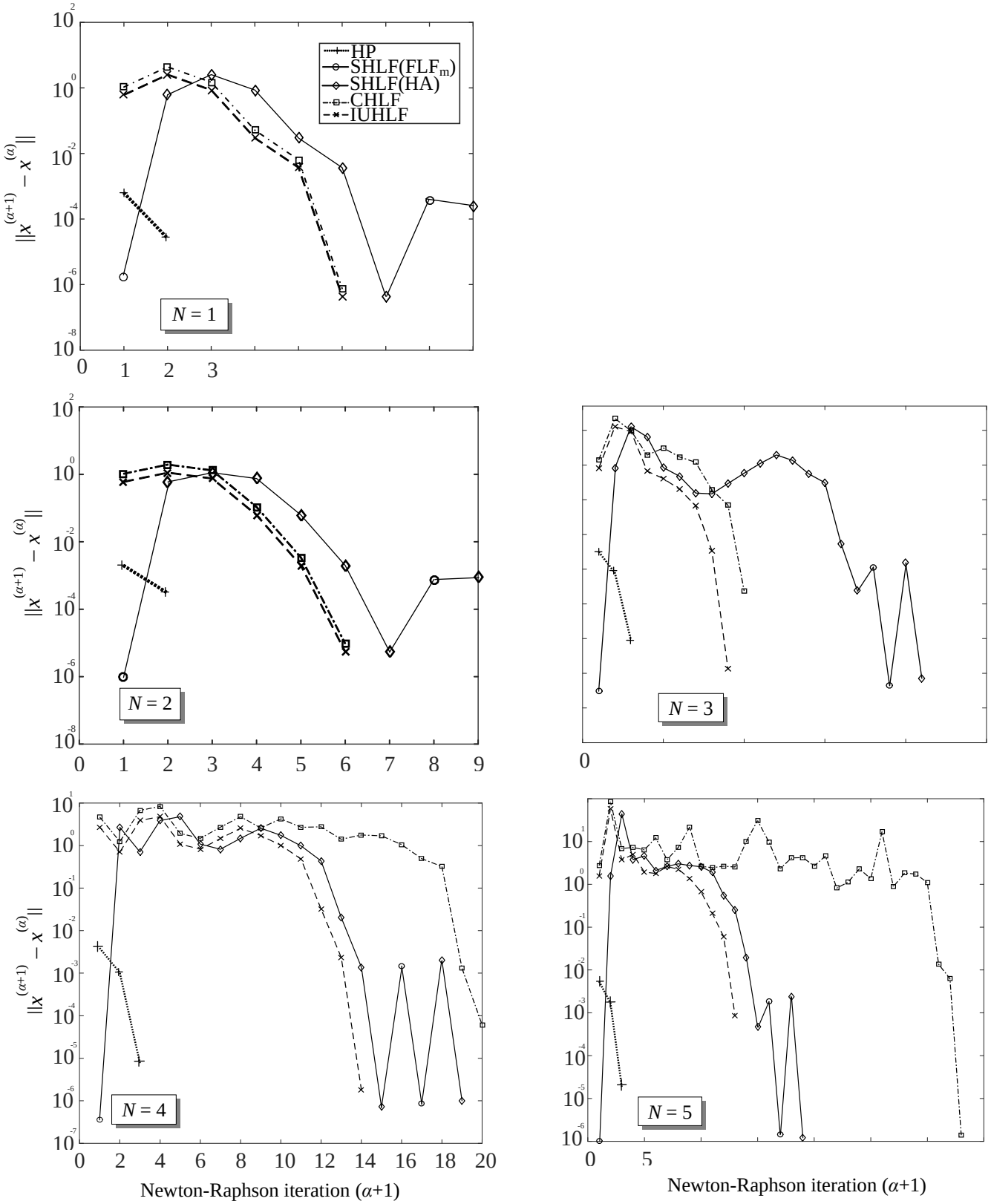

Figure 5.2(a): Evolution of $||x^{(\alpha+1)} - x^{(\alpha)}||$ versus the Newton-Raphson iteration (α+1)

Figure 5.2(b) shows the evolution of ||F(x)|| versus the Newton-Raphson iteration (α+1) for all used formulations and five different numbers N of single-phase uncontrolled rectifiers.

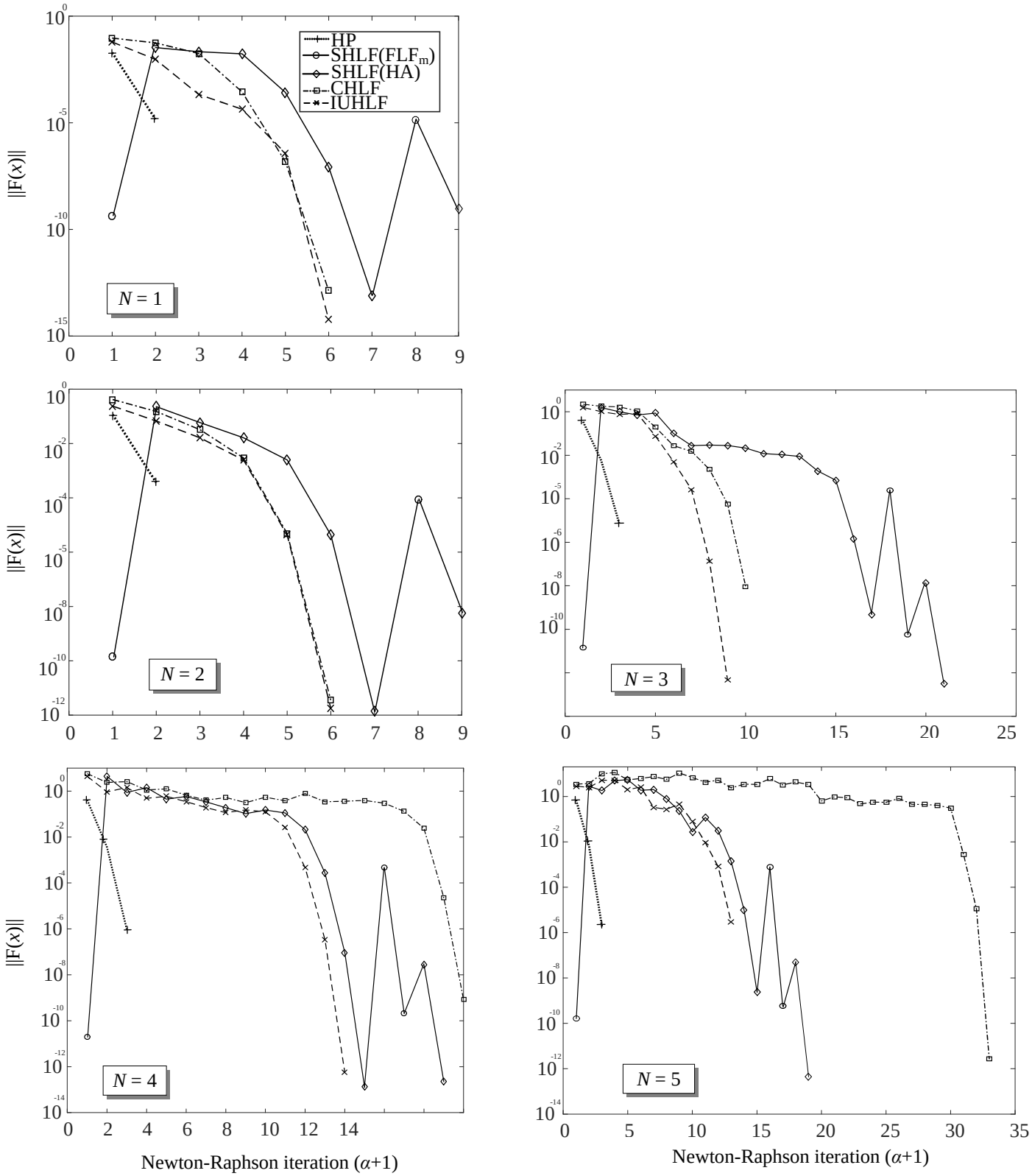

Figure 5.2(b): Evolution of ||F(x)|| versus the Newton-Raphson iteration (α+1)

It can be noticed that greater values of N generally lead to a higher number of iterations to the problem solution. This increase in the number of iterations is especially pronounced for CHLF

formulation, coherently exceeding for all values of N what is expected in a context of scarcely distorted voltages. It is also observed that HP and IUHLF formulations require a smaller number of iterations to the problem solution irrespective of N. Therefore, it can be concluded that both formulations are the best in terms of convergence.

Comparison between the evolutions of $||x^{(\alpha+1)} - x^{(\alpha)}||$ and $||F(x)||$ also leads to some interesting findings. It is observed that evolution of the step size $||x^{(\alpha+1)} - x^{(\alpha)}||$ towards the tolerance limit is very slow as compared to the evolution of error function $||F(x)||$. E.g. when $N = 1$, for IUHLF the step size $||x^{(\alpha+1)} - x^{(\alpha)}||$ takes 6 iterations to reach tolerance limit of 10^{-3} whereas the error function $||F(x)||$ reaches the limit 10^{-14} in these 6 iterations.

The total number of iterations taken by each HLF formulation to reach the numerical solution of the harmonic problem setting the step size tolerance limit at $||x^{(\alpha+1)} - x^{(\alpha)}|| < 10^{-3}$ is summarised in Table 5.1.

Number of NLLs (N)	HP number of iterations	CHLF number of iterations	SHLF number of iterations	IUHLF number of iterations
1	2	6	(1+1)+(6+1)	6
2	3	6	(1+1)+(6+1)	6
3	3	10	(1+2)+(16+2)	9
4	3	20	(1+2)+(14+2)	14
5	3	33	(1+2)+(15+2)	13

Table 5.1: Total number of iterations taken by each HLF formulation with varying NLLs (N)

As observed from Table 5.1, the CHLF, SHLF and IUHLF have almost the same performance when the value of N is at its minimum. However, when the value of N is changed to higher values, the difference between HLF formulations becomes more significant. The highest increase in number of iterations observed is CHLF, which exposes CHLF to convergence problems for higher number of nonlinear loads. HP is the most economical HLF, but provides inaccurate results when nonlinearity is increased by increasing values of N. SHLF is also a feasible solution for the numerical resolution of the harmonic problem, but has the disadvantage of using two numerical procedures to reach the numerical solution which might result in convergence problems.

In order to increase the accuracy of the results for the HLF formulations, the step size tolerance is set to a lower value and numerical resolution is performed again. From a common initial value $x^{(0)}$ for all used formulations, Newton-Raphson convergence was checked from the condition $||x^{(\alpha+1)} - x^{(\alpha)}|| < 10^{-4}$. Figure 5.3(a) shows the evolution of $||x^{(\alpha+1)} - x^{(\alpha)}||$ versus the Newton Raphson iteration (α+1) for all used formulations and five different numbers N of single-phase uncontrolled rectifiers.

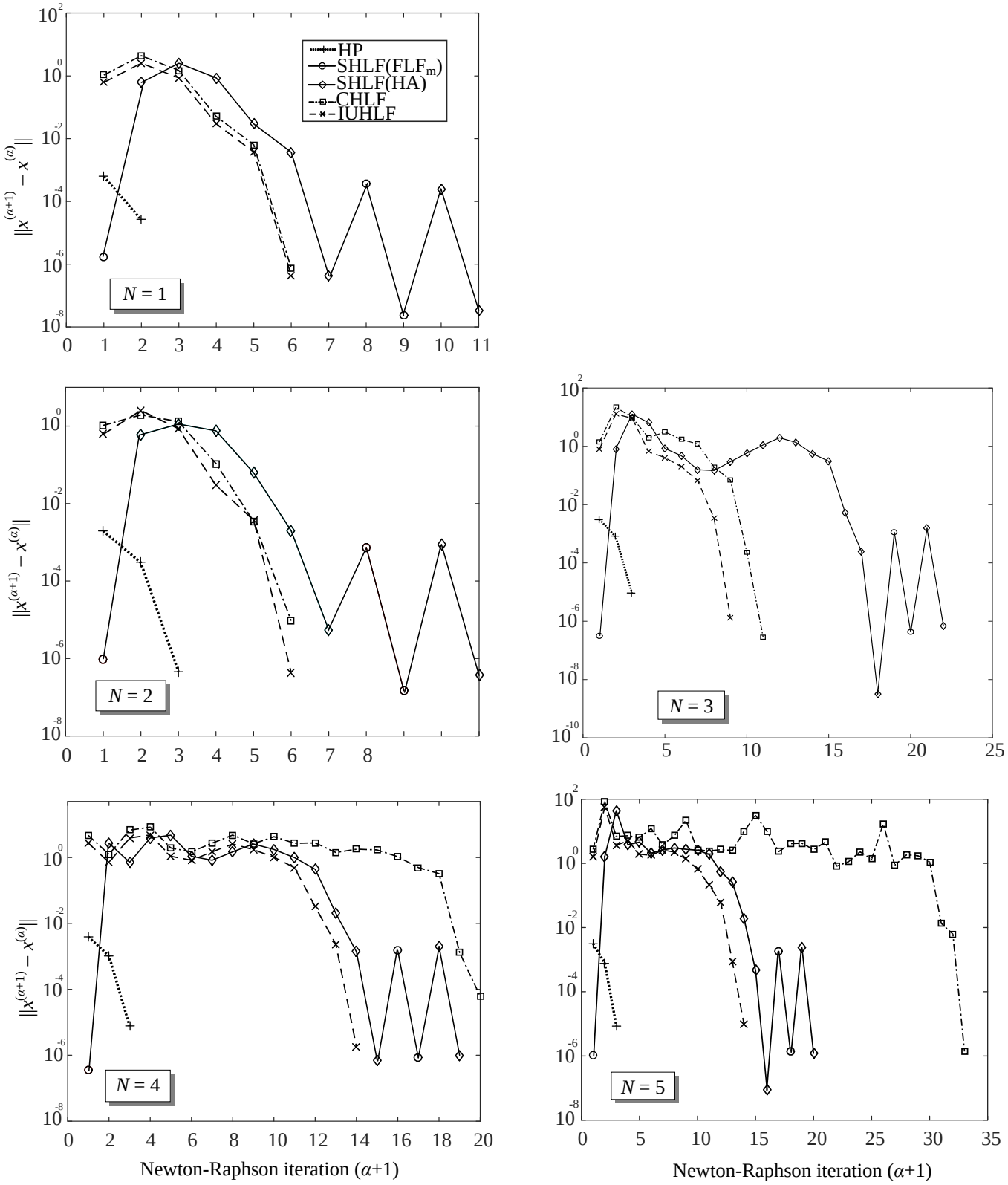

Figure 5.3(a): Evolution of $||x^{(\alpha+1)} - x^{(\alpha)}||$ versus the Newton-Raphson iteration (α+1)

Figure 5.3(b) shows the evolution of ||F(x)|| versus the Newton-Raphson iteration (α+1) for all used formulations and five different numbers N of single-phase uncontrolled rectifiers.

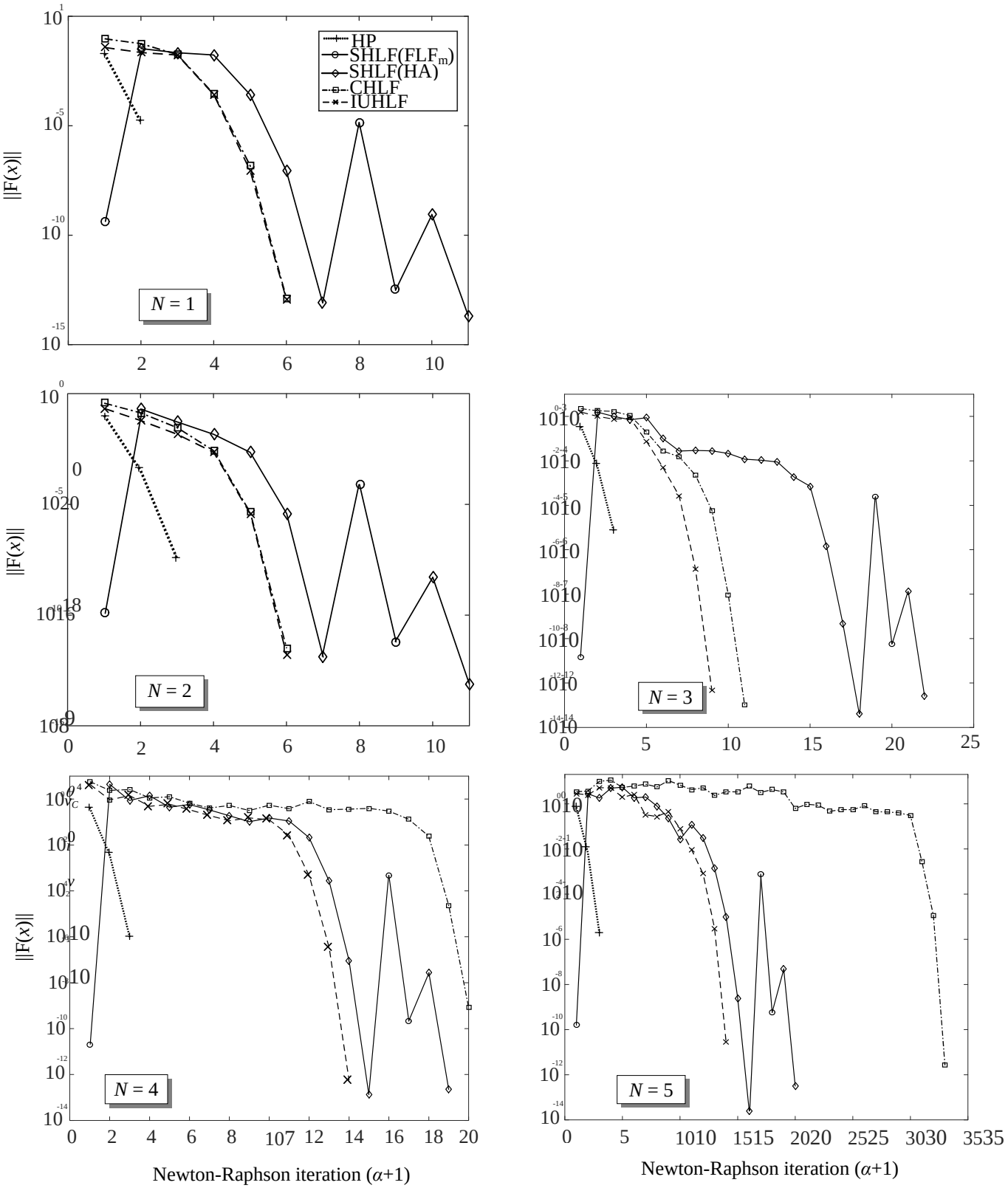

Figure 5.3(b): Evolution of ||F(x)|| versus the Newton-Raphson iteration (α+1)

The evolution of the plots for HP, IUHLF, CHLF remains almost identical when compared to evolution of the graphs with the tolerance limit of $||x^{(\alpha+1)} - x^{(\alpha)}|| < 10^{-3}$, but we observe a change

of convergence behaviour for the SHLF, as a constant increase in number of iterations is observed for every number *N* of nonlinear loads. So a decrease in the step size tolerance and an increase in voltage distortion may affect the convergence of SHLF as compared to other HLF formulations.

The total number of iterations taken by each HLF formulation to reach the numerical solution of the harmonic problem setting the step size tolerance limit at $||x^{(\alpha+1)} - x^{(\alpha)}|| < 10^{-4}$ is summarised in Table 5.2.

Number of NLLs (*N*)	HP number of iterations	CHLF number of iterations	SHLF number of iterations	IUHLF number of iterations
1	2	6	(1+2)+(6+2)	6
2	3	6	(1+2)+(6+2)	6
3	3	11	(1+2)+(17+2)	9
4	3	20	(1+2)+(14+2)	14
5	3	33	(1+2)+(15+2)	14

Table 5.2: Total number of iterations taken by each HLF formulation with varying NLLs (*N*)

The increase in the number of iterations taken by SHLF for every *N* might be attributed to the fact that there are two numerical procedures involved and a change in the step size tolerance limit affects both the procedures, which leads us to a very serious flaw in this formulation. Situation may arise during the numerical resolution of SHLF in which one of the numerical procedures converges to the solution, whereas the other procedure needs additional iterations to converge or even does not converge at all depending on the value of the step size tolerance limit given to the numerical procedure.

5.1.2. Levenberg-Marquardt method

The next technique employed in this thesis for the numerical resolution of harmonic problem is Levenberg-Marquardt method based on nonlinear least-squares approach. The theoretical background of the technique is briefly explained in Section 3.4 of the thesis memory. Even though Newton-Raphson is an efficient numerical method to solve the HLF problem, it suffers from convergence problems when starting points are not close to the solution and when voltage distortion is increased in the network. This disadvantage forces us to look at alternatives for the numerical resolution of the harmonic problem. The Levenberg-Marquardt method offers better convergence when voltage distortion is increased in the network.

From a common initial value $x^{(0)}$ for all used formulations, Levenberg-Marquardt convergence was checked from the condition $||x^{(\alpha+1)} - x^{(\alpha)}|| < 10^{-3}(||x^{(\alpha)}||+10^{-3})$. SHLF fixed-point iteration convergence was checked by considering $\varepsilon = 10^{-5}$ in equation (3.16). Figure 5.4(a) shows the evolution of $||x^{(\alpha+1)} - x^{(\alpha)}||$ versus the Levenberg-Marquardt iteration (α+1) for all used formulations and five different numbers *N* of single-phase uncontrolled rectifiers.

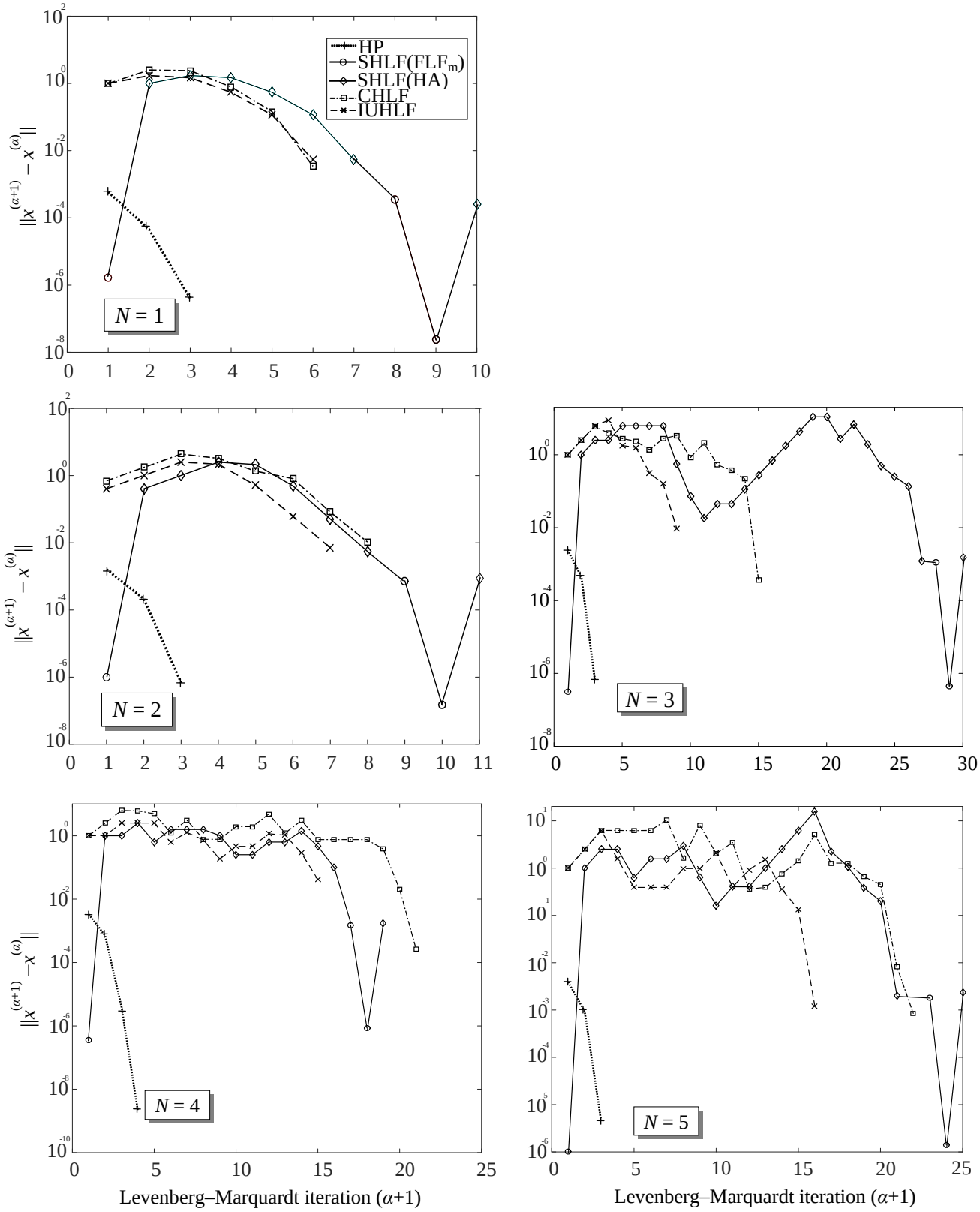

Figure 5.4(a): Evolution of $||x^{(\alpha+1)} - x^{(\alpha)}||$ versus the Levenberg-Marquardt iteration (α+1)

Figure 5.4(b) shows the evolution of S versus the Levenberg-Marquardt iteration (α+1) for all used formulations and five different numbers N of single-phase uncontrolled rectifiers.

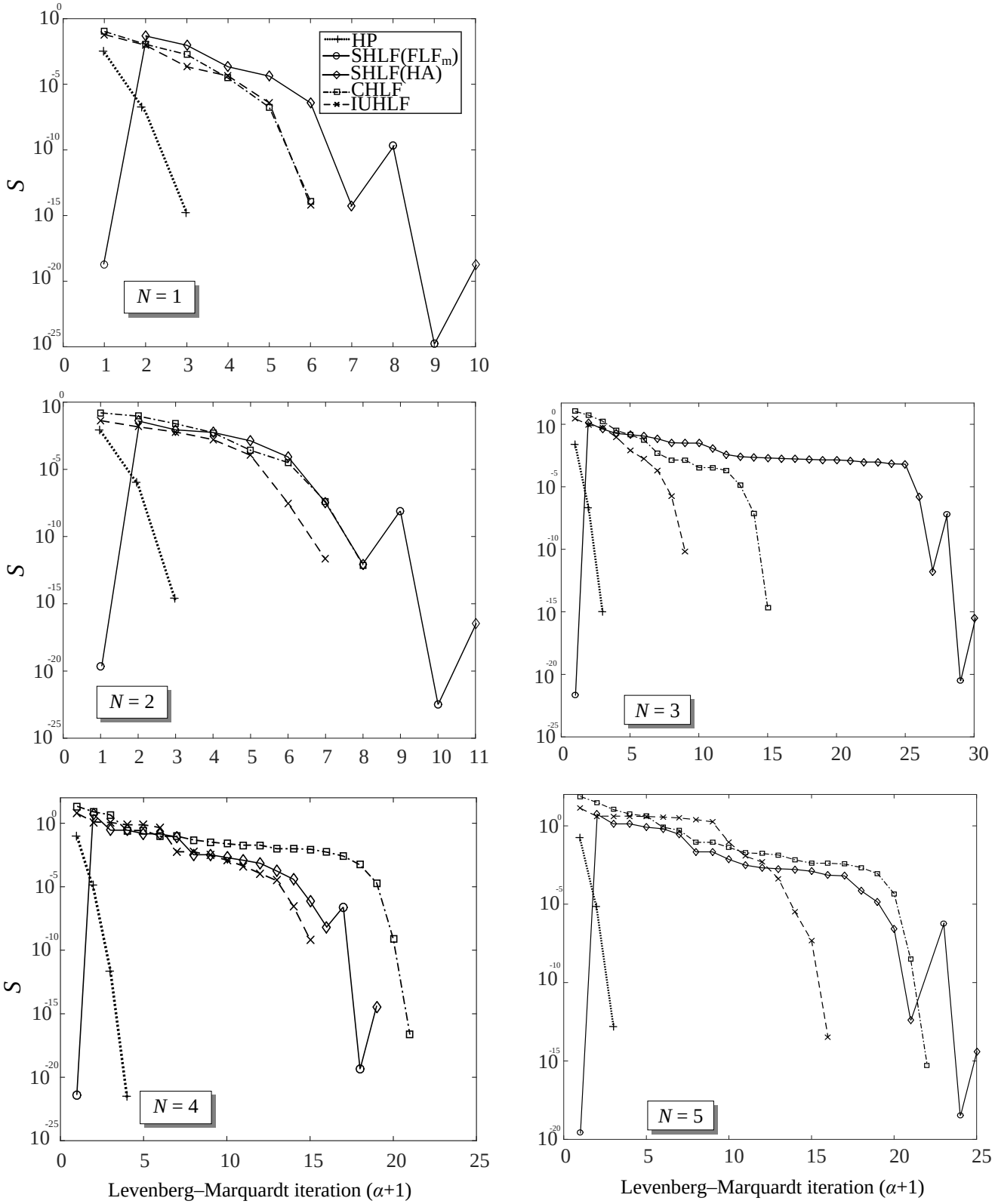

Figure 5.4(b): Evolution of S versus the Levenberg-Marquardt iteration (α+1)

Observation of the plots in Figure 5.4(a) and 5.4(b) leads us to the conclusion that for a certain step size tolerance limit $||x^{(\alpha+1)} - x^{(\alpha)}|| < 10^{-3}(||x^{(\alpha)}||+10^{-3})$, the numerical method gives us more

accuracy of the results at the cost of relatively slow convergence as compared to Newton-Raphson method.

The total number of iterations taken by each HLF formulation to reach the numerical solution of the harmonic problem setting the step size tolerance limit at $||x^{(\alpha+1)} - x^{(\alpha)}|| < 10^{-3}(||x^{(\alpha)}||+10^{-3})$ is summarised in Table 5.3.

Number of NLLs (N)	HP number of iterations	CHLF number of iterations	SHLF number of iterations	IUHLF number of iterations
1	3	6	(1+2)+(6+1)	6
2	3	8	(1+2)+(7+1)	7
3	3	15	(1+2)+(26+1)	9
4	4	21	(1+2)+(15+1)	15
5	3	22	(1+2)+(20+1)	16

Table 5.3: Total number of iterations taken by each HLF formulation with varying NLLs (N)

Comparison of the two numerical methods, i.e., Newton-Raphson and Levenberg-Marquardt results using Table 5.1 and Table 5.3, yields some interesting findings. For both the methods, the starting points being considered are the same and lie close to the solutions to avoid convergence problems. Regarding the IUHLF and SHLF formulations, Newton-Raphson method offers rapid convergence as compared to Levenberg-Marquardt method if we have starting points close to the solution. The behaviour of HP formulation remains almost the same for both the methods, as we know that HP does not consider harmonic interaction of nonlinear load with the AC network, therefore posing not much of a challenge for both the numerical methods.

Regarding CHLF formulation, we observe a very contrasting behaviour as compared to SHLF and IUHLF, i.e., CHLF exhibits better convergence when used in conjunction with Levenberg-Marquardt method as it utilizes a fewer number of iterations to reach the numerical solution even for greater number N of nonlinear loads as compared to Newton-Raphson method. This unusual phenomenon can be explained looking at the theoretical foundation of the HLF formulation. As we know from Chapter 2 that CHLF is the most computationally complex harmonic formulation having greater number of unknowns and equations as compared to other HLF formulations, it performs better when the numerical method being used is Levenberg-Marquardt based on nonlinear least-squares approach. In short, Levenberg-Marquardt method holds an edge over Newton-Raphson method if the number of unknowns to be solved is greater. This property of Levenberg-Marquardt method becomes very useful when handling bigger AC networks with multiple buses and nonlinear loads.

In order to increase the accuracy of the results for the HLF formulations, the step size tolerance is set to a lower value and numerical resolution is performed again. From a common initial value $x^{(0)}$ for all used formulations, Levenberg-Marquardt convergence was checked from the condition $||x^{(\alpha+1)} - x^{(\alpha)}|| < 10^{-4}(||x^{(\alpha)}||+10^{-4})$. Figure 5.5(a) shows the evolution of $||x^{(\alpha+1)} - x^{(\alpha)}||$ versus the

Levenberg-Marquardt iteration (α+1) for all used formulations and five different numbers N of single-phase uncontrolled rectifiers.

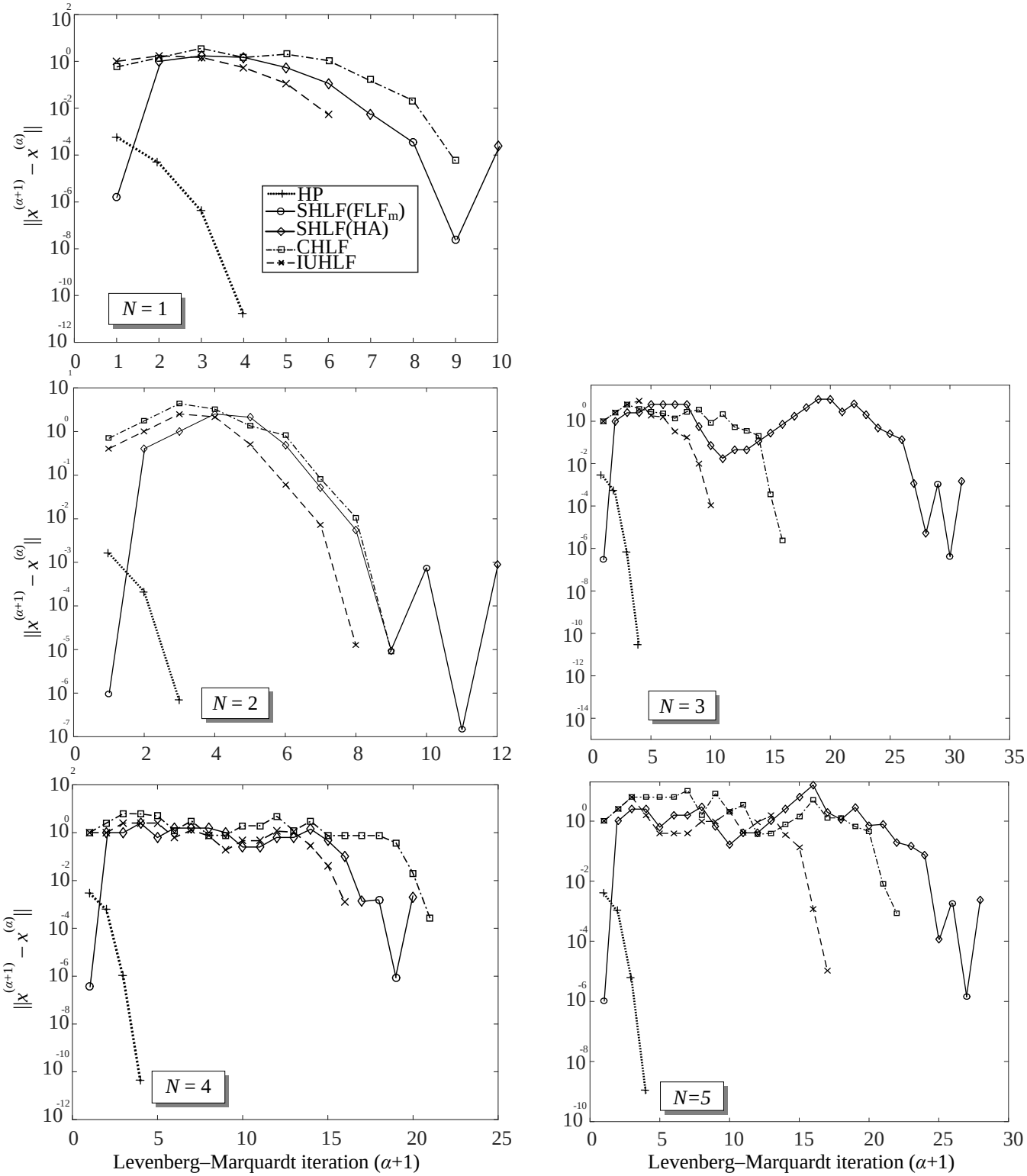

Figure 5.5(a): Evolution of $\|x^{(\alpha+1)} - x^{(\alpha)}\|$ versus the Levenberg-Marquardt iteration (α+1)

Figure 5.5(b) shows the evolution of S versus the Levenberg-Marquardt iteration (α+1) for all used formulations and five different numbers N of single-phase uncontrolled rectifiers.

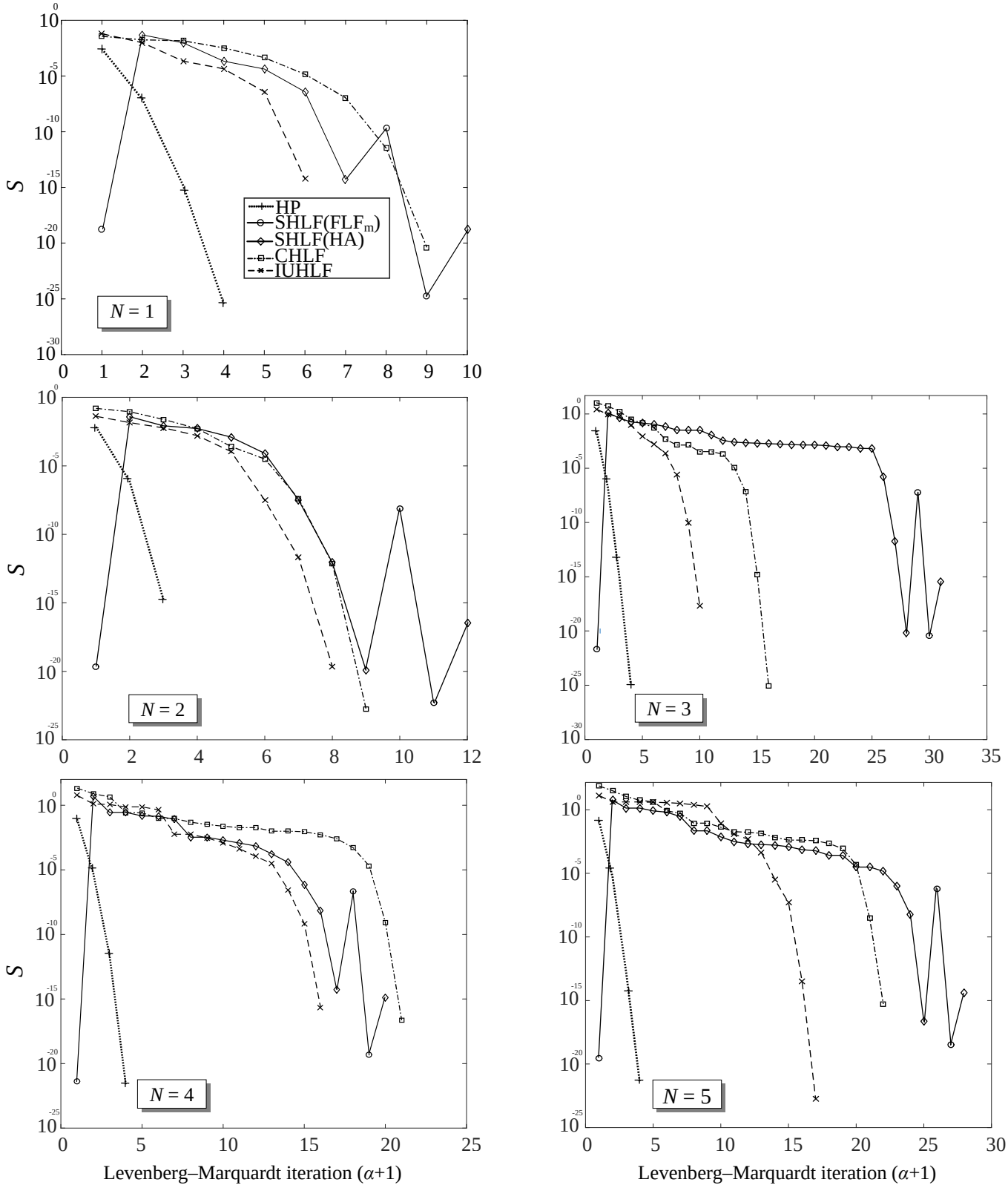

Figure 5.5(b): Evolution of S versus the Levenberg-Marquardt iteration (α+1)

As expected, increasing the accuracy of the results yields an increase in the number of iterations taken by each HLF formulation to reach the numerical solution of the harmonic problem.

The total number of iterations taken by each HLF formulation to reach the numerical solution of the harmonic problem setting the step size tolerance limit at $||x^{(\alpha+1)} - x^{(\alpha)}|| < 10^{-4}(||x^{(\alpha)}||+10^{-4})$ is summarised in Table 5.4.

Number of NLLs (N)	HP number of iterations	CHLF number of iterations	SHLF number of iterations	IUHLF number of iterations
1	4	9	(1+2)+(6+1)	6
2	3	9	(1+2)+(8+1)	8
3	4	16	(1+2)+(27+1)	10
4	4	21	(1+2)+(16+1)	16
5	4	22	(1+2)+(24+1)	16

Table 5.4: Total number of iterations taken by each HLF formulation with varying NLLs (N)

The increase in the number of iterations is more profound for SHLF formulation but not so much for the other HLF formulations (HP, CHLF and IUHLF). This is due to the reason that tolerance limit is applied to two numerical procedures in SHLF formulation.

5.2. Study of HLF formulation accuracies

Regarding the voltage at bus 3, Figure 5.6 plots the values of individual *Harmonic Distortions* (*HD*s) versus the harmonic order h, as well as the value of *Total Harmonic Distortion* (*THD*) for all used formulations and five different numbers N of single-phase uncontrolled rectifiers connected to this bus. As it is evident from Figure 5.6 and Tables 5.1 to 5.4, IUHLF offers the same accuracy of results compared to CHLF and SHLF, with the advantage of requiring a fewer number of iterations. Even when the number N of NLLs is increased, IUHLF maintains the accuracy of results while also keeping the number of iterations required for the numerical resolution to a minimum. From the observation of the Tables 5.1 to 5.4, it can be stated with some assurance that if provided an AC network with highly distorted voltages, IUHLF is more capable of solving the harmonic problem as compared to the other three formulations.

The high values of individual *HD* at $h = 15$ for all used formulations can be explained by the existence of a parallel resonance near $h = 15$ in the equivalent circuit of the network "observed" from bus 3. The reason for placing the resonance at such a high harmonic frequency is that the addition of the resonance to a lower harmonic frequency has a very significant effect on the AC network, increasing the harmonic voltage distortions and making the system difficult to solve by using the existing numerical methods. The bar graphs of Figure 5.6 only show the results of individual *HD* at bus 3 and at no other buses. This was done to avoid repetition of results, as

individual *HD*s at other buses give similar range of values. A more detailed summary of harmonic voltage distortion at all buses is given through Tables 4.13 to 4.18.

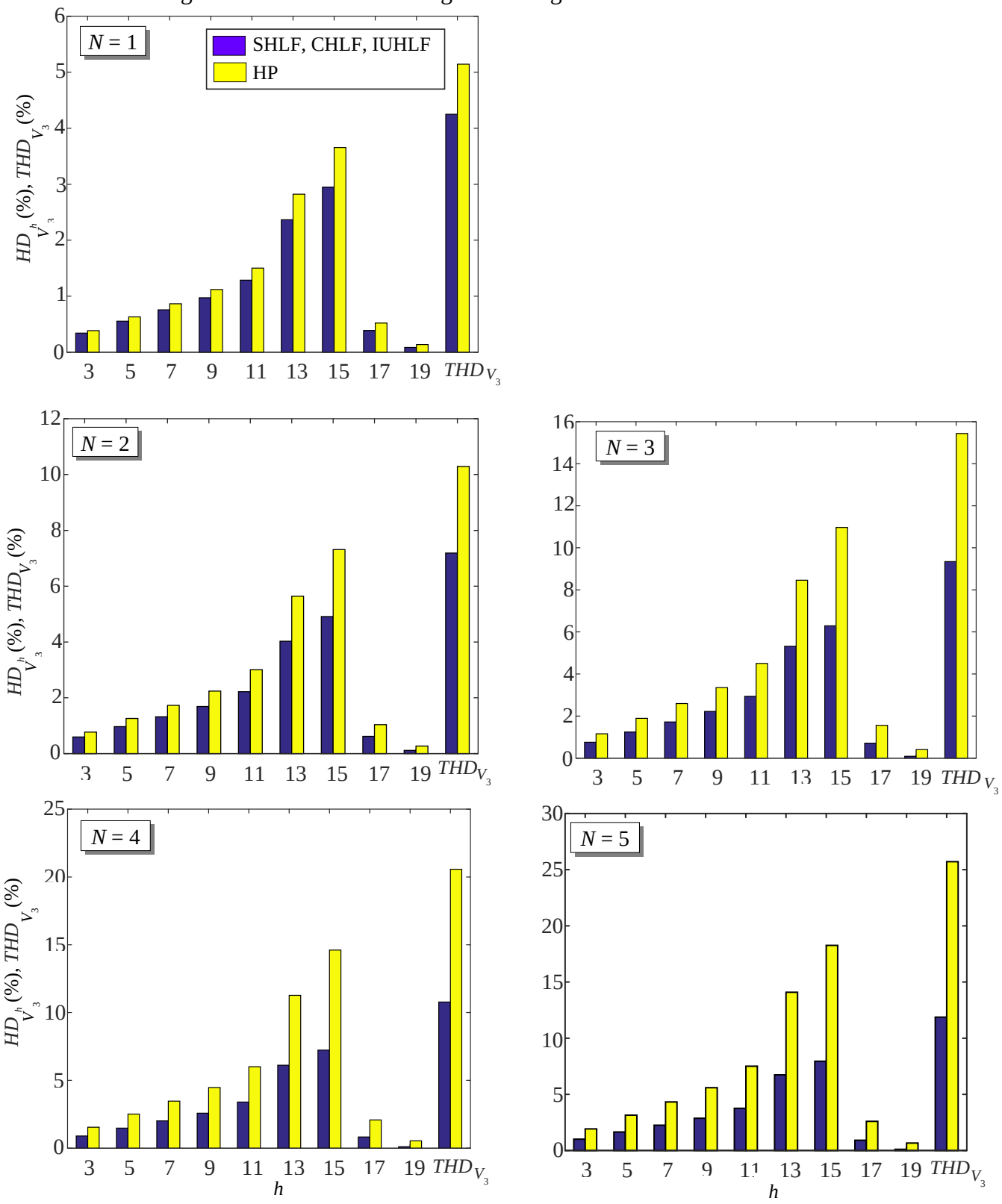

Figure 5.6: Voltage at bus 3: Individual *HD*s versus the harmonic order *h*, as well as *THD*, for all used formulations and five different values of *N*.

Higher values of N lead to greater discrepancy between the results obtained from the HP formulation and those obtained from the other three formulations. This is because NLL harmonic interaction is not considered in HP formulation, rendering the other three formulations better in terms of accuracy.

6. Conclusions

The study of harmonics in power systems is a very important field of research in Power Quality. The dynamics of AC networks is rapidly changing nowadays due to addition of nonlinear loads and renewable energy devices into the energy mix. It is very important to know how these nonlinear loads are interacting with the AC network and their potential impact on the power system. The thesis was aimed to study the harmonic load flow formulations and the numerical resolution of their nonlinear equation systems. The objective was to propose an improved HLF formulation, which considers the harmonic interaction of nonlinear loads with the AC network and offers simplicity and equal accuracy as compared to other HLF formulations. The study of numerical resolution of HLF formulations is focused on the analysis of the numerical method convergence and the comparison of numerical methods which try to obtain global convergence. The main conclusions of this thesis are presented below:

- First of all, basic understanding for the modelling of nonlinear loads was developed. For this purpose, equations of a commonly used nonlinear load were studied and implemented on the computing tool MATLAB. This load was the single-phase uncontrolled rectifier. This practise gave us a fair estimation of the harmonic characterization we can expect if we integrate this load into an electrical network with multiple buses.

- A study was conducted on the most important harmonic load flow formulations present in literature. The harmonic load flow formulations studied in this thesis are harmonic penetration (HP), simplified harmonic load flow (SHLF), complete harmonic load flow (CHLF) and unified harmonic load flow (UHLF). The equations pertaining to each harmonic formulation for Slack, PQ and NL buses were identified and presented. The unknowns for each formulation were also identified and presented in tabular form. The in-depth study of the harmonic formulations helped in understanding the complexity of each technique, level of harmonic interaction considered and mathematical orientation of each formulation.

- To further illustrate the concepts of harmonic formulations, an electrical network example was considered for which the equations and unknowns are developed for each harmonic formulation. Resonance was also introduced into the electrical network to study the harmonic behaviour of the AC network under unstable conditions. It was observed that setting resonance to a harmonic frequency close to fundamental frequency makes the network highly unstable for the presence of highly distorted voltages and it becomes very difficult to achieve the numerical resolution of the AC network.

- An improved harmonic load formulation was proposed, called improved unified harmonic load flow (IUHLF). This enhanced formulation is based on the best properties of HP, SHLF, CHLF and UHLF formulations: use of harmonic equivalent circuits to reduce the number of harmonic voltages which are unknowns in nonlinear equations systems, and construction of a single nonlinear equation system which is numerically solved by the Newton-Raphson method with true Jacobian matrix and by the Levenberg-Marquardt method.

- For all the HLF formulations applied to the electrical network example, it was noticed that Newton-Raphson method performs efficiently if the proposed starting point is close to the solution of the HLF problem, but it faces convergence problems if the starting point is set far from the solution. Newton-Raphson method was also observed to be vulnerable if voltage distortion in the AC network is increased to a certain limit. In addition, the use of Newton-Raphson method with constant Jacobian matrix in IUHLF formulation was studied through the same network and in the same context of voltage distortion. It was checked that it leads to serious convergence problems. Therefore, this strategy should be avoided in scenarios of highly distorted voltages. These observations forced us to look for alternative and more robust options for the numerical resolution of the HLF problem.

- To overcome the aforementioned deficiencies of Newton-Raphson method when solving the HLF problem, the electrical network example was solved by using the Levenberg-Marquardt method, which is a method based on nonlinear least-squares approach. It was observed that Levenberg-Marquardt method has better convergence properties when the number of unknowns in the HLF problem increases, which makes the method suitable for the numerical resolution of the HLF problem in large AC networks.

- IUHLF formulation allows the numerical resolution of the HLF problem to be simplified, i.e., the number of iterations required by the proposed formulation is smaller than that required by the other formulations with identical accurate results (SHLF, CHLF and UHLF). This is particularly critical in scenarios of highly distorted voltages.

7. Suggestions for future work

This thesis covers the basic fundamentals of harmonic load flow formulation and numerical resolution, with some new findings in the HLF problem treatment. The following lines of research are proposed as future work for this field of study:

- Only a specific nonlinear load was considered in this thesis: the single-phase uncontrolled rectifier. There is a need to extend the study of the HLF problem considering other important nonlinear loads such as discharge lamps, LED lamps, battery chargers, three-phase uncontrolled rectifiers, etc.

- Convergence properties for two numerical methods were explored in the thesis, one being the Newton-Raphson method and the other being the Levenberg-Marquardt method. There are many other numerical methods in literature which can be implored for the numerical resolution of the HLF problem.

- It was observed during the numerical resolution of the HLF problem that starting points play a significant role in attaining the correct solution of the problem. There is a need to develop a more robust technique which gives a good estimate of starting points for any type of HLF problem.

- For this thesis, the electrical network example taken was a 3-bus system. It would be highly advisable to implement the IUHLF formulation for electrical networks with a larger number of buses. In addition, convergence properties of IUHLF must be studied to know how this formulation performs for large networks as compared to other HLF formulations.

- An in-depth study of the HLF problem in electrical networks with highly distorted voltages is suggested, as well as an investigation of specific numerical methods which might be helpful in the numerical resolution of such networks.

- An analysis of the HLF problem in a context of renewable energy resources is recommended, which entails the harmonic characterization of the renewable energy resources and their harmonic interaction with the AC network.

8. Bibliography

8.1. References consulted by the PhD candidate

[1] B. Stott, *Review of load-flow calculation methods*, Proc. IEEE, Vol. 62, No. 7, pp. 916–929, July 1974.

[2] A. Keyhani, *Evaluation of power flow techniques for personal computers*, IEEE Trans. Power Syst., Vol. 4, pp. 817–826, May 1991.

[3] J. Arrillaga and C. P. Arnold, *Computer Analysis of Power Systems*, New York: Wiley, 1990.

[4] E. F. Fuchs, M. A. S. Masoum, *Power quality in power systems and electrical machines*, Academic Press, 2008.

[5] EN 50160, *Voltage characteristics of electricity supplied by public electricity networks.*

[6] IEEE 519-2014: *IEEE Recommended Practice and Requirements for Harmonic Control in Electrical Power Systems.*

[7] IEC 61000-2-2: *Electromagnetic compatibility (EMC) - Part 2-2: Environment - Compatibility levels for low-frequency conducted disturbances and signalling in public low-voltage (V < 1 kV) power supply systems.*

[8] IEC 61000-2-12: *Electromagnetic compatibility (EMC) - Part 2-12: Environment - Compatibility levels for low-frequency conducted disturbances and signalling in public medium-voltage (1 kV < V < 35 kV) power supply systems.*

[9] IEC 61000-3-2: *Electromagnetic compatibility (EMC) - Part 3-2: Limits - Limits for harmonic current emissions (equipment input current ≤16 A per phase).*

[10] IEC 61000-3-4, 3-12: *Electromagnetic compatibility (EMC) - Part 3-4, 3-12: Limits - Limitation of emission of harmonic currents in low-voltage power supply systems for equipment with rated current > 16 A (3-4), Limits - Limits for harmonic currents produced by equipment connected to public low-voltage systems with input current > 16 A and ≤75 A per phase (3-12).*

[11] IEC 61000-3-6: *Electromagnetic compatibility (EMC) - Part 3-6: Limits - Assessment of emission limits for the connection of distorting installations to MV, HV and EHV power systems.*

[12] O. Boix, *Estudio y modelización en régimen permanente de cargas no lineales para el análisis armónico de redes eléctricas*, PhD Thesis, ETSEIB, UPC, Barcelona, 1996.

[13] J. J. Mesas, *Estudio y caracterización de cargas no lineales*, PhD Thesis, ETSEIB, UPC, Barcelona, 2009.

[14] G. T. Heydt, *Electric Power Quality*, Stars in a Circle Publications, 1991.

[15] J. Arrillaga, N. R. Watson, *Power System Harmonics*, John Wiley & Sons, 2003.

[16] S. Herraiz, *Aportaciones al estudio del flujo armónico de cargas*, PhD Thesis, ETSEIB, UPC, Barcelona, 2002.

[17] H. W. Dommel, *Electromagnetic Transients Program Reference Manual (EMTP Theory Book)*, Microtran Power System Analysis Corporation, 1996.

[18] J. Usaola, *Régimen permanente de sistemas eléctricos de potencia con elementos no lineales mediante un procedimiento hibrido de análisis en los dominios del tiempo y de la frecuencia*, PhD Thesis, UPM, Madrid, 1990.

[19] Y. Sun, G. Zhang, W. Xu, J. G. Mayordomo, *A harmonically coupled admittance matrix model for AC/DC converters*, IEEE Trans. on Power Systems, Vol. 22, No. 4, November 2007, pp. 1574-1582.

[20] J. Molina, *Caracterización armónica de dispositivos de iluminación de eficiencia energética*, PhD Thesis, ETSEIB, UPC, Barcelona, 2014.

[21] S. Herraiz, L. Sainz, J. Clua, *Review of harmonic load flow formulations*, IEEE Trans. on Power Delivery, Vol. 18, No. 3, July 2003, pp. 1079-1087.

[22] T. J. Densem, P. S. Bodger, J. Arrillaga, *Three phase transmission system modelling for harmonic penetration studies*, IEEE Trans. on Power Apparatus and Systems, Vol. PAS-103, No. 2, February 1984, pp. 310-317.

[23] A. A. Mahmoud, R. D. Shultz, *A method for analyzing harmonic distribution in A.C. power systems*, IEEE Trans. on Power Apparatus and Systems, Vol. PAS-101, No. 6, June 1982, pp. 1815-1824.

[24] J. Arrillaga, C. D. Callaghan, *Double-iterative algorithm for the analysis of power and harmonic flows at AC/DC convertor terminals*, IEE Proceedings C (Generation, Transmission and Distribution), Vol. 136, No. 6, November 1989, pp. 319-324.

[25] J. Arrillaga, C. D. Callaghan, *Three phase AC-DC load and harmonic flows*, IEEE Trans. on Power Delivery, Vol. 6, No. 1, January 1991, pp. 238-244.

[26] M. Valcárcel, *Análisis del régimen permanente de los sistemas eléctricos de potencia con elementos no lineales mediante un método de reparto de cargas con armónicos*, PhD Thesis, UPM, Madrid, 1991.

[27] M. Valcárcel, J. G. Mayordomo, *Harmonic power flow for unbalanced systems*, IEEE Trans. on Power Delivery, Vol. 8, No. 4, October 1993, pp. 2052-2059.

[28] D. Xia, G. T. Heydt, *Harmonic power flow studies, Part I and Part II*, IEEE Trans. on Power Apparatus and Systems, Vol. PAS-101, No. 6, June 1982, pp. 1257-1265 and pp. 1266-1270.

[29] W. Xu, J. R. Marti, H. W. Dommel, *A multiphase harmonic load flow solution technique*, IEEE Trans. on Power Systems, Vol. 6, No. 1, February 1991, pp. 174-182.

[30] W. Xu, J. E. Drakos, Y. Mansour, A. Chang, *A three-phase converter model for harmonic analysis of HVDC systems*, IEEE Trans. on Power Delivery, Vol. 9, No. 3, July 1994, pp. 1724-1731.

[31] M. A. Moreno, J. Usaola, *A new balanced harmonic load flow including nonlinear loads modeled with RBF networks*, IEEE Trans. on Power Delivery, Vol. 19, No. 2, April 2004, pp. 686-693.

[32] M. A. Moreno, J. Usaola, *Three-phase harmonic load flow in frequency and time domains*, IEE Proceedings - Electric Power Applications, Vol. 150, No. 3, May 2003, pp. 295-300.

[33] S. Iwamoto, Y. Tamura, *A load flow calculation method for ill-conditioned power systems*, IEEE Trans. on Power Apparatus and Systems, Vol. PAS-100, No. 4, April 1981, pp. 1736-1743.

[34] S. C. Tripathy, G. Durga, O. P. Malik, G. S. Hope, *Load-Flow solutions for ill-conditioned power systems by a Newton-like method*, IEEE Trans. on Power Apparatus and Systems, Vol. PAS-101, No. 10, October 1982, pp. 3648-3656.

[35] J. Pedra, M. Salichs, *Harmonic power flow studies, Part II, Numerical solution and implementation*, International Symposium on "Electrical energy conversion in power systems", W-H.2, Capri, May 1989.

[36] J. G. Mayordomo, M. Izzeddine, J. Usaola, *Comparative study of algorithms for iterative harmonic analysis and its application to static converters*, IEEE VI-ICHPS, Bologna, 21-23 Sept. 1994, pp. 303-310.

[37] M. Dehnel, H. W. Dommel, *A method for identifying weak nodes in nonconvergent load flows*, IEEE Trans. on Power Systems, Vol. 4, No. 2, May 1989.

[38] V. A. Venikov, V. A. Stroev, V. I. Idelchick, V. I. Tarasov, *Estimation of electrical power system steady-state stability in load flow calculations*, IEEE Trans. on Power Apparatus and Systems, Vol. PAS-94, No. 3, May/June 1975, pp. 1034-1041.

[39] S. Abe, N. Hamada, A. Isono, K. Okuda, *Load flow convergence in the vicinity of a voltage stability limit*, IEEE Trans. on Power Apparatus and Systems, Vol. PAS-97, No. 6, Nov./Dec. 1978, pp. 1983-1993.

[40] J. Pedra, *El problema del flujo de cargas en redes con armónicos*, PhD Thesis, ETSEIB, UPC, Barcelona, 1986.

[41] L. Sainz, J. Pedra, *Infeasible harmonic power flow solutions*, IEEE VI-ICHPS, Bologna, 21-23 Sept. 1994, pp. 296-302.

[42] L. Sainz, J. Pedra, O. Boix, *Non-divergent numerical method for the harmonic load-flow resolution*, European Transactions on Electrical Power (ETEP), Vol. 9, No. 5, Sep./Oct. 1999, pp. 317-326.

[43] W. Ma, J. S. Thorp, *An efficient algorithm to locate all the load flow solutions*, IEEE Trans. on Power Systems, Vol. 8, No. 3, August 1993, pp. 1077-1083.

[44] MathWorks (2015). *Optimization Toolbox: User's Guide (R2018a)*, retrieved May 11, 2018 from https://www.mathworks.com/help/optim/ug/fsolve.html

[45] Levenberg, Kenneth (1944), *A method for the solution of certain nonlinear problems in least squares*, Quarterly of Applied Mathematics 2: 164–168.

[46] Marquardt, Donald (1963), *An algorithm for least-squares estimation of nonlinear parameters*, SIAM Journal on Applied Mathematics 11 (2): 431–441, doi: 10.1137/0111030.

[47] https://www.rose-hulman.edu/~bryan/lottamath/leastsqrs2.pdf

[48] B. C. Smith, J. Arrillaga, *Power flow constrained harmonic analysis in AC-DC power systems*, IEEE Trans. on Power Systems, Vol. 14, No. 4, November 1999, pp. 1251-1261.

[49] J. Arrillaga, B. Smith, *AC-DC power system analysis*, IEE Power and Energy Series (27), Institution of Engineering and Technology, 1998.

[50] J. J. Mesas, L. Sainz, J. Molina, *Parameter estimation procedure for models of single-phase uncontrolled rectifiers*, IEEE Trans. on Power Delivery, Vol. 26, No. 3, July 2011, pp. 1911-1919.

8.2. Scientific productivity of the PhD candidate

[51] A. Rashid, J. J. Mesas, L. Sainz, *An improved harmonic load flow formulation*, Electric Power Systems Research, Current Status (September 2018): Under Review.